Guidelines for Authors

This periodical is a publication of the Academic Publishing and Translation Directorate of Qassim University. Its purpose is to provide an opportunity for scholars to publish their original research.

Manuscripts will be published in on of the following platforms:

i)   **Article:** It should be original and has a significant contribution to the field in which the research was conducted.

ii) **Review Article:** A critical synthesis of the current literature in a particular field, or a synthesis of the literature in a particular field during an explicit period of time.

iii) **Brief Article (Technical Notes):** A short article (note) having the same characteristics as an article.

iv) **Innovation and Invention Reports**

v)   **Forum:** Letters to the Editor, comments and responses, preliminary results or findings, and miscellany.

vi) **Book Reviews**

The Editorial Board will consider manuscripts in the following fields:

- Electrical Engineering
- Civil Engineering
- Mechanical Engineering
- Chemical Engineering
- Computer Engineering

- Mining and Petroleum Engineering
- Computer Science
- Information Technology
- Information Systems
- Basic Engineering and Computer Sciences

A manuscript should be submitted in English, and, if accepted for publication, it should not be published elsewhere without the written permission of the Editor-in-Chief.

General Instructions

1. **Submission of manuscripts for publication:** Papers must be presented in final page format (not more than 20 pages, A4 size), along with a compact disk (CD) containing the contribution executed on a PC using MS Word or any updated version of it. Manuscripts should be typed using Times New Roman, 12 points font, and one and half space. Pages are to be numbered consecutively and are to include all illustrative material, such as tables and figures, in their appropriate places in the text. If the author does not follow these guidelines, the paper is likely to be rejected or delayed.

2. **Abstracts:** Manuscripts for articles, review articles, and brief articles require both Arabic and English abstracts, using not more than 200 words..

3. **Keywords:** Each article must have keywords before both abstracts (English and Arabic) and they should not exceed 10 words.

4. **Tables and other illustrations:** Tables, figures, charts, graphs and plates should be planned to fit the Journal's page size (A4 incl. running heads). Line drawings are to be presented on high quality tracing paper using black India ink. Copies are not permitted for use as originals. Line quality is required to be uniform, distinct, and in proportion to the illustration. Photographs may be submitted on glossy print paper, in either black and white, or color, or made by using Adobe Photoshop. Tables and other illustrative material must include headings or titles, and captions for figures.

5. **Abbreviations:** The names of periodicals should be abbreviated in accordance with *The World List of Scientific Periodicals.* e.g., *et al., J. of Food Sci.*

For weights and measurements, and where appropriate, abbreviations rather than words are to be used, e.g., cm, mm, m, km, cc, ml, g, kg, min, %, etc., Fig.

Latin abbreviations such as: *op. cit., loc. cit., ibid.,* are to be in italic (if they are used).

6. **References:** References are mentioned numerically [between brackets] in the text and a list of references are provided at the end of the manuscript as follows:

a- Journals: [number] followed by the last name of the author (authors), First name or abbreviation, "paper title" , journal title , volume and issue numbers, (the year of publications between parentheses) , and page numbers.

Example: Sawyer, D. A. "Pounding of Rainwater on Flexible Roof Systems," Proceedings ASCE, Journal of the Structural Division, Vol. 93, No. 1, (1967), pp.127-147.

b- Books: Book references must include author, book title, the publisher's location, and publisher, and the year of publication.

Example: Feld, J., and Carper, K., Construction failure, 2nd Ed., New York, Wiley, 1997.

7. **Content Note or Footnote:** A content note or footnote is a note from the author to the reader providing clarifying information.

A content note is indicated in the text by using a half-space superscript number (e.g. … books[3] are …). Content notes are to be sequentially numbered throughout the text. A reference may be cited in a content note by the use of the standard (Author, Date) style in the same way they are used in the text.

Content notes are to be presented below a solid half-line separating them from the text of the page in which the footnote is mentioned (in single column). Use the same half-space superscript number assigned in the content note(s) in the text to precede the content note itself.

8. **Proofs:** No changes, additions or deletions will be allowed in the pageproof stage.

9. **Opinions:** Manuscripts submitted to the Journal for publication contain the author's conclusions and opinions and, if published, do not constitute a conclusion or opinion of the Editorial Board.

10. **Offprints:** Two copies of the journal and twenty reprints of the accepted papers will be sent to the authors.

11. **Correspondence:** All correspondence may be addressed to:

Prof. Mohamed A Abel-halim (Editor in Chief)
E-mail: quecjour@qec.edu.sa

12. **Frequency:** …Two issues per year…….

13. **Subscription and Exchange:**

Prof. Mohamed A Abel-halim (Editor in Chief)
E-mail: quecjour@qec.edu.sa

**In The Name of ALLAH,
Most Gracious, Most Merciful**

Volume (2)   No. (1)

Journal
of
Engineering and Computer Sciences

(January 2009)   **(Muharram 1430H)**

Qassim University Scientific Publications

(Refereed Journal)

Deposif: 1429/2023

Contents   **Page**

Voltage-Firing Control of Grid_Connected Induction Generator

A. F. Almarshoud[*], M.A. Abdel-halim[**], M. Munawer Shees[***]
College of Engineering, Qassim University, Buraydah
*[*]amarshoud@yahoo.com   ** masamie@qec.edu.sa   *** munawwarshees@qec.edu.sa*

Abstract. This paper presents a complete analysis of an induction generator linked to the power network through an ac voltage controller aiming to control the generated active and reactive power at different speeds. The ac voltage controller uses the firing angle strategy to control the generator terminal voltage. The generator performance characteristics regarding the harmonic distortion factors, active power, reactive power, power factor, torque ripples and efficiency have been computed at different speeds. These characteristics have been determined with the help of a novel equivalent circuit in the frequency domain.
***Keywords*:** induction generator, ac voltage controller, grid-connected

1. Introduction

Wind is a promising source of renewable energy in the world. This power may be utilized to generate electrical power using the induction generators [1-2].

The performance of a grid-connected induction generator using a solid state ac voltage controller as an interface between the grid and the stator terminals of the generator is studied in this paper. In this regard a forced-commutated ac voltage controller which utilizes a set of power transistor devices has been used.

Many authors have analyzed the self excited induction generators [3-8] which are utilized in far and isolated sites. The performance of controlled generators using ac voltage controller has been analyzed in previous publications for naturally commutated voltage controllers, and forced commutated voltage controllers [9-11]. The analysis has been determined using numerical techniques based upon a dq-abc reference frame models. In the present paper the steady-state electrical and mechanical performance of the generator has been analyzed through modeling the induction generator and the static converter by novel equivalent circuits in the frequency domain. This is expected to give more accurate results, and enables the iron losses to be taken into consideration which leads to accurate estimation of the generator efficiency.

Computer programs have been developed to determine the performance characteristics of the uncontrolled grid-connected induction generator and the controlled generator for a wide range of operating conditions and a specified switching strategy of the ac voltage controller. In this regard, the firing angle control strategy has been used. The computed performance characteristics included the generator current and its distortion factors, the generator active and reactive powers and the generator efficiency. Also, the bus current, its distortion factors, reflected harmonics on the supply, the displacement angle, the bus active and reactive powers, and the power factor has been computed. On the other side the mechanical performance characteristics regarding the unidirectional-developed torque and the pulsating components appearing as a result of the use of the ac voltage controller have been determined.

When using the ac voltage controllers, the active and reactive powers of the grid connected induction generator can be controlled. The bus reactive power is clearly controlled when using the firing angle control strategy to the extent that it becomes positive over certain ranges of firing angle. This means that the output current lags the voltage. Consequently, the reactive power will be delivered to the network by the induction generator.

2. Solid State Control of the Induction Generator

Forced commutated AC voltage controller is suggested to be used as an interface between the grid and the induction generator.

Control Using a Forced Commutated AC Voltage Controller

The proposed circuit is shown in Fig. (1). Each stator phase has control circuit that contains series and shunt power transistor in bridges of diodes to allow the current to pass in the two directions [10]. The two transistors are operated alternatively, when the series transistor is turned on, the shunt transistor is turned off and vice versa. This control circuit links the induction generator with the network. The terminal voltage as well as the active and reactive power of the generator can be controlled by variation of the on and off periods of the series transistors. The shunt transistor bridge allows the clamped current in the stator phase during the off state of the series bridge to continue flowing as freewheeling path.

The transistorized AC voltage controller may be controlled using different control strategies. In the present paper the firing angle control strategy is applied. The control of the generator terminal voltage is done by varying the firing angle (α), while the extinction angle (β) is kept at 180 degree as shown in Fig. (2).
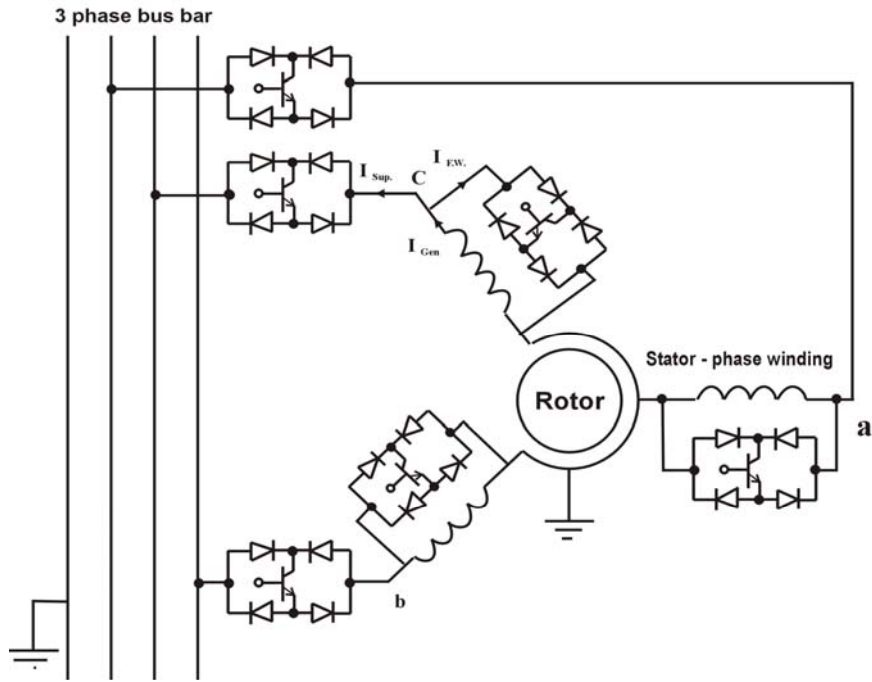
Fig. (1). Induction generator connected to grid via ac voltage controller.

he terminal voltages of the induction generator are as follows:

$$v_a = V_m \sin \omega t \qquad\qquad n\pi + \alpha \le \omega t \le (n+1)\pi \qquad\qquad (1)$$

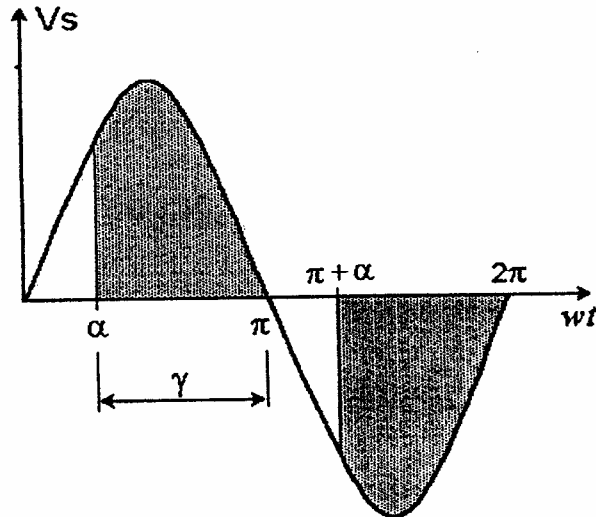v_b and v_c lag behind v_a by $2\pi/3$ and $4\pi/3$ respectively.

Fig. (2). Firing angle control strategy.

3. Steady State Modeling

Frequency Domain Equivalent Circuits

The stator terminal voltage of the induction Generator when using an ac voltage controller is no more pure sinusoidal voltage (Fig. 2). Using Fourier series [12] this voltage can be analyzed to a series of fundamental voltage and higher order voltage harmonics. Let, the bus voltage; v_{bb}, to be

$$v_{bb}(\theta) = V_m \sin \theta \quad ; \theta = \omega t \tag{2}$$

Then, the generator terminal voltage; v_g, is given by

$$v_g(\theta) = SF(\theta).v_{bb} \tag{3}$$

Where $SF(\theta)$ is a switching function that is fully determined according to the control technique such that, in the case of firing angle control technique

$$SF(\theta) = 1 \qquad\qquad n\pi + \alpha \leq \theta \leq (n+1)\pi; n = 0, 1, 2, .. \tag{4}$$

Otherwise it is zero.

To get the Fourier series of the generator voltage, $SF(\theta)$ is easily analyzed using Fourier series rules, to get

$$SF(\theta) = a_o + \sum_n c_n \sin(n\omega t + \varphi_n) \tag{5}$$

Where n is even number; n = 2, 4, 6, …

Then,

$$v_g(\theta) = V_m \sin\theta \ \{ a_o + \sum_n c_n \sin(n\omega t + \varphi_n) \} \tag{6}$$

which yields the following equation:

$$v_g(t) = \sum_h V_h \sin(h\omega t + \varphi_h) \tag{7}$$

Where h is odd numbers.

V_h and φ_h are given for the control techniques in Appendix A.

The generator applied voltage components, obtained by Fourier series, are classified as follows:

Positive sequence voltage components:

Components of order nf = 1 + 6k; where k = 0, 1, 2, 3,…., are called positive sequence voltages. These voltages generate rotating fluxes in the same direction of rotation of the flux produced by the fundamental voltage. The slip w.r.t the flux of any positive sequence voltage is obtained as follows:

$$S_P = \frac{nf \times N_s - N_r}{nf \times N_s} \tag{8}$$

Negative sequence voltage components:

Components of order nb = 5 + 6k; where k = 0, 1, 2,…., are called negative sequence voltages. These voltages generate rotating fluxes in the opposite direction of rotation of the flux produced by the fundamental voltage. The slip w.r.t the flux of any negative sequence voltage is obtained as follows:

$$S_N = \frac{nb \times N_s + N_r}{nb \times N_s} \tag{9}$$

Zero sequence voltage components:

Harmonics of order no = 3 + 6k; where k = 0, 1, 2, 3,…., are called zero sequence or triplex voltages. The net flux of these harmonic components in the air gap is zero. Therefore, they neither contribute to the torque output nor induce currents in the rotor.

The positive and negative sequence equivalent circuits of the slip ring and plain cage induction machines are as shown in Fig. 3(a). Fig. 3(b) shows the zero sequence equivalent circuit which applies for all induction machine types. The zero sequence voltage drives zero sequence currents if the induction generator circuit allows. This happens in case of delta connected generator or four wire system.

Generator Current, Power and Torque Calculations

For each voltage component (of order h) the appropriate equivalent circuit is used to calculate the corresponding stator, magnetizing and rotor currents. Also, the power factor is obtained. Then, the terminal active- and reactive- electrical power, rotor air gap power and the induced torque are calculated as follows:

$$P_{eh} = V_h I_h \cos(\varphi_h - \psi_{gh}) \quad \text{p.u} \tag{10}$$

$$Q_{eh} = V_h I_h \sin(\varphi_h - \psi_{gh}) \tag{11}$$

$$P_{gh} = I_h^2 R_2/S_h \quad \text{p.u} \tag{12}$$

$$T_{eh} = P_{gh}/h \qquad p.u \tag{13}$$

Where φ_h is the phase angle of the hth voltage component; V_h, ψ_h is the phase angle of the hth current component; I_h, and S_h is the slip w.r.t the flux of the hth voltage component.
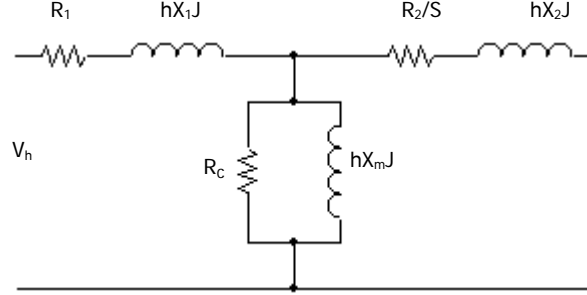
(a) Positive and negative sequence equivalent circuits
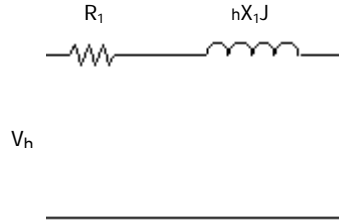
(b) The zero sequence equivalent circuit of the induction machine.

Fig. (3). The generator equivalent circuits.

(S = S_P in case of +ve sequence harmonics and S = S_N in case of -ve sequence harmonics).

$$THD = \frac{\sqrt{I^2 - I_1^2}}{I_1} \tag{14}$$

THD defines the total harmonic content [13], but it does not indicate the level of each harmonic component. If a filter is used at the output of the converters, the higher-order harmonics would be attenuated more effectively. Therefore, knowledge of both the frequency and the magnitude of each harmonic is important. The distortion factor indicates the amount of the harmonics distortion that remains in a particular waveform after the harmonics of that waveform have been subjected to a second order attenuation (i.e. divided by n^2). Thus, D.F [13] is a measure of effectiveness in reducing unwanted harmonics without having to specify the values of the second order load filter and is defined as [13]

$$D.F = \frac{1}{I_1}\left[\sum_{h=2,3}\left(\frac{I_h}{h^2}\right)^2\right]^{1/2} \tag{15}$$

$$D.F_h = \frac{I_h}{I_1 . h^2}$$

The total terminal active- and reactive- electrical power are calculated by

$$P_e = \sum_k P_{ek} \tag{16}$$

$$Q_e = \sum_k Q_{ek} \tag{17}$$

The total steady induced torque is calculated by

$$T_e = \sum_k T_{ek} \tag{18}$$

Interaction between the fluxes that rotate at different speeds results in pulsating torques. The steady and pulsating torque components are calculated in p.u using the following formula [14]:

$$T_{e1} = X_m \sum_{ks} \sum_{kr} (I_{s(ksf)} I_{r(krf)} \sin((ksf - krf)\omega_s t + \psi_{s(ksf)} - \psi_{r(krf)})$$

$$T_{e2} = X_m \sum_{ks} \sum_{kr} (I_{s(ksb)} I_{r(krb)} \sin((ksb - krb)\omega_s t + \psi_{s(ksb)} - \psi_{r(krb)})$$

$$T_{e3} = X_m \sum_{ks} \sum_{kr} (I_{s(ksb)} I_{r(krf)} \sin((ksb + krf)\omega_s t + \psi_{s(ksb)} + \psi_{r(krf)})$$

$$T_{e4} = X_m \sum_{ks} \sum_{kr} (I_{s(ksf)} I_{r(krb)} \sin((ksf + krb)\omega_s t + \psi_{s(ksf)} + \psi_{r(krb)})$$

$$T_e = T_{e1} - T_{e2} + T_{e3} - T_{e4} \tag{19}$$

Where ksf, krf are the stator and rotor harmonic orders which induce forward rotating magnetic fields and ksb, krb are the stator and rotor harmonic orders which induce backward rotating magnetic fields.

Bus Current and Power Calculations

As at any instant the instantaneous bus power equals the instantaneous generator power, then

$$p_g = p_b \tag{20}$$

which means

$$v_g \, i_g = v_{bb} \, i_{bb} \tag{21}$$

Using Eqns. 3 and 21, leads to

$$i_{bb} = i_g \, SF(\theta) \tag{22}$$

i_g has components calculated from the equivalent circuits corresponding to the voltage components and $SF(\theta)$ has its Fourier Series form. Thus i_{bb} could be expressed as a summation of current components as given in Appendix A.

The active- and reactive- electrical powers are calculated, keeping in mind that the bus voltage is pure sinusoidal, as follows:

$$P_e = V_b \, I_{bb1} \cos(-\psi_{bb1}) \tag{23}$$
$$Q_e = V_{bb} \, I_{bb1} \sin(-\psi_{bb1}) \tag{24}$$

The angle between the fundamental bus current; I_{bb1}, measured in the output sense and the bus voltage, called the displacement angle; Dangle, is calculated as follows:

$$DAngle = \psi_{bb1} + \pi, \tag{25}$$

The bus power factor is calculated from [13]

$$PF = PuF \cdot DF \tag{26}$$

Where PuF is the purity factor and is given by; $PuF = I_1/I$

The bus current total distortion factor and the individual distortion factors are calculated using the formula applied to the generator current (Eqns 14, 15).

4. Performance Characteristics of the Controlled Generator
Generator Performance Characteristics

A program based upon the steady state (frequency domain) equivalent circuits, with the terminal voltage represented as a series of fundamental voltage and higher harmonic voltages has been developed. The terminal voltage is determined using Fourier series analysis (Appendix A.1) which gives the voltage components as a function of the firing angle. The program has been used to compute the performance characteristics of the generator having the data given in Appendix B. Various performance characteristics of the generator such as the fundamental current, total current, various distortion factors, the active power, the reactive power and the efficiency of the generator have been computed versus the generator speed at different firing angles. These characteristics are depicted in Figs. (4-9). These figures indicate that at a certain speed the fundamental current decreases as the firing angle increases (Fig. 4). Also, as the firing angle increases the harmonic current contents increases. It should be mentioned here that only odd harmonic currents exist (Figs. 5-7). It is obvious from Fig. (8) that the active power decreases as the firing angle increases. The generator efficiency decreases as the firing angle increases due to the increase of the harmonic contents (Fig. 10).

Fig. (4). Generator fundamental current.
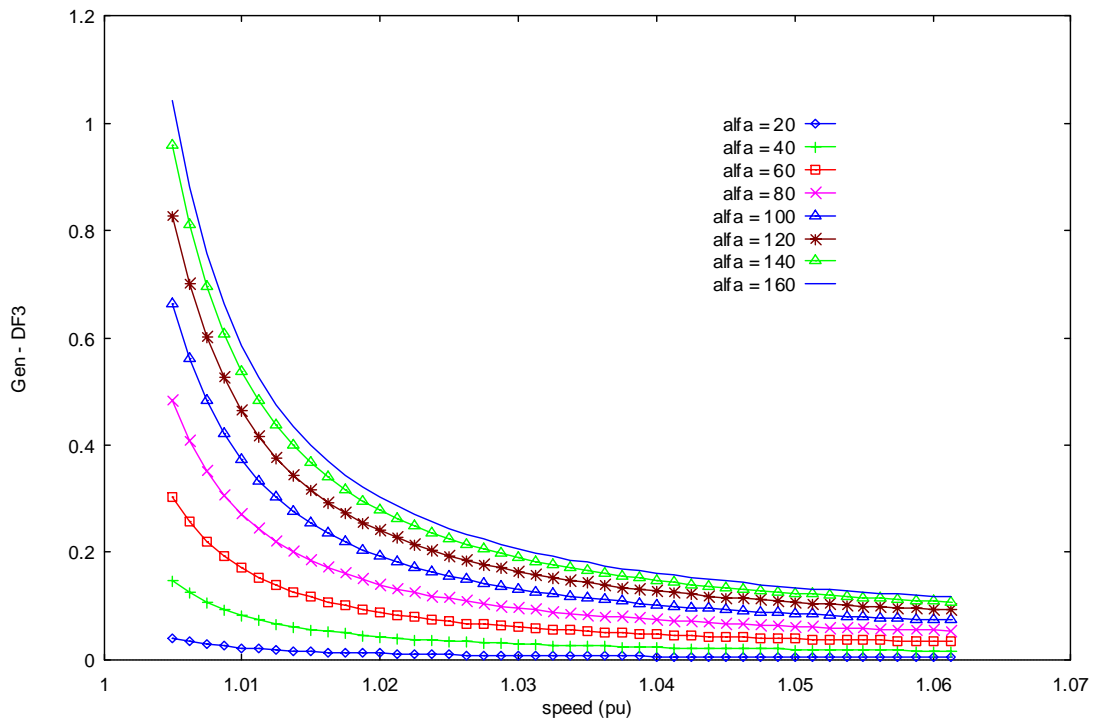
Fig. (5) Distortion factor of the third order generator harmonic current.
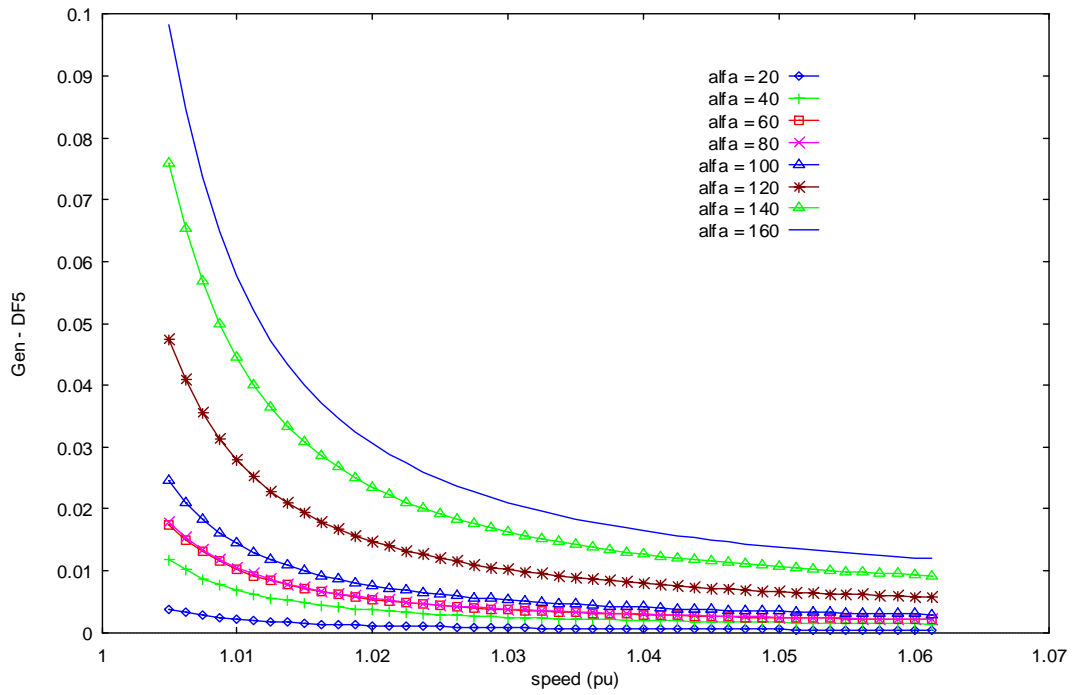
Fig. (6). Distortion factor of the 5th order generator harmonic current.
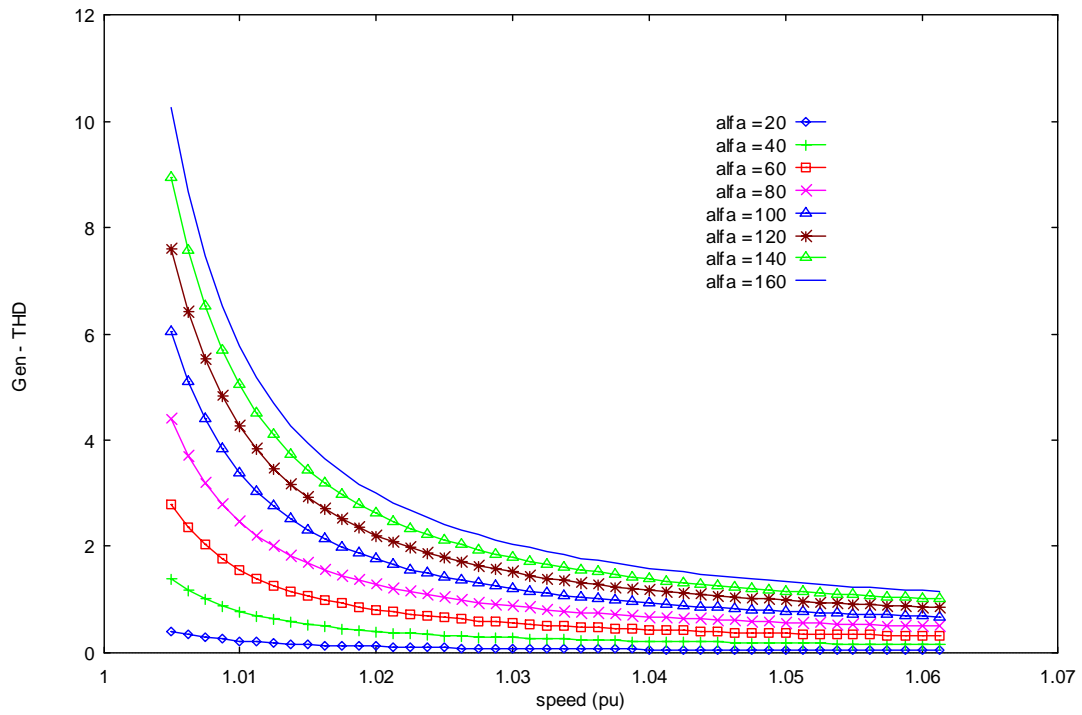
Fig. (7). Total harmonic distortion factor of the generator current.
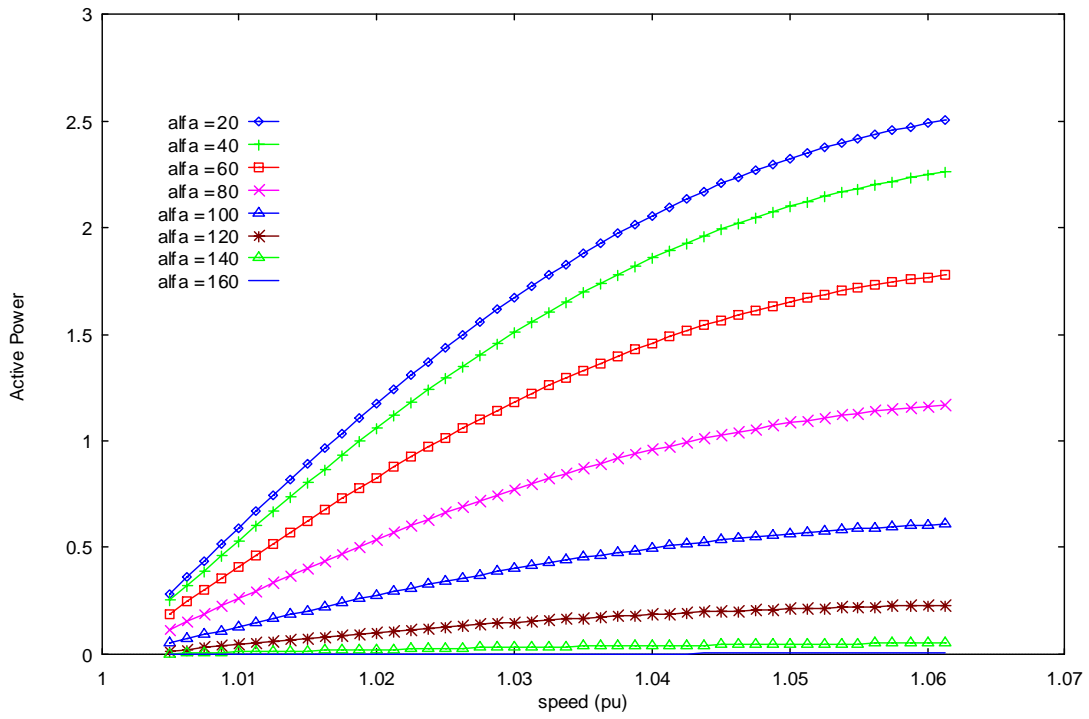
Fig. (8). Generator active power.
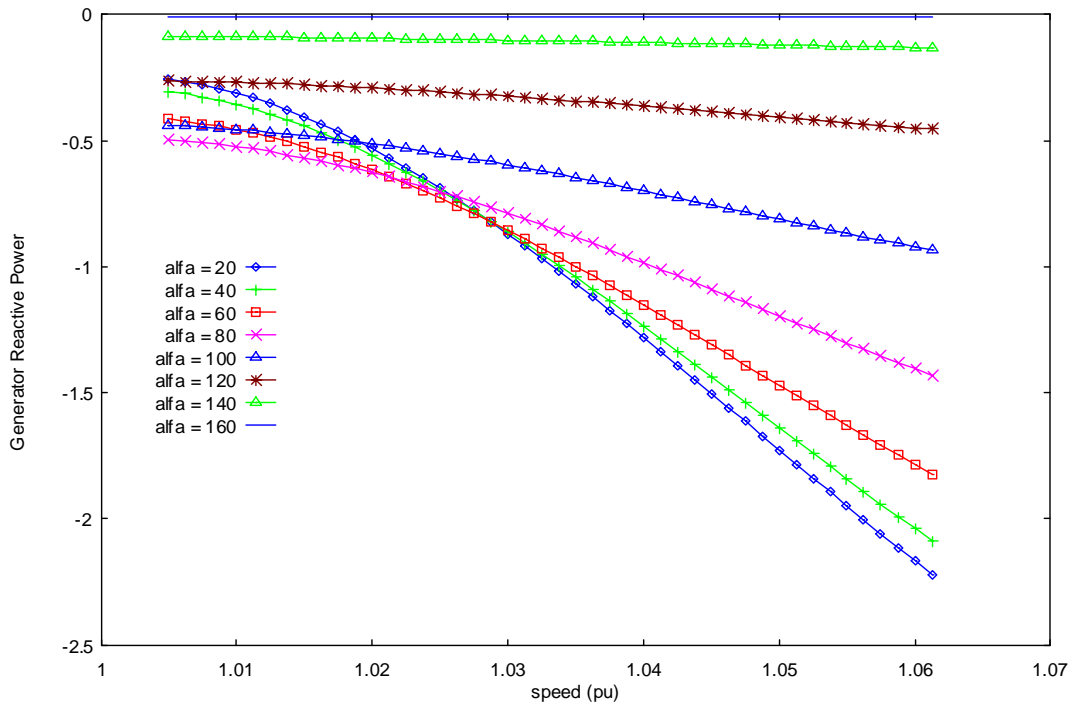
Fig. (9). Generator reactive power.
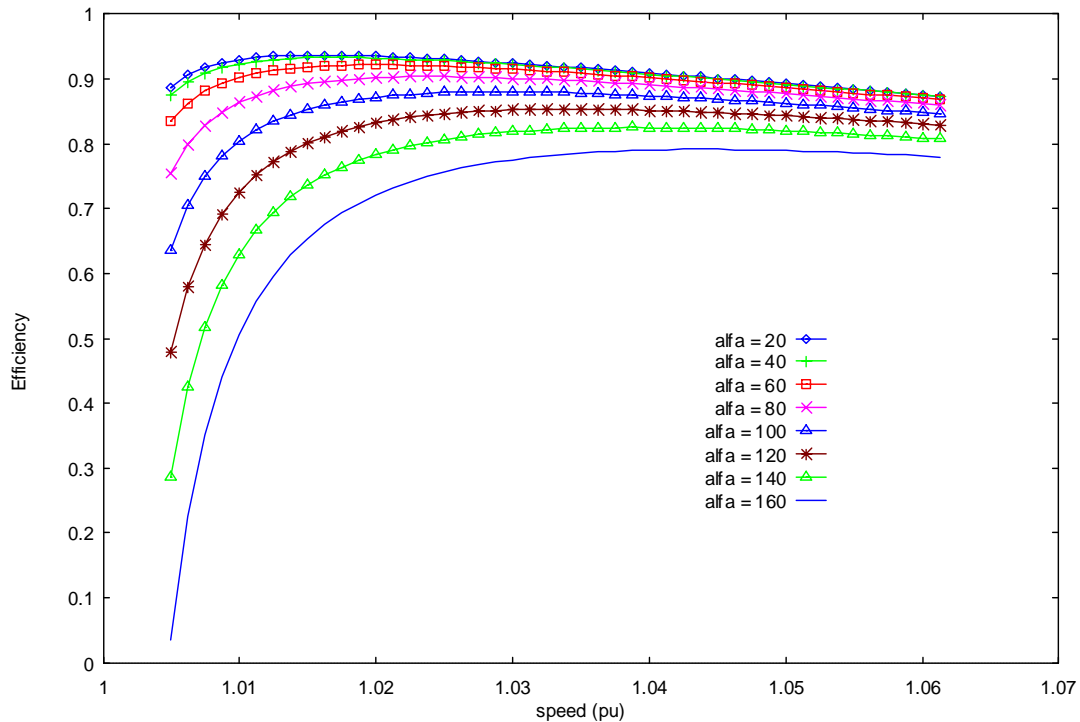
Fig. (10). Efficiency of the generator.

Impact upon the Supply

The effect of using the ac voltage controller when employing the firing angle-control strategy upon the supply (bus-bar) has been investigated. The concerned quantities include the bus fundamental current, different current distortion factors, the active- and reactive- power, the displacement angle and power factor. The computed results showing the effect of the firing angle are depicted in Figs 11-17. The bus fundamental current decreases as the firing angle increases. The bus current, like the generator current, contains odd harmonics. Each harmonic current component has maximum value at a speed which increases as the firing angle increases. The maximum value itself increases as the firing angle increases (Figs. 12-13). The total harmonics behave in the same way as the individual harmonic contents (Fig. 14). The firing angle control strategy drives the generator to work at lower leading power factors, and it may lead to generator operation at a lagging power factor (Fig. 15). In this case, the induction generator behaves unusually, and delivers reactive power to the bus (Fig. 16). The effect of the firing angle upon the power factor is depicted in Fig. 17. The increase of the firing angle improves the displacement factor. Nevertheless, the power factor decreases as a result of the increasing harmonic contents.
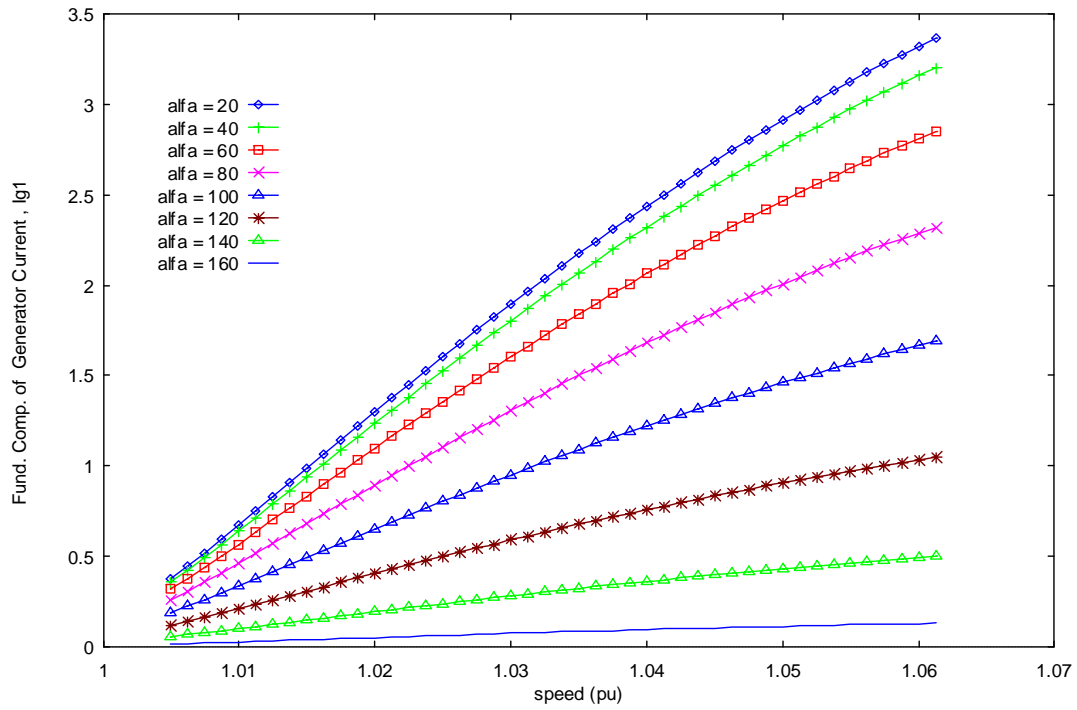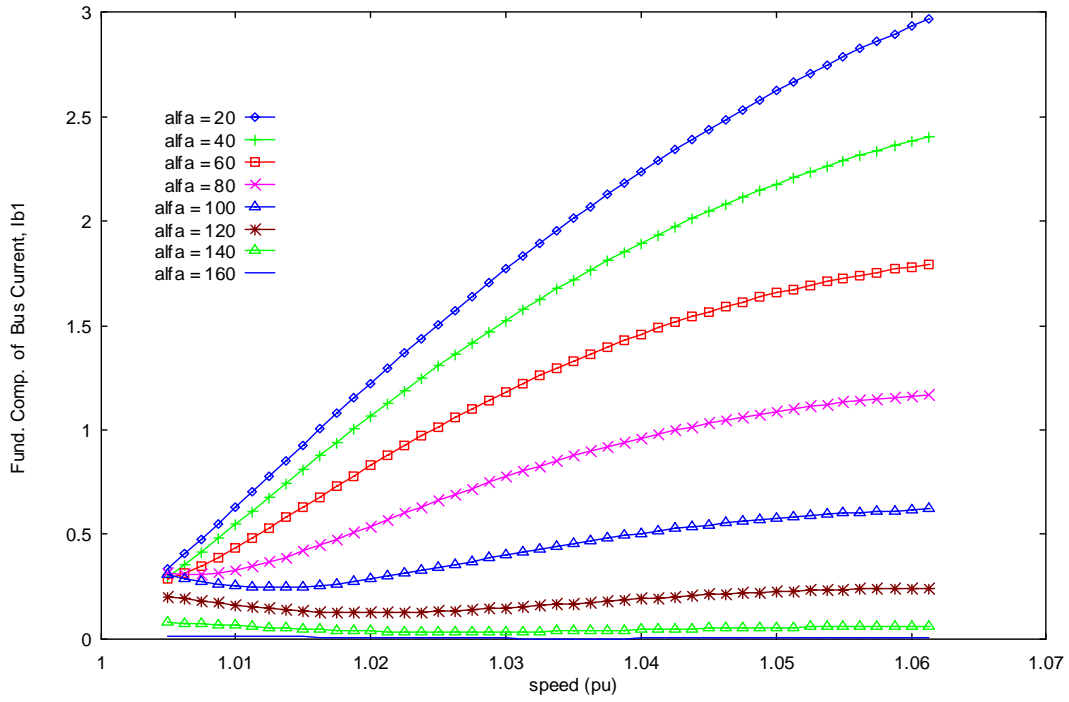
Fig. (11). Bus fundamental current.
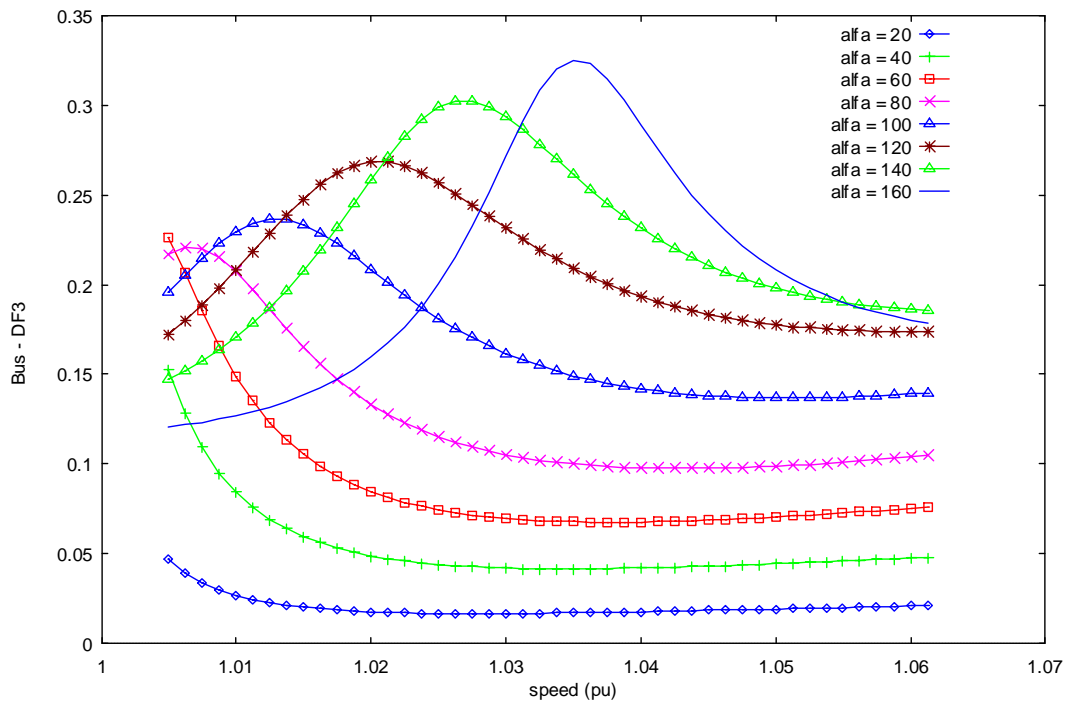
Fig. (12). Distortion factor of the third order bus harmonic current.
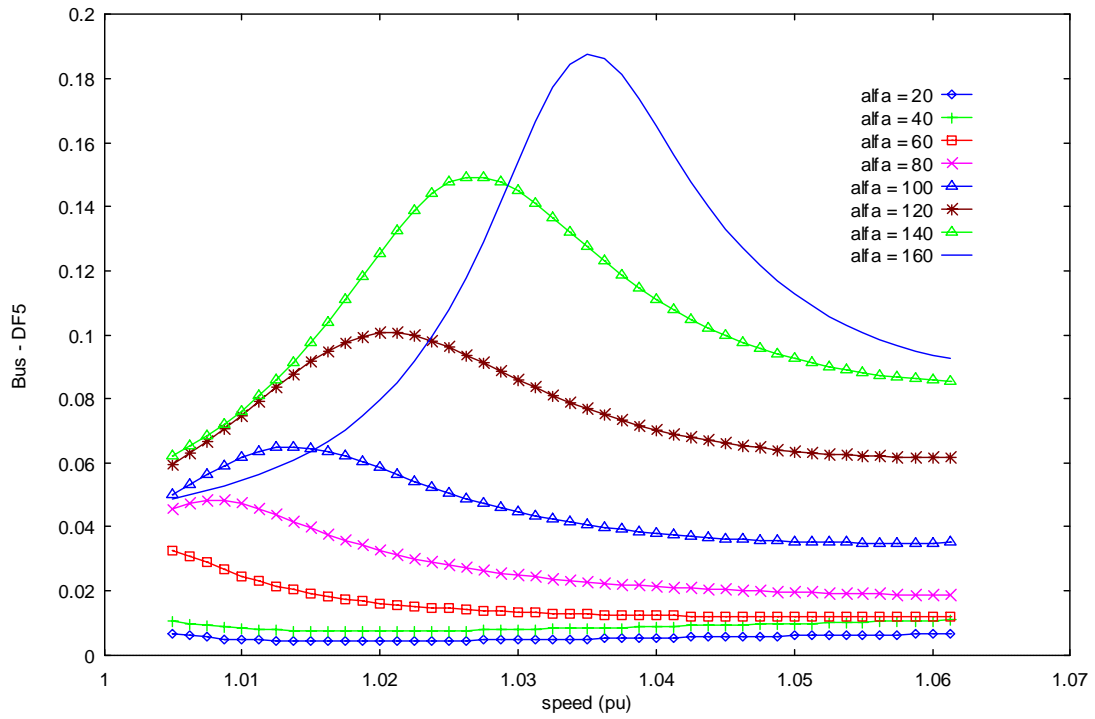
Fig. (13). Distortion factor of the 5th order harmonic bus current.
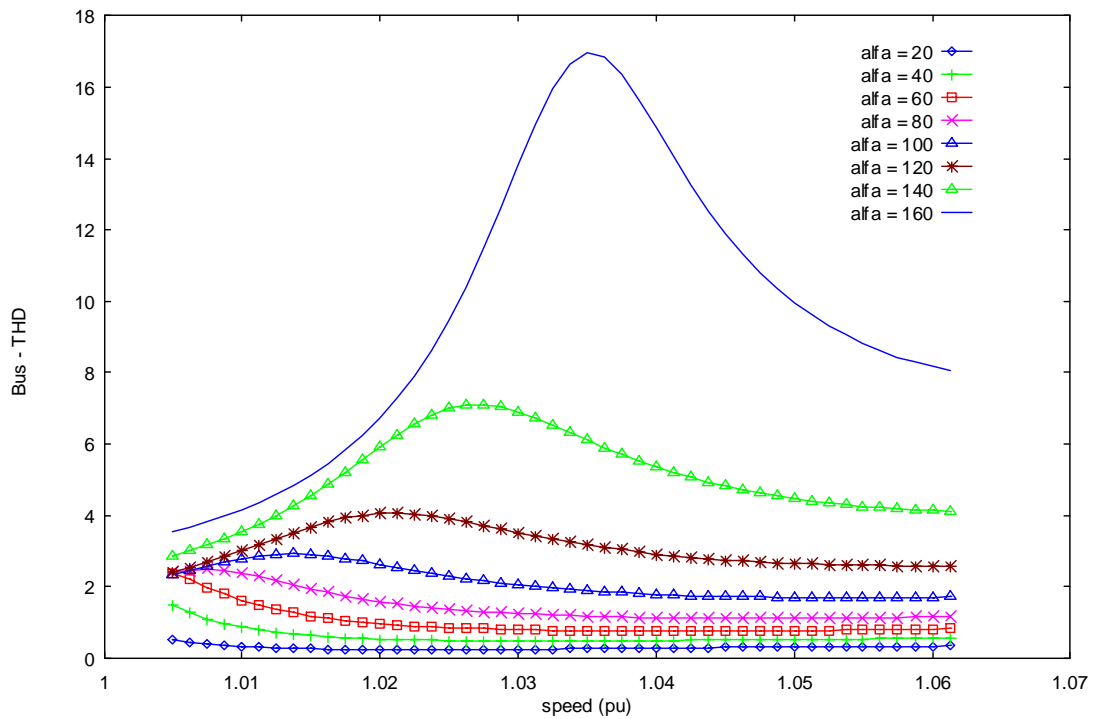
Fig. (14). Total harmonic distortion factor of the bus current.
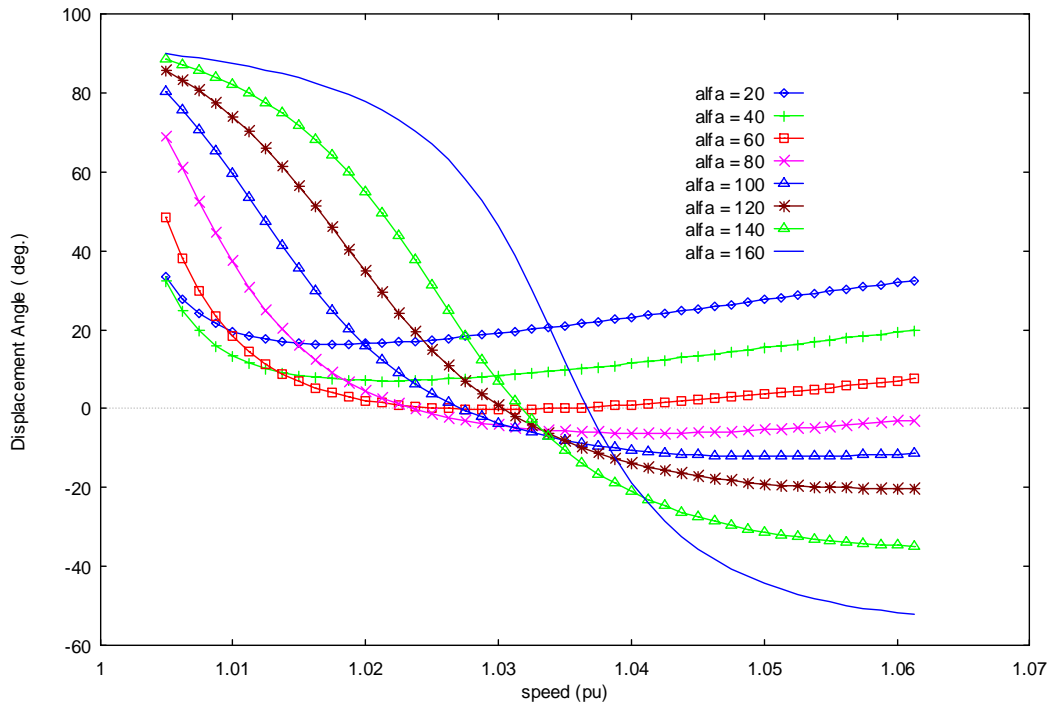
Fig. (15). Displacement angle of the bus current.
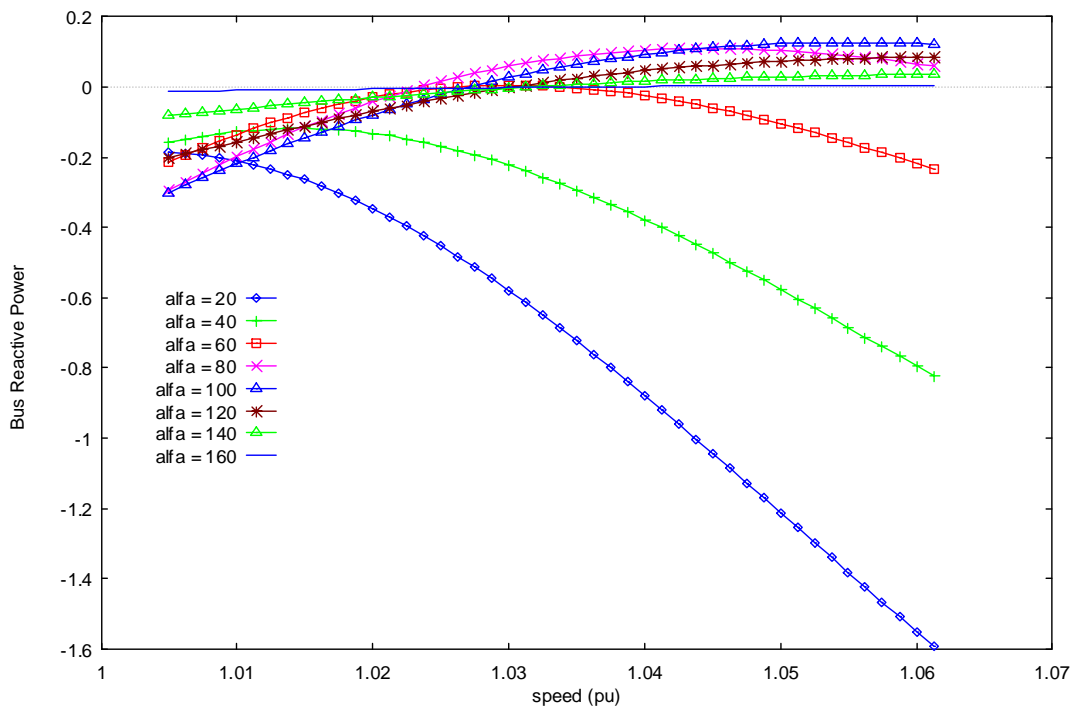
Fig. (16). Bus reactive power.
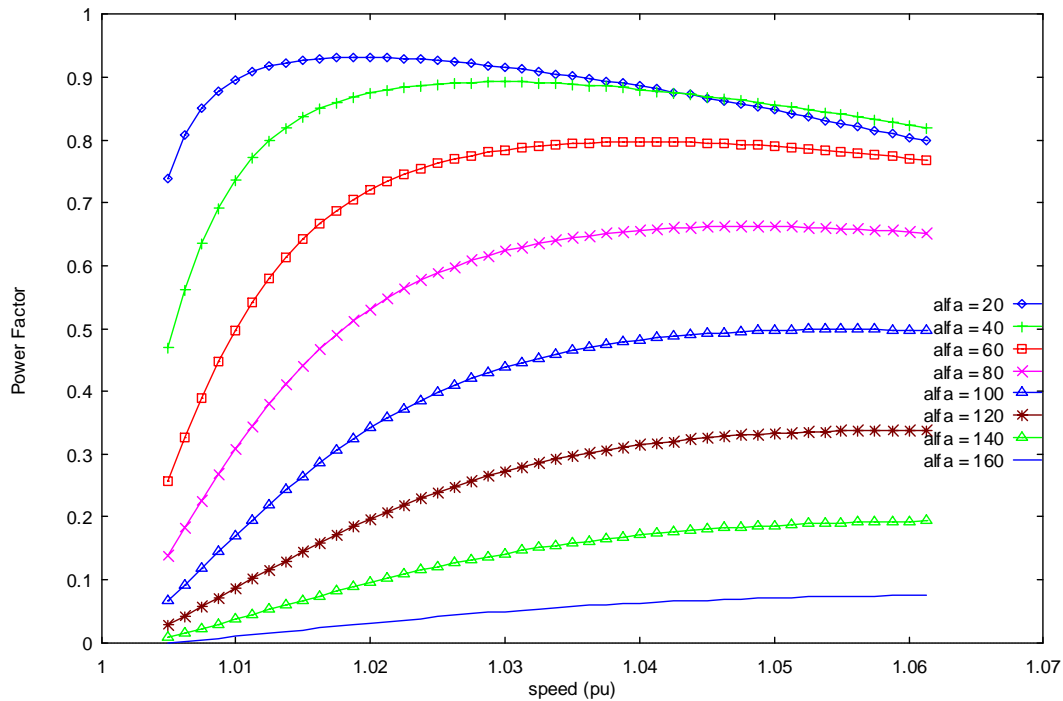
Fig. (17). Bus power factor.

Mechanical Performance Characteristics of the Controlled- Generator

The effect of using the ac voltage controller upon the induced torque as regarding the produced average torque and the added pulsating torques has been investigated. The computed results are shown in Figs. (18-21). The total average steady torque produced by all the voltage components is shown in Fig. (18) versus the generator speed at different firing angles. That produced by the fundamental voltage is shown in Fig. (19). The 6th order and 12th order pulsating torques are shown in Figs. (20 and 21) as a percentage of the total steady induced torque. As the firing angle increases the 6th order pulsating torque (computed as a ratio of the steady torque) has the tendency to increase but with a fluctuating manner. The 12th order pulsating torque (computed as a ratio of the steady torque) increases as the firing angle increases.
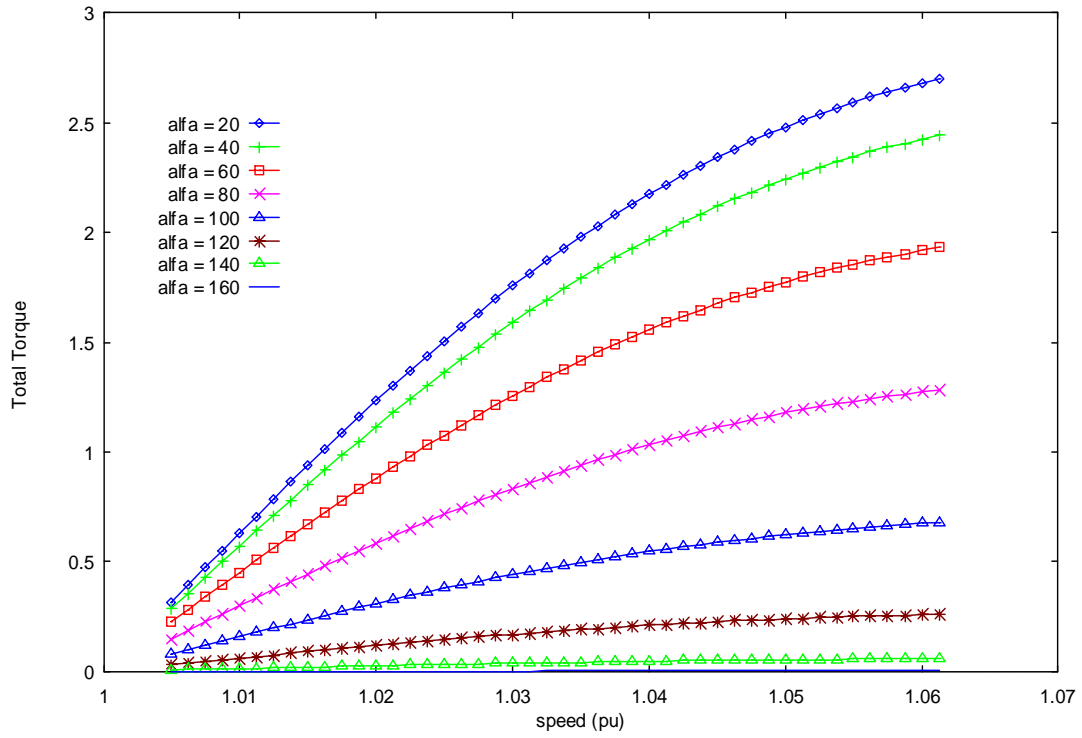
Fig. (18). Total average induced torque.
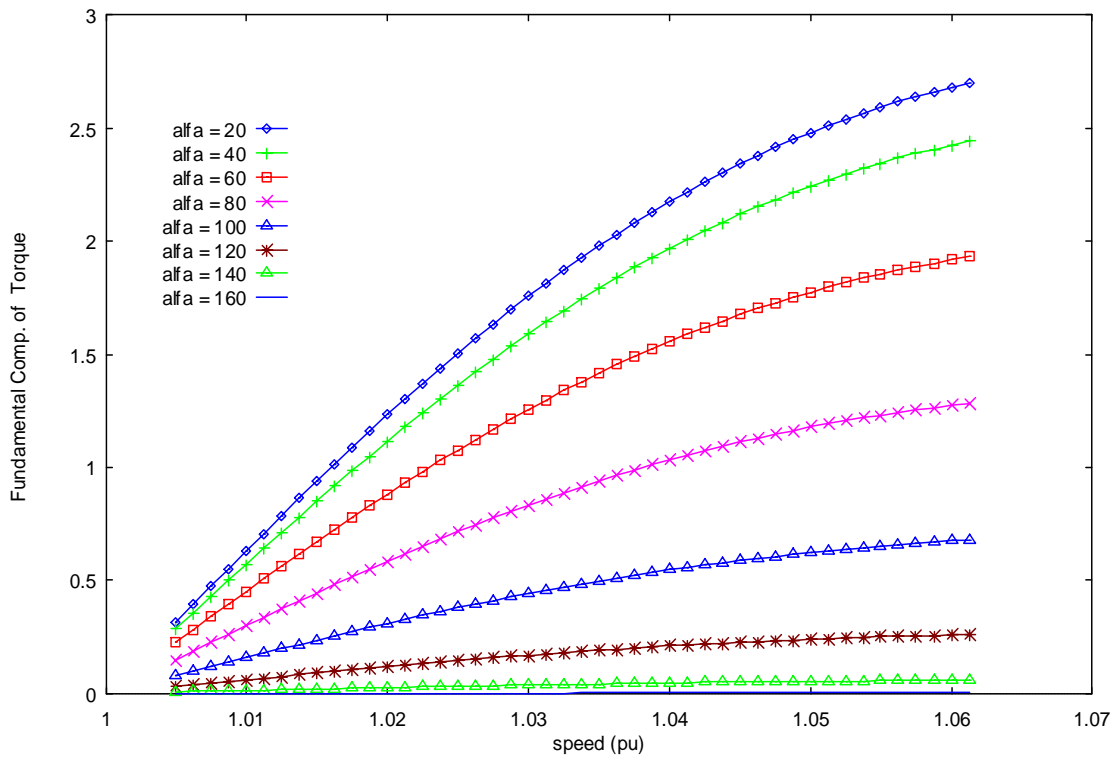
Fig. (19). Average torque induced by the fundamental voltage.
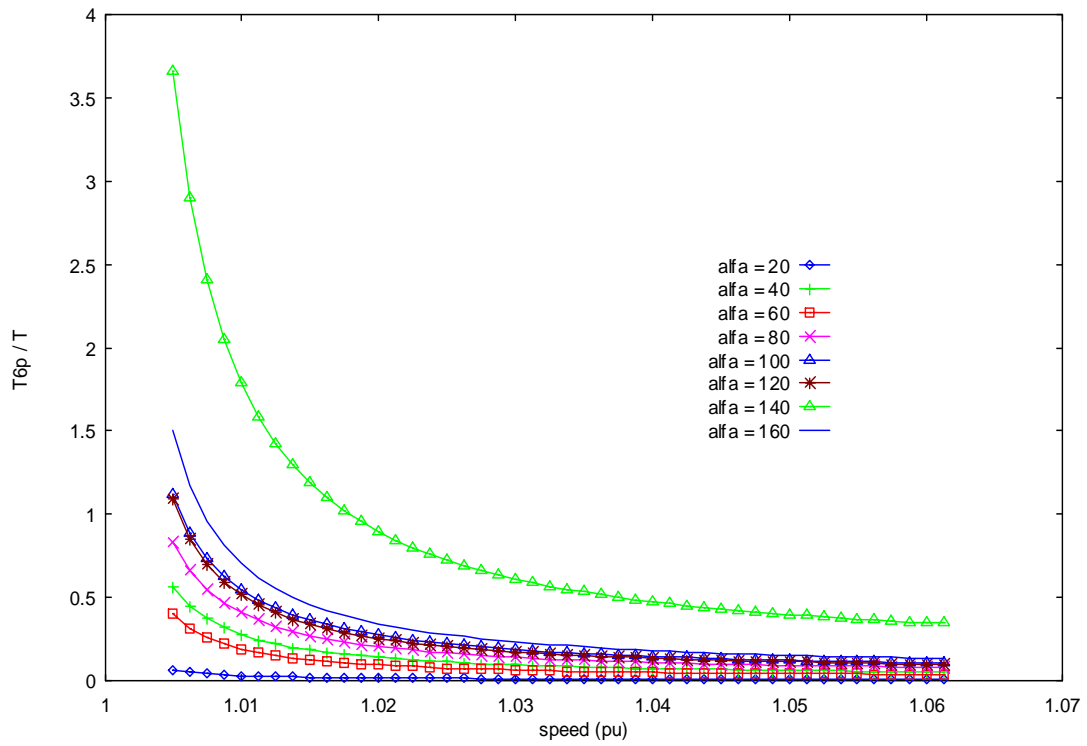
Fig. (20). The 6th order pulsating torque.
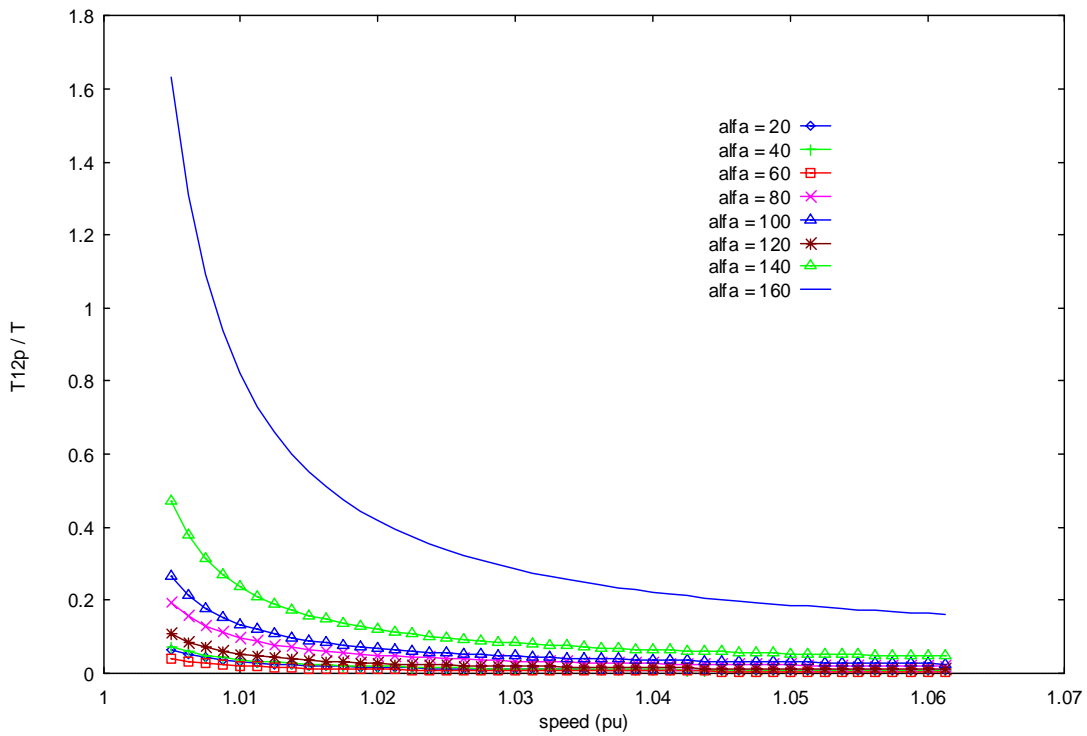
Fig. (21). The 12th order pulsating torque.

5. Conclusions

The performance of a grid-connected induction generator using a solid state ac voltage controller as an interface between the grid and the stator terminals of the generator has been studied. In this respect forced-commutated ac voltage controller which utilizes a set of power transistor devices has been used.

The steady-state electrical and mechanical performance has been analyzed through modeling the induction generator and the static converter by novel equivalent circuits in the frequency domain. The presented model is more accurate compared with the time domain models, which usually neglect the iron losses. The computed performance characteristics included the generator current and its distortion factors, the generator active and reactive powers and the generator efficiency. Also, the bus current, its distortion factors, reflected harmonics on the supply, the displacement angle, the bus active and reactive powers, and the power factor has been computed. On the other side the mechanical performance characteristics regarding the developed torque and the pulsating components appearing as a result of the use of the ac voltage controller have been determined.

When using the ac voltage controllers, the active and reactive powers of the grid connected induction generator can be controlled. The bus reactive power is clearly controlled when using the firing angle control strategy to the extent that it becomes positive over certain ranges of firing angle. This means that the output current lags the voltage. Consequently, the reactive power will be delivered to the network by the induction generator.

Using the solid state electronic switches is associated with the existence of current harmonic contents in the generator and harmonic currents reflected on the supply. Only the odd harmonics especially the third harmonics exist extensively. The existence of harmonic contents increases the generator losses, and leads to the existence of two operation regions; practical and impractical. The impractical operating region is the region where the internal generated power is not even enough to cover the stator losses.

6. References

[1] Fernando D. Bianchi, Herna'n De Battista and Ricardo J. Mantz, "*Wind Turbine Control Systems- Principles, Modelling and Gain Scheduling Design*," Springer, London, 2007.

[2] Singh, B., "Induction generators- A prospective", *Electric Machines and Power Systems*, Vol.23 (1993), 163-177.

[3] Raina, G., and Malik, O. P., "Wind Energy Conversion using a Self-Excited Induction Generator", *IEEE Transactions on Power Apparatus and Systems*, Vol. PAS-102, No. 12 (December 1983), 3933-3936.

[4] Shaltout, A.A., and Abdel-halim, M.A. ,"Solid State Control of a Wind Driven Self-Excited Induction Generator", *Electric Machines and Power Systems*, Vol. 23 (1995), 571-582.

[5] Shaltout, A. A., and El-Ramahi , A.F. ,"Maximum power tracking for a wind driven induction generator connected to a utility network", *Applied Energy*, Vol.52 (1995), 243-253.

[6] Singh, B., Shridhar, L., and Jha, C.S., "Improvements in the Performance of Self-Excited Induction Generator through Series Compensation", *IEE Proceedings Generation, Transmission and Distribution*, Vol. 146, No. 6 (November 1999), 602-608.

[7] Shaltout, A., Abdel-Halim, M., and Al-Ramahi, A., "Optimised Solid-State Exciter for Wind Powered Pumping Applications", *Proceedings of the Fourth Arab International Solar Energy Conference*, Amman, Jordan, 20-25 November 1993, 233-242.

[8] Brennen, M. B., and Abbondanti, A., "Static Exciters for Induction Generator", *IEEE Transactions on Industry Applications*, Vol. IA-13, No. 5 (September/October 1976), 422-428.

[9] Abdel-halim, M.A., "Solid State Control of a Grid Connected Induction Generator", *Electric Power Components and Systems*, Vol. 29 (2001), 163-178.

[10] Almarshoud, A. F., Abdel-halim, M. A., Alolah, A. I., "Performance of Grid Connected Induction Generator under Naturally Commutated AC Voltage Controller", *Electric Power Components and Systems*, Vol. 32 (2004), 691-700.

[11] Abdel-halim, M.A, Abdel-aziz, M. M. and Mostafa, H. G., "AC chopper controlled grid-connected induction generator", *Qassim University Scientific Journal- Engineering and Computer Sciences*, Vol.1, No. 1 (2008), 1- 19.

[12] Ralaston, A., "*A First Course in Numerical Analysis*", New York, USA, McGraw-Hill, 1995.

[13] Rashid, M. H., "*Power Electronics: Circuits, Devices, and Applications*", Second Edition, Prentice-hall, USA, 1993.

[14] Abdulrahman S. M., Kettleborough, J. G. and Smith, I. R., "Fast Calculation of Harmonic Torque Pulsations in a VSI/Induction Motor Drive", *IEEE Trans. On Industrial Electronics*, Vol.40, No.6 (Dec. 1993), 561-569.

Appendix A: Fourier Series of the Generator Voltage and Bus Current

A.1- Generator Voltage

$v_g = V_m \sin(\theta) . F(\theta)$

where $F(\theta)$ is the switching function which is determined according to the control strategy as follows:

$SF(\theta) = 1 \qquad\qquad n\pi + \alpha \le \theta \le (n+1)\pi; \ n = 0, 1, 2, ..$

Otherwise it is zero.

Using Fourier series analysis of the switching function, the generator voltage can be expressed as follows:

$v_g = 0.5 V_m [(a_0-a_2) \sin(\theta) + (a_2-a_4) \sin(3\theta) + (a_4-a_6) \sin(5\theta) + (a_6-a_8) \sin(7\theta) + \ldots\ldots.$
$\qquad\qquad + b_2 \cos(\theta) + (b_4-b_2) \cos(3\theta) + (b_6-b_4) \cos(5\theta) + (b_8-b_6) \cos(7\theta) + \ldots\ldots]$

Thus, the fundamental component; $v_{g1} = 0.5 V_m (a_0-a_2) \sin(\theta) + 0.5 V_m (b_2) \cos(\theta)$,

3rd harmonic component; $v_{g3} = 0.5 V_m (a_2- a_4) \sin(3\theta) + 0.5 V_m (b_4-b_2) \cos(3\theta)$,

5th harmonic component; $v_{g5} = 0.5 V_m (a_4- a_6) \sin(5\theta) + 0.5 V_m (b_6-b_4) \cos(5\theta)$,

and so on.

a_0, a_n and b_n are given, for the three control strategies, as follows:

$a_0 = 2(\pi-\alpha)/\pi$

$a_n = [(-2/\{(2n-1)\pi\}] \times \sin(2n-1)\alpha , \quad n =1,2,3,\ldots.$

$b_n = \cos(2n\alpha-1)/n\pi , \qquad\qquad n =1,2,3,\ldots$

A.2- Bus Current

$i_{bb} = i_g SF(\theta)$

The fundamental bus current is given by

$i_{bb1} = \{0.5 \ I_{g1} ((a_0-a_2) \cos(\psi_{g1})+b_2 \sin(\psi_{g1})) + 0.5 \ I_{g3} ((a_2-a_4) \cos(\psi_{g3}) + (b_4-b_2) \ \sin(\psi_{g3})) + 0.5 \ I_{g5}$ $((a_4-a_6) \cos(\psi_{g5})+(b_6-b_4) \sin(\psi_{g5})) + \ 0.5 \ I_{g7} ((a_6-a_8) \cos(\psi_{g7}) + (b_8-b_6) \sin(\psi_{g7}) + \ldots.\}\times\sin(\theta) + \{0.5 \ I_{g1}$ $(b_2 \cos(\psi_{g1}) + (a_0+a_2) \sin(\psi_{g1})) + 0.5 I_{g3} ((b_4+b_2) \cos(\psi_{g3}) + (a_2+a_4) \sin(\psi_{g3})) + 0.5 \ I_{g5} ((b_6+b_4) \cos(\psi_{g5}) +$ $(a_4+a_6) \sin(\psi_{g5}) + 0.5 \ I_{g7} ((b_8+b_6) \cos(\psi_{g7}) + (a_6+a_8) \sin(\psi_{g7}) + \ldots.\}\times\cos(\theta)$

3rd harmonic bus current is given by

$i_{bb3} = \{0.5 \ I_{g1} ((a_2-a_4) \cos(\psi_{g1}) + (b_4+b_2) \sin(\psi_{g1})) + 0.5 \ I_{g3} ((a_0-a_6) \cos(\psi_{g3}) + b_6 \sin(\psi_{g3})) + \ 0.5 \ I_{g5}$ $((a_2-a_8) \cos(\psi_{g5}) + (b_8-b_2) \sin(\psi_{g5})) \ +\ldots.\}\times\sin(3\theta) \ + \ 0.5 \ I_{g7} ((a_4-a_{10}) \cos(\psi_{g7}) + (b_{10}-b_4) \sin(\psi_{g7})) +$ $\{0.5 \ I_{g1} ((b_4-b_2) \cos(\psi_{g1}) + (a_2+a_4) \sin(\psi_{g1})) + 0.5 \ I_{g3} (b_6 \cos(\psi_{g3}) + (a_0+a_6) \sin(\psi_{g3})) + 0.5 \ I_{g5} ((b_8+b_2)$ $\cos(\psi_{g5}) + (a_2+a_8) \sin(\psi_{g5}) + 0.5 \ I_{g7} ((b_{10}+b_4) \cos(\psi_{g7}) + (a_4+a_{10}) \sin(\psi_{g7}) + \ldots.\}\times\cos(3\theta)$

5th harmonic bus current is given by

$i_{bb5} = \{0.5 \ I_{g1} ((a_4-a_6) \cos(\psi_{g1})+(b_6+b_4) \sin(\psi_{g1})) + 0.5 \ I_{g3} ((a_2-a_8) \cos(\psi_{g3}) + (b_9+b_2) \sin(\psi_{g3})) + 0.5$ $I_{g5} ((a_0-a_{10}) \cos(\psi_{g5})+b_{10} \sin(\psi_{g5})) + \ldots.\}\times\sin(5\theta) \ + \ 0.5 \ I_{g7} ((a_2-a_{12}) \cos(\psi_{g7}) + (b_{12}-b_2) \sin(\psi_{g7})) + \{0.5$ $I_{g1} ((b_6-b_4) \cos(\psi_{g1}) + (a_4+a_6) \sin(\psi_{g1})) + 0.5 \ I_{g3} ((b_8-b_2) \cos(\psi_{g3}) + (a_2+a_8) \sin(\psi_{g3})) + 0.5 \ I_{g5} (b_{10} \cos(\psi_{g5}) + (a_0+a_{10}) \sin(\psi_{g5})) + 0.5 \ I_{g7} ((b_{12}+b_2) \cos(\psi_{g7}) + (a_2+a_{12}) \sin(\psi_{g7}) + \ldots.\}\times\cos(5\theta)$

where $I_{g1} , I_{g3} , I_{g5} \ I_{g7} \ldots\ldots$ are the generator harmonic currents.

a_0, a_n and b_n are as given before.

Appendix B: Generator Particulars and Parameters

Three phase generator, . connected, 600 V, 475 A, 50 Hz, having the following parameters:

$R_1 = R_2 = 0.015$ pu, $X_1 = X_2 = 0.091$ pu, $X_m = 4.251$ pu

***   **   *

*amarshoud@yahoo.com   ** masamie@qec.edu.sa   *** munawwarshees@qec.edu.sa

(/   /   /   /   )

.

.

.

.

Solar Heat Gain through Conical Skylight

M. A. Kassem
Mechanical Power Engineering Department, Faculty of Engineering,
Cairo University, Cairo, Egypt
mahmoudkassem@yahoo.com

Abstract. The calculation of the instantaneous rate of heat gain through a conical skylight requires extensive computational work. The problem is much more tedious when the computations are repetitively executed to evaluate the daily, seasonally or annual solar heat gain. The main objective of the present work is to systemize the procedure of calculating the solar heat gain through the conical skylight. The principles are presented, then a computer program is prepared to calculate the solar heat gain on instantaneous, daily, seasonally and annual bases. The program can be used for any location and any latitude and for any atmospheric clearness; moreover, it can deal with any type of glazing and any conical shape. Results are presented in a useful tabulation form, which can be readily implemented to calculate the solar heat gain in one step. The results are presented in a general way that can be applied to any conical skylight of any size. The effect of truncating a conical cap is investigated with different degrees of truncation. The results show that the conical skylights with conical ratio grater than four can be treated as a horizontal flat plate skylight.
Keywords: Solar, Heat gain, Skylight

List of Symbols

A, B and C	ASHARA constants	
Cn	Atmosphere clearance number	
d	Declination angle (3)	Degree
dN	Day number start from January 1st	
H	Complete cone height	m
h0	Outside heat transfer coefficient	W/m^2 ^{0}C
hi	Inside heat transfer coefficient	W/m^2 ^{0}C
Ht	Height of removed cone	M
I	Solar global insolation	W/m^2
Ib	Solar beam insolation	W/m^2
Id	Solar diffuse insolation	W/m^2
IN	Solar normal insolation	W/m^2
Ir	Solar reflected insolation	W/m^2
k	Glass extinction coefficient	mm^{-1}
L	Latitude	Degree
n	Glass refraction coefficient	
Q	Average daily solar heat gain	W h/m^2
ql	Instantaneous solar heat gain per unit area of element	W/ m 2
R	Cone base radius	m
Ru	Removed cone base radius	m
Rc	Conical ratio = R/H	
Rt	Truncation ratio = Ht / H	
T	Time	Hr
t	Glass thickness	Mm
T1	Sun rise time	
T2	Sun set time	
γ	Solar azimuth angle	Degree
αγ	Glass absorptivity	
β	Solar altitude angle	Degree
δ	Solar-element azimuth angle	Degree
φ	Element inclination	Degree
α	Surface azimuth angle	Degree
θ	Solar incidence angle	Degree
ρΓ	Ground reflectivity	
τγ	Glass transmissivity	

1. Introduction

The solar heat gain through glazing is one of the major factors constituting the indoor thermal environment. Whenever space heating is required; solar heat gain is welcomed, but in many instances it entails a load which has to be removed by the cooling system.

Skylights were originally intended to provide sunlight for interior building spaces. Form aesthetic or structural point of view; non planer skylight may be used. It is not infrequent to encounter conical skylight, especially in public buildings. The main target of the present work is to establish a method for quantifying the solar heat gain through conical skylights.

Information about the solar heat gain are available for horizontal, vertical [1-3], hemispherical [4] and cylindrical [5] glazing. Conical glazing shape characteristics are different from that of planer, cylindrical or hemispherical glazing. Conical glazing has three-dimensional, single-curved shape, while

planer glazing has one-dimensional zero-curved shape, cylindrical glazing has two-dimensional single curved shape, and hemispherical glazing has three-dimensional, two-curved shape. So the results tabulated for planer, cylindrical or hemispherical glazing can not be used accurately to evaluate solar heat gain through conical skylights.

In the present work, a computational procedure is established and a computer program is coded to calculate the solar heat gain through a conical skylight. The study covers the cases of complete conical skylight as well as that of truncated, incomplete one, both cases are shown in Fig. 1. The extent of truncation is defined by the (truncation ratio, R_t) which is the ratio between the height of the removed cone (H_t) to the height of complete one (H). The truncated skylight, having $0 < R_t < 1$, represents the general case; with the two special cases of complete conical and circular horizontal skylight falling at the two extremities $R_t = 0$ and $R_t = 1$, respectively. The present study deals with the side surface only of the cone, because of the upper surface is a horizontal plate which if it is glass its data is listed [1&2]. The current work; also, deals with conical skylights with different conical ratios (R $_c$) which is the cone radius (R) to height (H) ratio.

The results are submitted in convenient table and graph forms to be easily utilized by the user. The resulted average specific values have only to be multiplied by the skylight side area to yield the solar heat gain, either as instantaneous rate or as daily or seasonal integrated values.

2. Computation Basis and Procedure

In the present model, the cone is conceivably divided into a large number of identical narrow elements. Each element is consider being flat and has its own surface- azimuth angle ( ), on the other hand all elements have the same inclination angle ( ) as shown in Fig. 1. The local solar heat gain will be individually calculated for each element. Consequently, the total solar heat gain to the conical space will then be evaluated by summation the local values around the perimeter.
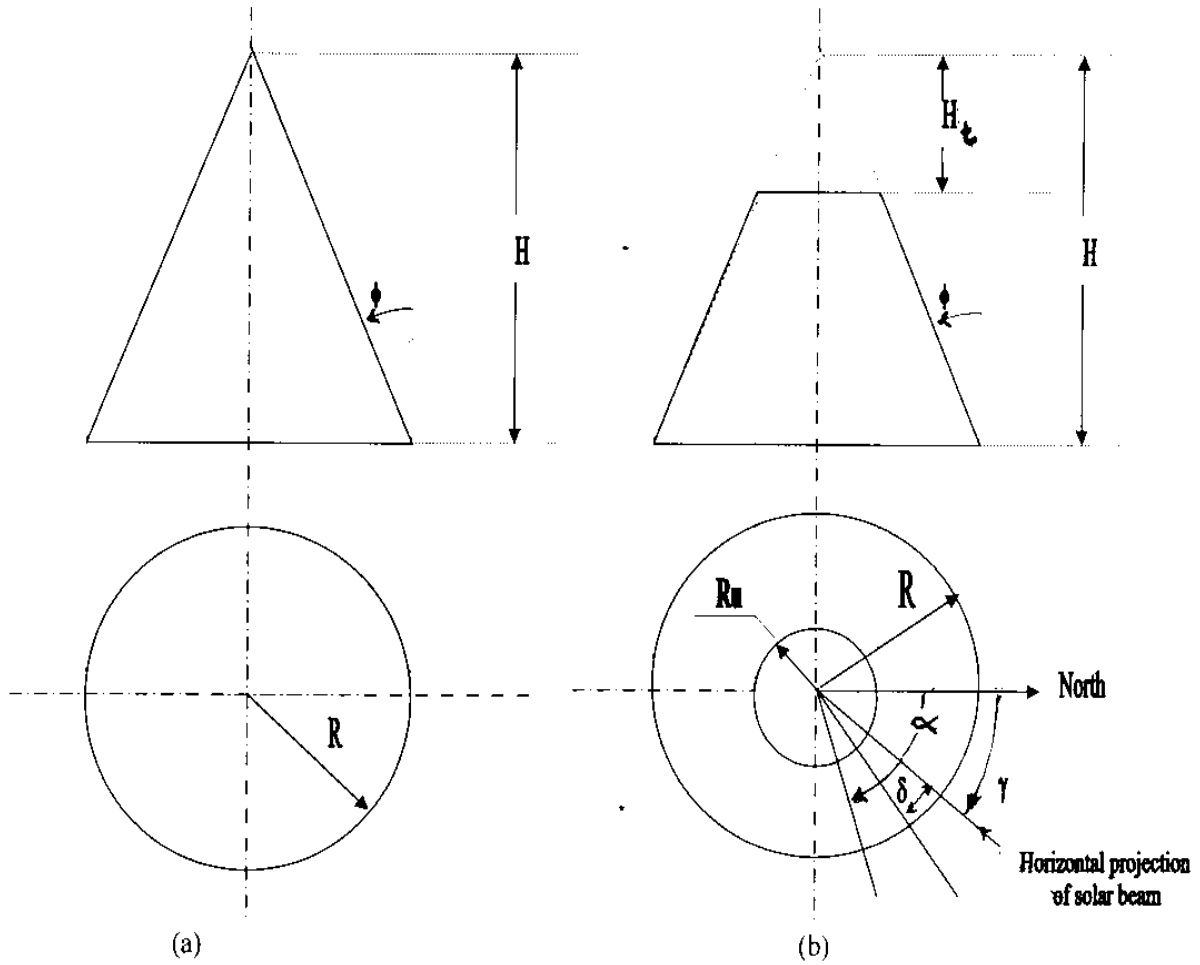
Fig. (1). Conical sky light and solar angels.
a) Complete conical skylight   a) Truncated conical skyligt

Solar angles

The solar altitude (β) and azimuth (γ) angels are defined as follows [6]:

$$\beta = \sin^{-1} (\cos L \cos h \cos d + \sin L \sin d) \tag{1}$$

$$\gamma = \cos^{-1} ((\cos L \sin d - \cos d \sin L \cos h)/ \cos \beta) \tag{2}$$

where the sun declination angle (d) is defined as [6] :

$$d = 23.45 \sin B_1 \tag{3}$$

$$B_1 = B_0 +0.4087 \sin B_0 + 1.8722 \cos B_0 - 0.0182 \sin (2 B_0)$$
$$+ 0.00831 \cos (2 B_0) \tag{4}$$

and

$$B_0 = 360 (dN +284) / 365.24 \tag{5}$$

dN is the day number measured from first of January

At any time, the direct solar radiation incidence angle θ is constant for a particular element, and is given by [6]

$$\theta = \cos^{-1} (\cos \beta \cos \delta \cos \phi + \sin \beta \sin \phi) \tag{6}$$

; where $\delta = |\gamma - \alpha|$

Instantaneous Insulation on an Element

Any element will be exposed to direct solar radiation at the times when   . is less than 90 [0]. On the other

hand, the element will receive diffuse and reflected radiations, if any, throughout the sunlight hours. In this research, the reflection of global radiation on ground is taken into account. The ground is considered as a diffuse reflector. The ground reflectivity (ρ_G) is set to the widely accepted value of 0.2 [1].

There are different models to calculate the intensity of solar radiation components (7 and 8). The ASHARE model [1-6] is used; and results presented hereinafter is based on an atmospheric clearness number (C_n) of unity.

The instantaneous beam (I_b), diffuse (I_d) and reflected (I_r) solar radiations falling on a surface of any general orientation, are given by [1-6]

$$I_b = I_N \cos \theta \ \text{ for } \ \theta < 90^0 \tag{7}$$

$$I_b = 0 \ \text{ for } \ \theta > 90^0 \tag{8}$$

$$I_d = \frac{CI_N(1+\sin\phi)}{2} \tag{9}$$

$$I_r = \frac{\rho_G I_N(\sin\beta + C)(1-\sin\phi)}{2} \tag{10}$$

Where the direct normal radiation intensity I_N is given by

$$I_N = C_n A e^{\frac{-B}{\sin\beta}} \tag{11}$$

and the coefficients A, B and C are tabulated for different months [1]

Since all elements under consideration has the same inclination angle (ϕ) given as

$$\phi = \tan^{-1} R_c \tag{12}$$

Then equations 9 and 10 reduce to

$$I_d = \frac{CI_N}{2}\left(1 + \frac{1}{\sqrt{1+R_c^2}}\right) \tag{13}$$

$$I_r = \frac{\rho_G I_N(\sin\beta + C)}{2}\left(1 - \frac{1}{\sqrt{1+R_c^2}}\right) \tag{14}$$

The instantaneous global insolation on any element will be

$$I = I_b + I_d + I_r \tag{15}$$

The direct component varies from one element to another; while the diffuse and reflected components are constant all around the cone.

Instantaneous Solar Heat Gain Through an Element

The solar heat gain through the glass comprises two distinct parts. The first is the directly transmitted radiation; and the second is a fraction of the absorbed radiation that is released, by inward convection and radiation. This fraction depends on the inside and outside temperatures as well as the heat transfer coefficients on both sides of the glass. A commonly-accepted approximation is to consider this fraction to be dependent only on the heat transfer coefficients [1&2].

The two parts, mentioned above depend on the glass transmissivity (τ_g) and absorptivity (α_g) which are given by [3&4]

$$\tau_g = \frac{(1-r)^2 a}{1-(ra)^2} \tag{16}$$

and

$$\alpha_g = 1 - r - \frac{(1-r)^2 a}{1-ra} \tag{17}$$

where:

$$r = \frac{1}{2}\left(\frac{\sin^2 \theta_1}{\sin^2 \theta_2} + \frac{\tan^2 \theta_1}{\tan^2 \theta_2} \right) \qquad (18)$$

$$\theta_1 = \theta - \sin^{-1}\left(\frac{\sin \theta}{n} \right) \qquad (19)$$

$$\theta_2 = \theta + \sin^{-1}\left(\frac{\sin \theta}{n} \right) \qquad (20)$$

$$a = e^{\Delta} \qquad (21)$$

$$\Delta = \frac{-kt}{\sqrt{1 - \left(\dfrac{\sin \theta}{n} \right)^2}} \qquad (22)$$

where t, n and k are glass thickness, refraction coefficient and extinction coefficient, respectively.

Equations (16-22) show that the glass transmissivity τ_g and absorptivity α_g are depending on glass properties as well as the incidence angle. Since the diffuse and reflected radiation have no specific direction; they can always be treated as if their incidence angle of 60^0 [1]. Therefore, the values of the glass transmissivity τ_g and absorptivity α_g , for diffuse and reflected radiation, are constant all around the cone and depend only on the glass type. However the glass transmissivity τ_g and absorptivity α_g for direct radiation vary from one time to another.

The instantaneous solar heat gain per unit side area of any element can now be evaluated as:

$$q_L = I_b \, (\tau_{g,b} + F \, \alpha_{g,b}) + (I_d + I_r)\,(\tau_{g,d} + F \, \alpha_{g,d}) \qquad (23)$$

where the fraction F is given by:

$$F = h_i \, / \, (\, h_i + h_o \,) \qquad (24)$$

h_i and h_o are the inside and outside heat transfer coefficients respectively. Although the value of the fraction (F) listed in references varies from 0.196 to 0.4 [1&2]; the results presented hereinafter are arbitrarily based on a value equal to 0.268 as shown in [1&5].

Instantaneous and Daily Integrated Solar Heat Gain

The average instantaneous solar heat gain, per unit side area of the glass cone (q)is calculated by integrating and averaging the local values, obtained before. Thus,

$$q = \frac{1}{2\pi} \int_{0}^{2\pi} q_L \, d\alpha \qquad \qquad \text{W/m}^2 \qquad (25)$$

The daily average energy gain per unit side area (Q), is given as:

$$Q = \int_{T_1}^{T_2} q \, dT \qquad \qquad \text{Wh/m}^2 \qquad (26)$$

where T_1 and T_2 are the sunrise and sunset times, respectively. They can be found by substituting a solar altitude angle of zero in eqn. (1). Thus,

$$T_1 = 12 - \frac{\cos^{-1}\left(-\tan L \, \tan d \right)}{15}$$

and,

$$T_2 = 12 + \frac{\cos^{-1}\left(-\tan L \, \tan d \right)}{15}$$

Equations 25 and 26 are numerically integrated, as follows,

$$q = \frac{1}{N} \sum_{i=1}^{N} q_L \qquad\qquad\qquad \text{W/m}^2 \qquad\qquad\qquad (27)$$

and

$$Q = \Delta T \sum_{J=1}^{M} q \qquad\qquad\qquad \text{Wh/m}^2 \qquad\qquad\qquad (28)$$

Equations (25, 26, 27) and 28 give instantaneous average and daily integrated values per unit side area. These equations can be easily modified to obtain the same parameters per unit area of the cone base by multiplying each equation by the ratio of side area to base area "F_s" given as;

$$F_s = \frac{\left(1 - R_t^2\right)\sqrt{1 + R_c^2}}{R_c} \qquad\qquad\qquad (29)$$

3. Computer Program

A computer program is coded using visual basic language to carry out the computations presented previously. The program is designed in a general form and can be used for any location and on any date. It can also deal with different glazing type as specified by thickness, extinction coefficient and index of refraction. The program can deal with the complete and truncated cone or a specified arc from it during a day light or a certain period of the day.

The validity of the program was achieved through comparing its results for two cases:

　　1. The case of conical ratio equal to zero with to that obtained for the case of vertical cylinder [5].
　　2. The case of very high conical ratio with that obtained for the case of horizontal plate skylight [1].

The results which obtained by using the computer program were in good agree with the results which listed in ref. 5 and 1 .The maximum error is within $\pm 1\%$

4. Results and Discussions

The presented sample of results are based on clear double strength glass (ADS) having a thickness of 3 mm, an extinction coefficient (k) of 0.00764 mm^{-1} and index of refraction (n) of 1.526 . This type of glass was intentionally considered as a reference in order to have the present results consistent with, and comparable to, the information available in the literature [1-8].

Complete Conical Skylight

Instantaneous Local Heat Gain

In this section, the results for non truncated conical skylight with conical ratio equal to unity are presented. The variation of the instantaneous local solar heat gain around the conical skylight is shown for different surface azimuth angles of the element, different latitudes, different solar times and dates as shown in Figs. (2-5). These figures show that, some times (morning and after noon); a part of the skylight is only exposed to diffuse and reflected radiation since the solar beam incidence angle to that part is grater than 90 ^{0}. The area of that part depends on the date and latitude. The figures show that when the sun is vertically over head at equator on March 21st and September 21st during noon, all elements of the cone receives the same solar radiation.
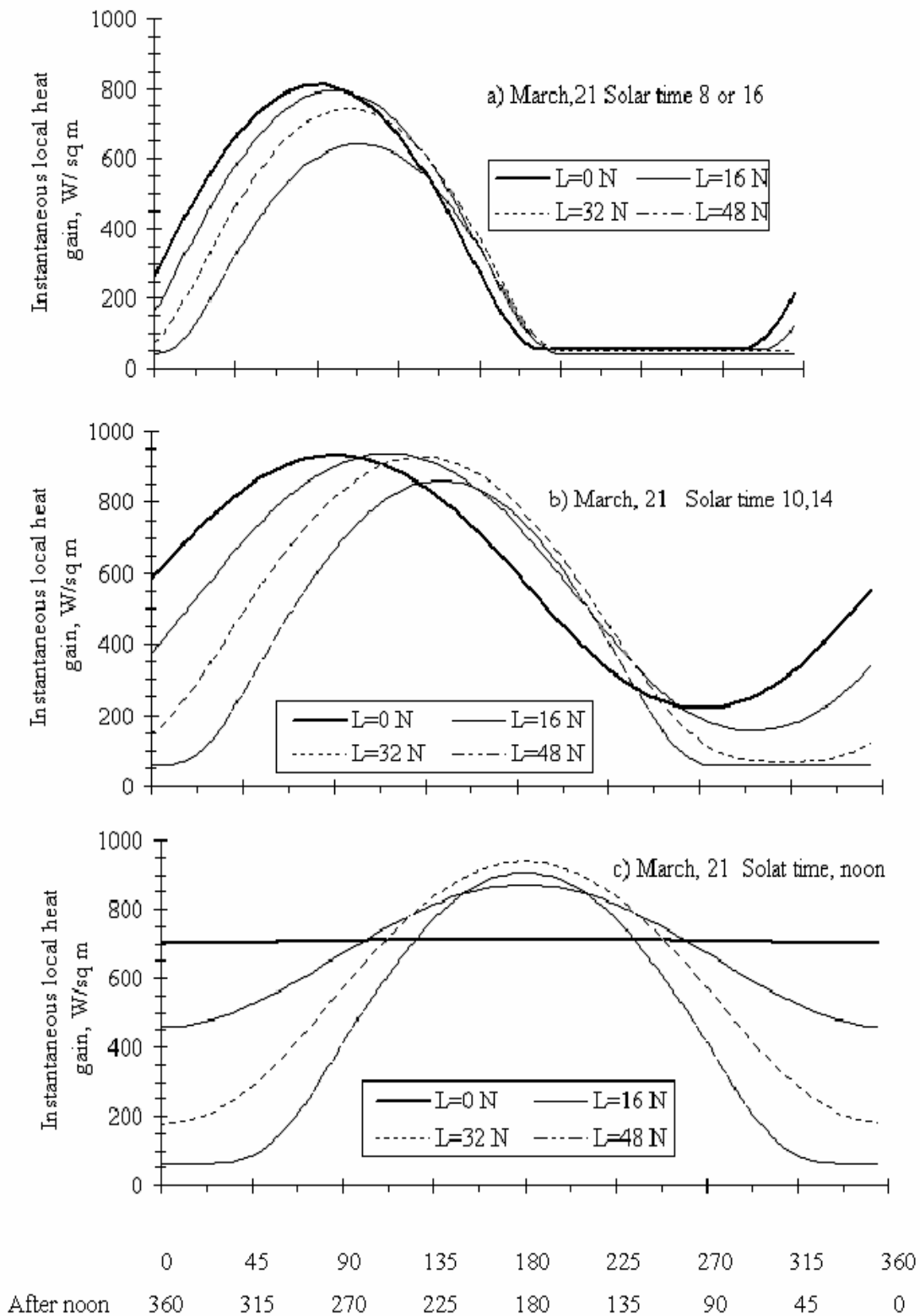
Fig. 2 Variation of the instantaneous local heat gain around a cone with conical ratio of unity on 21 Mar. and different latitudes and times
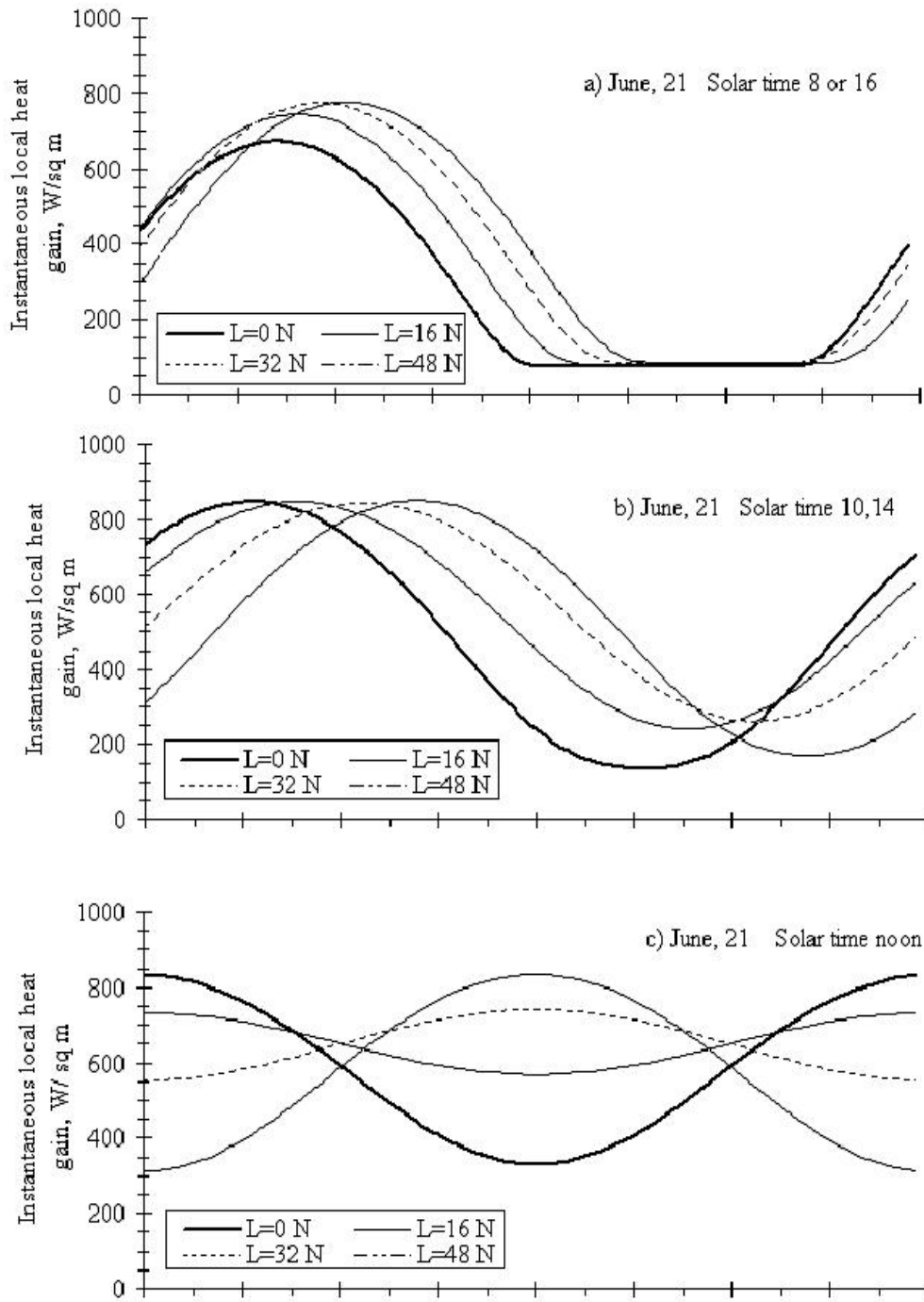
Fig. 3 Variation of the instantaneous local heat gain around a cone with conical ratio of unity on 21 Jun and different latitudes and times
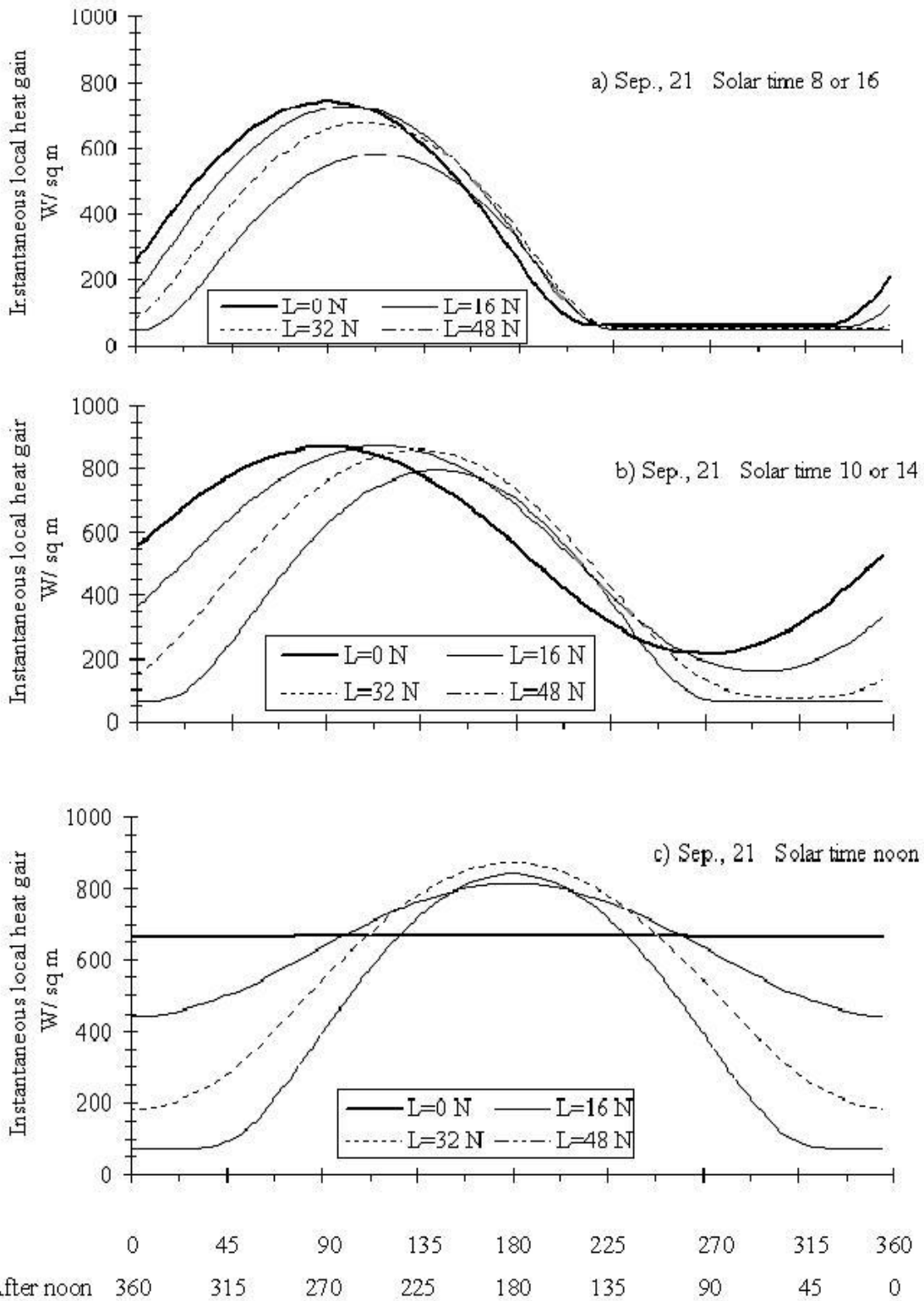
Fig. 4 Variation of the instantaneous local heat gain around a cone with conical ratio of unity on 21 Sep. and different latitudes and times
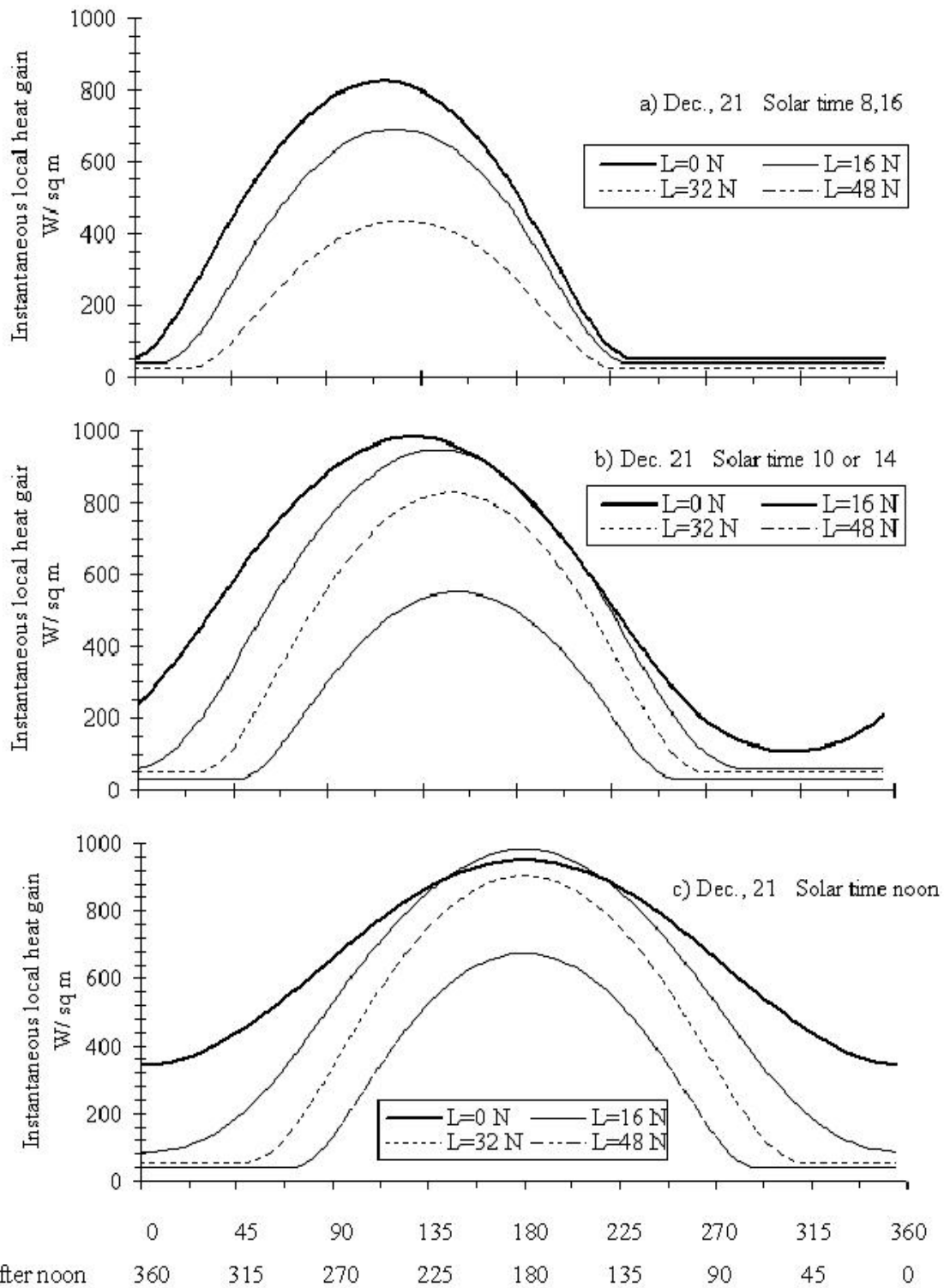
Fig.5 Variation of the instantaneous local heat gain around a cone with conical ratio of unity on 21 Dec. and different latitudes and times

Average instantaneous solar heat gain

The variation of the average instantaneous solar heat gain per unit side area of a cone with a conical ratio equal to unity at different dates, latitudes and solar times is shown in Fig. 6 and Table (1). The relationships in this figure are symmetric around the noon time, and represent the area under the corresponding curves in Figs. (2-5).

Fig. (6) also shows that, for the cone under consideration and around solar noon time, the average instantaneous solar heat gain is the highest in summer (21/6) for latitudes 32^0 N and 48^0 N; while at the equator the average instantaneous solar heat gain is the highest in spring. Moreover, the minimum average instantaneous solar heat gain occurs in winter in all latitudes except at the equator where it occurs in summer.

Daily average energy gain

The variation of the average daily energy gain, per unit side area, for the whole cone with a unity conical ratio, throughout the year is illustrated in Fig.. 7. The figure shows that during summer, the daily gain is higher at higher latitudes; the opposite is true in winter.

One can conclude that, the glass cone under consideration represent a load for air conditioning system during summer and winter. At the equator the daily energy gain throughout the considered cone is nearly constant around the year.

Effect of Conical Ratio

Figs. (8-11) show the variation of the average instantaneous solar heat gain ratio with conical ration (ratio between the average instantaneous solar heat gain for any complete cone to the average instantaneous solar heat gain through a complete cone unity conical ratio) for latitudes from 0^0 to 48^0 N. at different solar times and dates. The figures show that the average instantaneous solar heat gain ratio is nearly horizontally flat with conical ration grater than four. It could be concluded that; the cone can be treated as a horizontal flat skylight if its conical ration is grater than four. Also, if the conical ratio is zero (i.e. the cone is vertical cylinder), the date given in [5] is applicable. Finally, only cones with conical ratio grater than zero and less than four need special treatment listed hereinbefore.
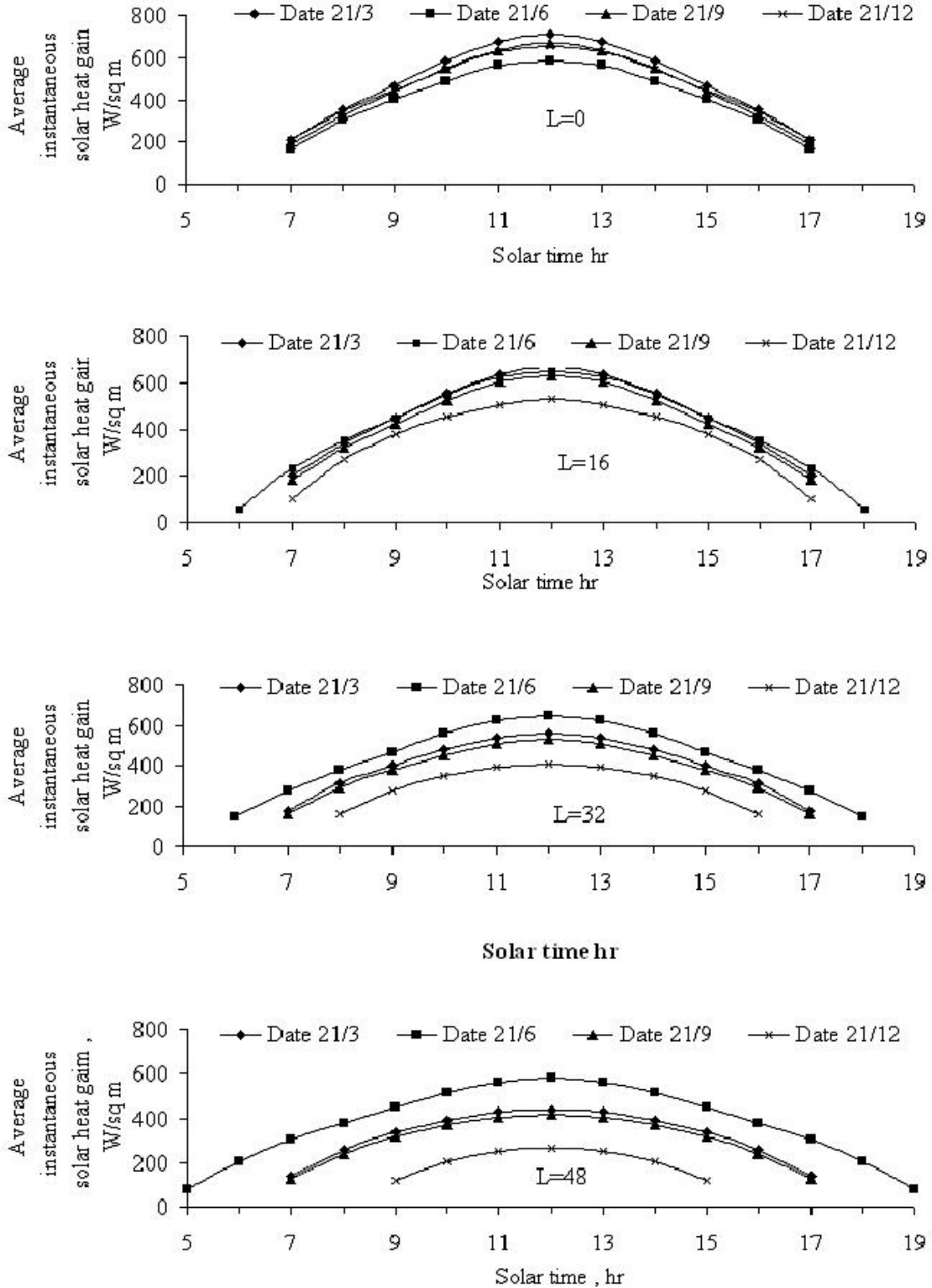
Fig. 6 Variation of the average instantaneous solar heat gain through a cone with conical ratio equal unity for different dates and latitudes.

Effect of truncation

The parameters presented in the current study are calculated per unit side cone area for complete cone. They can also be applied for truncated cone. The instantaneous average or daily heat gain through the complete con can be obtained by multiplying the cone side area and the corresponding values obtained from graphs. The parameters for truncated cone can be calculated from those of complete one by multiplying the corresponding values by $(1-R_t^2)$.
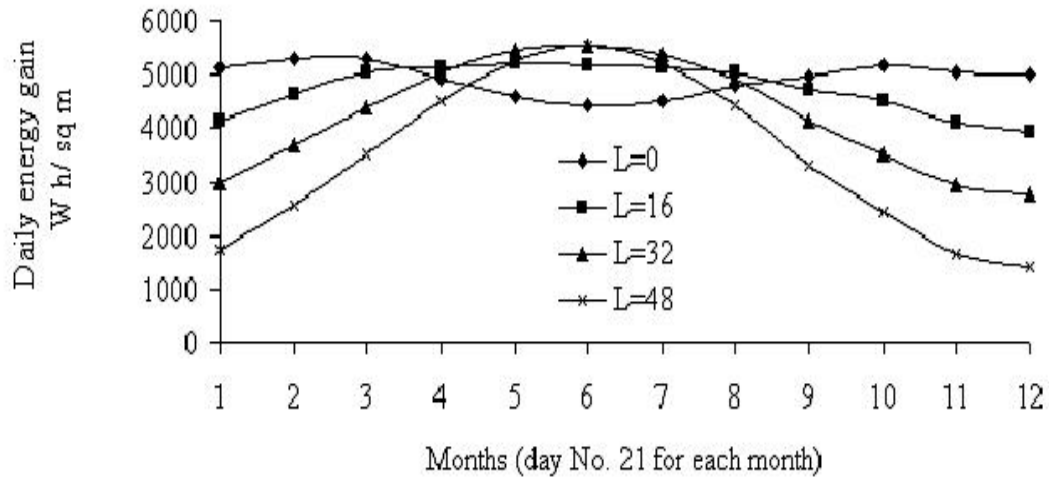
Fig.7 Variation of the daily energy per unit area of the conical glass with conical ratio equal unity through the year and latitudes
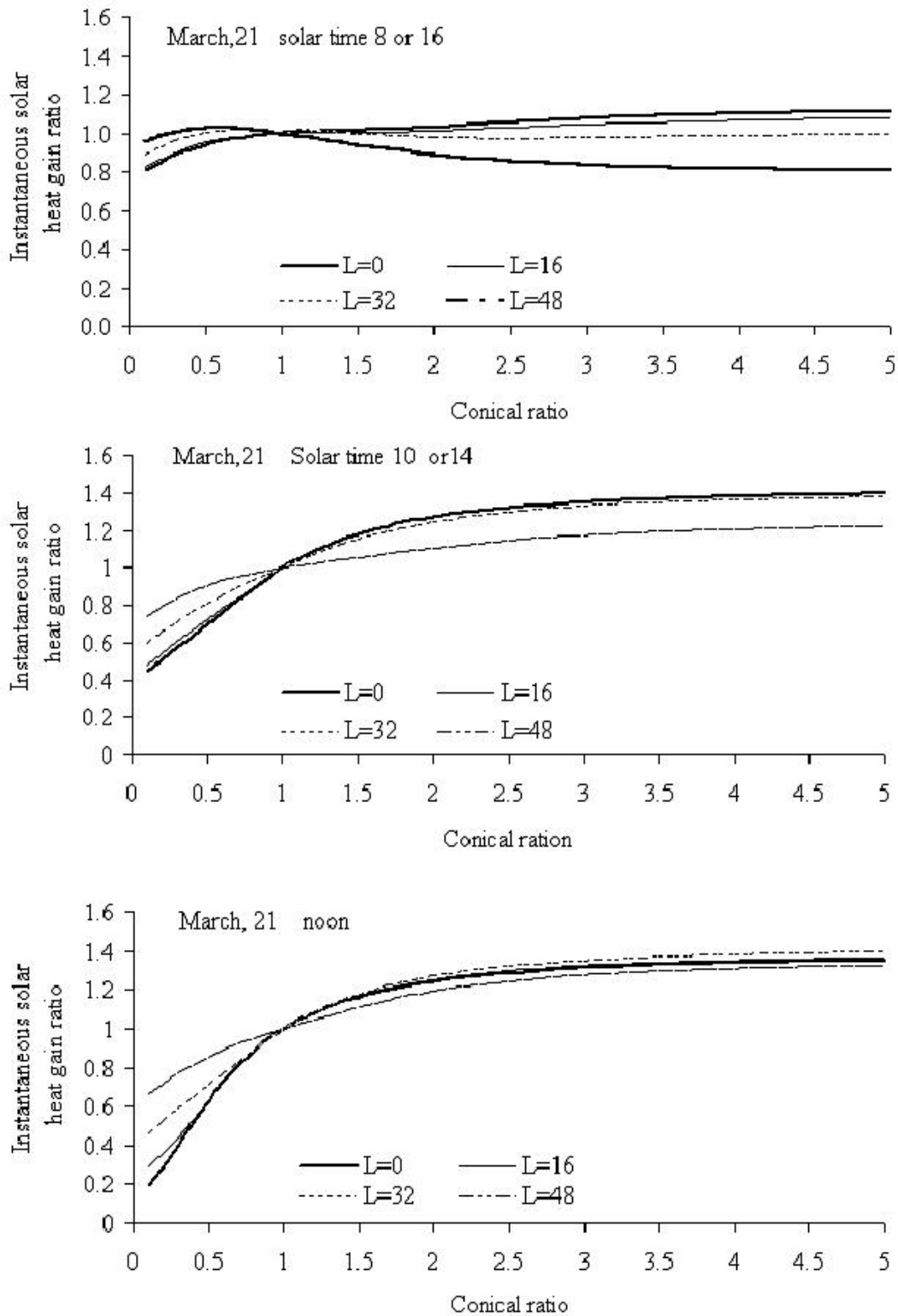
Fig. 8 Variation of the average instantaneous solar heat gain ratio with
conical ratio for different latitudes and times on 21 Mar.
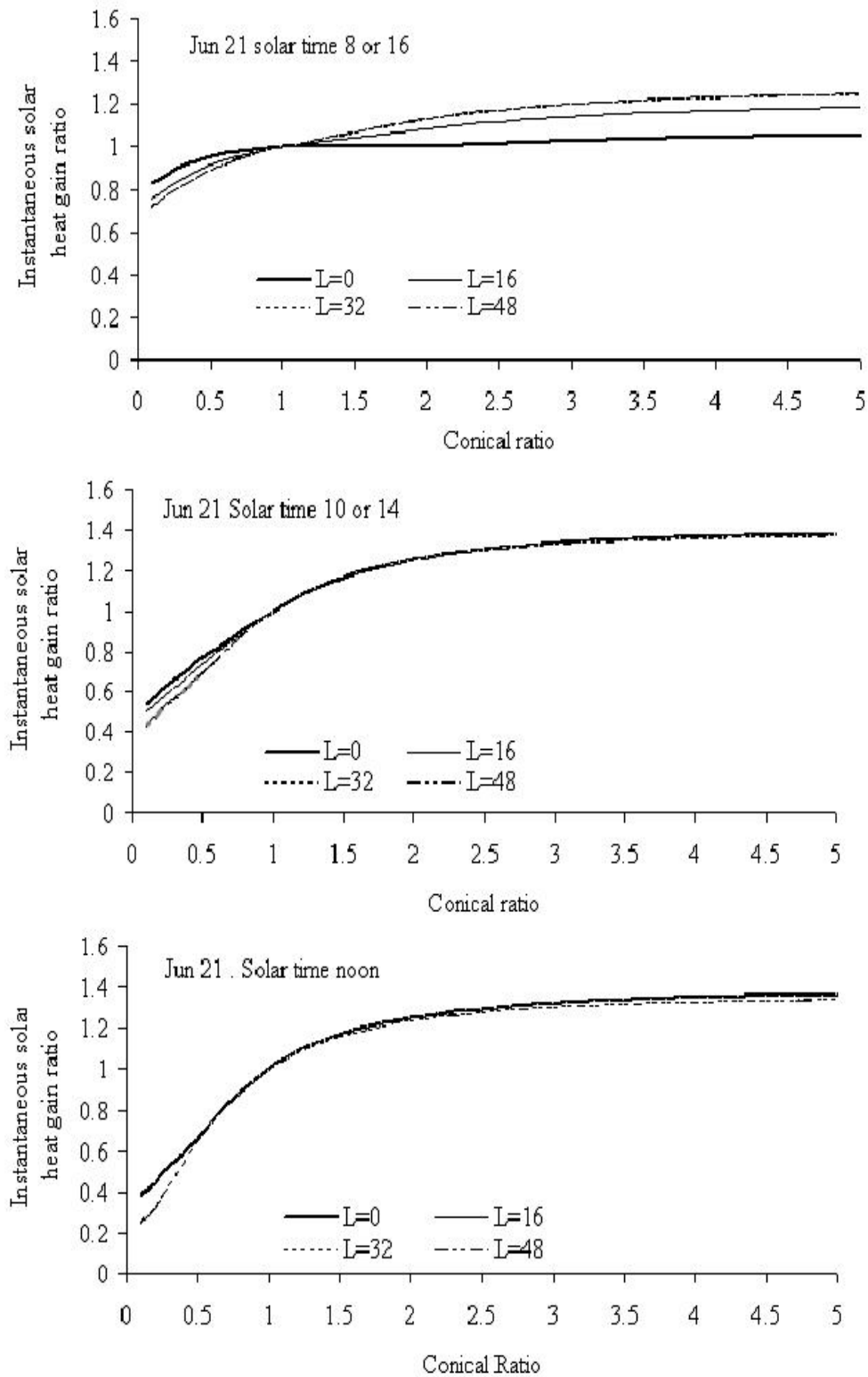
Fig. 9 Variation of the average instantaneous solar heat gain ratio with conical ratio for different latitudes and times on 21 Jun.

Table (1). Instantaneous and daily average solar heat gain through a cone with unity conical ratio and different latitude.

Latitude =		0	16	32	48
	Time	q, W /m²	or		Q W.H /m²
21/1	7	211.7	120.6	0.8	0.0
	8	351.9	287.1	190.4	26.4
	9	456.4	391.5	301.5	167.5
	10	558.5	469.4	372.1	243.4
	11	643.5	529.5	414.4	283.7
	12	674.6	553.9	428.9	296.6
Total		5118.8	4149.9	2987.2	1738.7
21/2	7	216.2	166.3	88.8	0.9
	8	358.2	318.4	255.6	159.8
	9	467.0	422.7	355.0	259.7
	10	582.0	511.9	424.8	321.4
	11	673.7	588.6	470.7	357.2
	12	706.4	617.9	488.2	369.1
Total		5300.6	4633.8	3678.3	2567.3
21/3	7	210.0	201.1	177.2	136.1
	8	353.3	341.8	309.8	256.1
	9	463.6	446.7	403.0	335.7
	10	582.7	552.1	477.9	391.6
	11	675.3	637.8	539.5	426.6
	12	707.9	668.7	563.5	438.9
Total		5277.7	5027.7	4378.1	3531.2
21/4	6			60.2	102.6
	7	190.1	221.3	235.5	233.6
	8	331.9	350.7	348.2	324.6
	9	437.5	453.7	437.8	394.8
	10	545.4	564.0	526.8	450.9
	11	630.6	647.4	596.7	493.9
	12	661.0	676.7	622	510.4
Total		4932.1	5150.6	5032.6	4511.3
21/5	5				40.3
	6		42.6	125.3	183.3
	7	174.5	232.9	269.0	286.0
	8	314.2	354.1	371.5	366.1
	9	414.5	453.1	460.7	433.8
	10	508.0	558.2	554.4	498.0
	11	584.0	636.1	622.7	546.7
	12	611.8	663.4	646.7	564.4
Total		4602.2	5217.4	5453.9	5272.6
21/6	5				79.4
	6		53.6	145.0	207.3
	7	165.9	234.8	278.9	302.3
	8	304.5	352.6	377.7	379.1
	9	402.5	448.9	466.5	446.9
	10	489.4	550.1	559.4	513.8
	11	560.5	624.9	625.7	562.8
	12	586.8	651.1	648.9	580.4
Total		4432.5	5181.1	5555.2	5563.7
21/7	5				41.2
	6		40.2	122.4	181.0
	7	168.2	227.9	265.1	282.9
	8	308.1	348.9	367.2	362.6
	9	407.8	447.0	455.7	429.8
	10	499.5	550.2	548.0	493.6
	11	573.8	626.6	615.0	541.7
	12	601.0	653.3	638.5	559.2
Total		4515.7	5135.1	5385.5	5224.8

Table (1). Cont.

Latitude =	Time	0	16	32	48
		q, W /m² or		Q W.H /m²	
21/8	6		9.6	54.1	96.0
	7	179.5	212.1	227.5	226.4
	8	322.9	342.6	341.0	318.0
	9	428.2	445.2	430.3	388.2
	10	533.6	553.0	518.0	444.1
	11	616.4	634.1	586.2	486.6
	12	645.9	662.6	610.8	502.8
Total		4807.2	5056.0	4925.1	4421.3
21/9	7	190.6	183.3	161.3	123.1
	8	330.4	320.2	290.1	238.9
	9	436.3	421.2	380.2	316.0
	10	548.6	521.3	452.0	369.9
	11	635.4	601.9	510.7	403.6
	12	666.0	630.9	533.4	415.4
Total		4948.6	4726.7	4122.0	3318.4
21/10	7	205.0	153.2	74.3	0.1
	8	348.1	307.1	242.6	143.9
	9	456.4	411.6	343.1	245.9
	10	569.0	499.2	412.8	308.5
	11	658.6	573.9	458.1	344.5
	12	690.5	602.5	475.1	356.5
Total		5164.8	4492.5	3536.8	2442.3
21/11	7	206.2	114.0	0.3	
	8	346.6	281.2	183.2	20.5
	9	450.8	385.6	295.0	159.4
	10	551.8	463.1	365.7	236.1
	11	635.6	522.3	408.0	276.6
	12	666.3	546.3	422.4	289.6
Total		5048.5	4078.5	2926.8	1674.7
21/12	7	207.6	99.1		
	8	346.0	271.7	158.9	
	9	448.1	375.9	276.7	120.4
	10	543.4	451.0	348.3	206.4
	11	624.0	504.4	390.2	249.8
	12	653.9	526.1	404.2	263.4
Total		4991.9	3930.4	2752.3	1416.7

5. Conclusions

Recalling the main objective set in the introduction, the prime outcome of this research would be the complete code together with underlying the computational procedure. This useful tool can be used easily and accurately to evaluate the solar heat gain through any conical skylight with any given dimensions or glass type, located at any latitude, at any time of the day and any day of the year.

Another useful conclusion is that, cones with high conical ratio can be treated as horizontal flat plate sky lights. Moreover cones with law conical ration can be treated as vertical cylindrical skylight. Only cones with conical ratio less than four need the special treatment described.

Useful data for instantaneous and daily average solar heat gain through a cone with unity conical ratio on different dates and latitudes are shown in Table (1). Using this table, instantaneous or daily solar heat gain can be obtained in one step. For a cone with a conical ratio other than unity, Figs. (8-11) are suitable for the correction. Truncated cone can be treated by multiplying results from table (1) by $(1-R_t^{2})$; this means that table (1) and Figs. (8-11) represent a helpful tool in dealing with conical sky lights.

6. References

[1]   ASHRAE, ASHRAE. *Handbook of fundamentals, American Society of Heating, Refrigerating and Air Conditioning Engineer Inc*. Atlanta, GA, USA, 2001.

[2]   Carrier Air Conditioning Company. *Hand Book of Air Conditioning System Design.* MC Grow Hill, USA, 1965.

[3]   Kassem, M. A., "Controlling the Solar Heat Gain by Changing the Glass Inclination Angle" *Engineering Research Journal, Faculty of Engineering, Helwan University, Egypt*, Vol. 75, (2001).

[4]   Kassem, M.A., Kaseb, S., and EL-Refaie, M. F., "Solar Heat Gain Through Hemispherical skylight", *Journal of Engineering and Applied Science, Faculty of Engineering Cairo University, Egypt*, Vol. 45, No. 3, (1998), pp. 409- 425.

[5]   Kassem, M.A., Kaseb, S., and EL-Refaie, M. F., "Solar Heat Gain Through Vertical Cylindrical glass", *Journal of Building and Environment*, Pergamon press, Vol. 34 (1999), pp. 253- 262.

[6]   EL-Sayed, M.M., Taha, I.S., and Sabbagh, J.A., "Design of Solar Thermal Systems", *Scientific Publishing Center, King – Abdul-Aziz University Jeddah, Saudi Arabia*, (1994).

[7]   Jager, C., "Solar Forcing of Climate ", *Space Science Reviews*, Vol. 120, No. 3-4, pp. 197-241, (2005).

[8]   Myers, Daryl R., "Solar radiation modeling and measurements for renewable energy applications: data and model quality", *National Renewable Energy Laboratory 1617 Cole Boulevard, Golden, CO80401, USA*, (2004).

(/ /   / /   )

.

.

.

.

.

.

Automation of Component Matching for Automotive-Cooling Systems

M. A. Kassem* and M. F. El-Refaie**

Mechanical Power Engineering Department
Faculty of Engineering , Cairo University , Cairo , Egypt
* mahmoudkassem@yahoo.com   ** aymr@link.net

Abstract. The matching of components to constitute an integrated refrigeration system is a rather involved and tedious task. In particular, the refrigeration subsystem of an automobile air-conditioning system represents a very special application. The compressor speed is continuously varying and the operating and loading conditions experience frequent sharp changes. This adds further complexities to the component-matching procedure. Hence, automation of the process would be quite in place.

In this work, a systematic mathematical foundation is established; and a versatile computer program is coded to execute the component-matching procedure. The program input includes specifications of the suggested components and information about the operating conditions. The program works out the common balance point of the system; and evaluates the refrigeration capacity. Other important byproducts are also delivered by the program; such as the balance evaporation and condensation temperatures, the required power input and the condenser duty.

The program is an easy-to-use tool which helps to save time and effort. It can be repetitively run to compare alternative components or to investigate different working conditions.

Keywords: Automotive air conditioning, refrigeration system, component matching, automation

List of Symbols

A_f face area, m^2

A_f fin area, m^2

A_i inner area, m^2

A_m mean area, m^2

A_o outer area, m^2

A_p prime area, m^2

c   compressor clearance factor

c_1 to c_9 coefficients of the polynomial in Eqn. (1)

C_{pa} specific heat of air at constant pressure, kJ/kg.K

d_1 to d_9 coefficients of the polynomial in Eqn. (2)

D   compressor cylinder diameter, m

D_h hydraulic diameter on refrigerant side, m

e_1 to e_9 coefficients of the polynomial in Eqn. (4)

F   condenser factor, defined in Eqn. (6), kW/K

G   evaporator factor, defined in Eqn. (9), kW/K

h   enthalpy, kJ/kg

h_B boiling heat-transfer coefficient, $kW/m^2.K$

h_{cond} condensation heat-transfer coefficient, $kW/m^2.K$

h_o heat-transfer coefficient on air (outer) side, $kW/m^2.K$

k_m thermal conductivity of tube material, kW/m.K

L   piston stroke, m

m_a air mass-flow rate, kg/s

$\dot{m}_{ref}$ refrigerant mass-flow rate, kg/s

n   index of compression process

N   compressor rotational speed, rpm

P   indicated power input to compressor, kW

P_c condensing pressure, MPa

P_e evaporating pressure, MPa

PD total piston displacement of compressor, m^3

q_c rate of heat rejection in condenser, kW

q_e refrigeration capacity, kW

t_a ambient-air temperature, °C

$t_{a,o}$ air temperature at exit from heat exchanger, °C

t_c condensing temperature, °C

t_e evaporating temperature, °C

t_i air temperature at inlet to evaporator, °C

TTD   terminal temperature difference, °C

U_o overall heat-transfer coefficient based on outer area, $kW/m^2.K$

v_f face velocity of air, m/s

Z   number of compressor cylinders

Greek Letters

δ tube-wall thickness, m

Δt_a air-temperature rise in condenser, °C

η_f fin efficiency

η_{vol} volumetric efficiency

ρ refrigerant density, kg/m^3

ρ_a air density, kg/m^3

1. Introduction

An automotive-cooling system, similar to any other vapor-compression refrigeration system, is constituted by integrating a number of main components; namely, the compressor, condenser, expansion device and evaporator. When developing such a system, the designer has the liberty to choose each component from a variety of available models. Although the individual performance characteristics, of the components, may usually be known, there is always an uncertainty concerning the collective performance of the integrated system; which depends on the individual characteristics as well as the working conditions.

The particular nature of vehicular cooling is very much different from other cooling applications; such as household and commercial refrigeration and residential air conditioning. In actual practice, the operation of an automobile-cooling system is quite far from being steady. The compressor runs at different speeds, depending on traffic and traction needs, and the working conditions pertaining to both heat source and heat sink are always varying. This dynamic nature adds very much to the inherent complexity of the component-matching procedure for automobile-cooling applications. The collective-performance prediction should be repeated to cover different possible situations. This calls for automation of the matching procedure.

The objective of the present study is to provide a handy tool, in the form of a computer program, for non-experimental execution of the lengthy component-matching procedure. This will evade expensive and wasteful experimentation and trials. Moreover, the wide spectrum of working conditions, intrinsic to automotive-cooling applications, will be conveniently accommodated.

In more details, the program facilitates the evaluation of the cooling capacity realizable when combining any four particular components into one integrated system; and putting it into operation under any set of working conditions. In addition, the program provides other important and instructive information; e.g. the balance evaporation and condensation temperatures, the indicated power input necessary to drive the compressor and the required condenser duty.

2. Component-Matching Procedure

Any component of the cooling system does not have a singular capacity. Instead, it has a range of capacities depending on the evaporating and condensing temperatures and, implicitly, on the externally-imposed working conditions. Thus, when the components are integrated, in a complete system, and operated under a set of working conditions, their capacity characteristics will be interdependent. The system will autonomically reach, and settle at, an equilibrium state of operation, or a balance point, where all the individual performance characteristics of the components, as isolated elements, will be simultaneously satisfied. It is to be realized that this balance condition can in no way be readily concluded just from the knowledge of the individual characteristics.

The elaborate process of determining this balance point is what is practically known as "Component-Matching Procedure" [1, 2]. This can be achieved in two different ways; graphically or analytically.

The graphical method is time consuming and must be conducted manually. It is not amenable to computerization. Therefore, it is excluded from the scope of the present work. Nevertheless, it is very indicative and establishes a sound understanding of the matching procedure. That is why it is fully detailed in different locations in the literature [3, 4, 5].

3. Analytical Method

Rudiments of the Method

This method, which is also referred to as "System Simulation", is performed through mathematical rather than graphical procedure. It is well known that to get the intersection point of two performance curves, which determines the mutual balance point of a two-component combination, is nothing but the simultaneous solution of the two equations representing the two curves.

Extending this concept to more than two components, the method can be summarized as the simultaneous solution of the equations describing the performance characteristics of all components. This ends up in one singular balance point which determines the operating condition of the system as a whole.

For the case under consideration, four equations will be dealt with simultaneously. These represent:
   1- The cooling capacity achievable by the compressor.
   2- The condenser duty as dictated by the compressor.
   3- The heat-rejection capacity of the condenser as a heat exchanger.
   4- The heat-extraction capacity of the evaporator as a heat exchanger.

In this method, and unlike the graphical one, the components do not have to be combined in pairs. All of them can be simulated simultaneously. Moreover, and being conducted through a mathematical course, this method can be automated; by coding it into a computer program. In fact, computerization is a necessity to execute the lengthy computations, which will be outlined hereinafter, and to facilitate repetitions for different configurations and under different working conditions. If necessary, the program may be validated experimentally [6].

Mathematical Expression of Performance

In order to go through the analytical procedure of component matching (system simulation), the performance of each component of the system must be properly expressed in a mathematical form. These expressions, or equations, represent the raw material for the system simulation which will evolve in determining the balance point for the whole system.

In general, the performance equations may be derived from catalogue data, test results or repetitive performance calculations under different conditions. The third source will be employed because this is the most rigorous and detailed; it also allows for free arbitrary variations in component characteristics or working conditions.

The forms of the performance equations for the different components are overviewed in what follows:

Compressor Performance

The cooling capacity produced by running the compressor and the required indicated power input, can be represented by the following two equations [3] which were obtained through curve fitting of performance data for different compressors:

$$q_e = c_1 + c_2\, t_e + c_3\, t_e^2 + c_4\, t_c + c_5\, t_c^2 + c_6\, t_e\, t_c +$$
$$c_7\, t_e^2\, t_c + c_8\, t_e\, t_c^2 + c_9\, t_e^2\, t_c^2 \tag{1}$$

and

$$P = d_1 + d_2\, t_e + d_3\, t_e^2 + d_4\, t_c + d_5\, t_c^2 + d_6\, t_e\, t_c +$$
$$d_7\, t_e^2\, t_c + d_8\, t_e\, t_c^2 + d_9\, t_e^2\, t_c^2 \tag{2}$$

The rate of heat rejection, dictated by the compressor, is practically equal to the sum of the refrigeration capacity and the indicated power input. Thus,

$$q_c = q_e + P \tag{3}$$

This can be put in the form

$$q_C = e_1 + e_2\, t_e + e_3\, t_e^2 + e_4\, t_c + e_5\, t_c^2 + e_6\, t_e\, t_c +$$
$$e_7\, t_e^2\, t_c + e_8\, t_e\, t_c^2 + e_9\, t_e^2\, t_c^2 \tag{4}$$

where the coefficients e_1 to e_9 are given by

$$e_i = c_i + d_i \quad \{ \text{ for i = 1,2,....,9 } \} \tag{5}$$

Condenser Performance

A rigorous expression of the heat-transfer performance of the condenser can be quite complex. However, a satisfactory representation of air-cooled condenser performance, for most engineering calculations, is available in the straight-line form [3]:

$$q_c = F\, (\, t_c - t_a\,) \tag{6}$$

The factor F is worth some further in-depth investigation. This factor quantifies the condenser capacity per unit of temperature difference; i.e. per unit of temperature split (where the "Temperature Split" is the difference between condensing temperature and incoming-air temperature).

It is important to have an idea about the practical range of the value of F. A theoretical maximum limit for its value can be set through the following brief analysis. Referring to Fig. 1, the temperature split is the sum of the air-temperature rise through the condenser Δt_a and the terminal temperature difference TTD.

$$t_c - t_a = \Delta t_a + TTD \tag{7}$$

$$\Delta t_a = q_c \ / \ m_a \ C_{pa}$$
$$t_c - t_a = q_c \ / \ m_a \ C_{pa} + TTD$$

substituting for q_c from Eqn. (6)

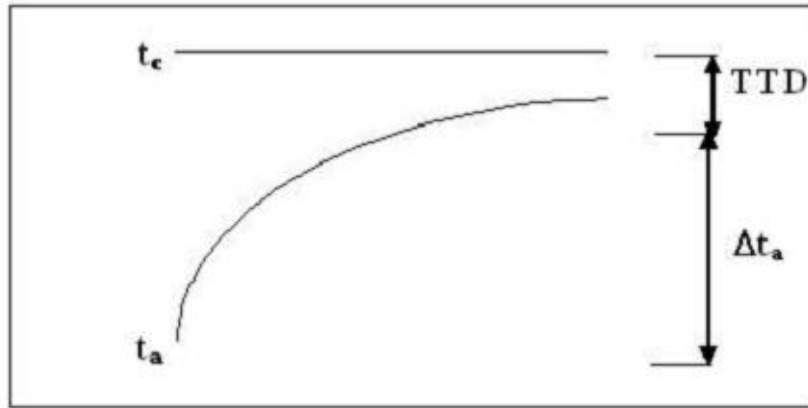$$TTD = (\ 1 - F/m_a \ C_{pa} \ ) \ (\ t_c - t_a \ ) \tag{8}$$

Fig. (1). Temperature-surface diagram of an air-cooled condenser.

Equation (8) reveals that the terminal temperature difference TTD will have a positive value for all values of $F < (m_a c_{pa})$. Accordingly, the theoretical maximum limit which bounds the value of F is the product $(m_a c_{pa})$. This limit would only be reached under impractical conditions; represented by an infinitely large surface area. In actual practice, the value of F is expected to be considerably lower than this theoretical limit.

Evaporator Performance

The heat-transfer performance of an air-cooling evaporator is expressed by [3]

$$q_e = G \ (\ t_i - t_e \ ) \tag{9}$$

It can be shown through an analysis, similar to that presented before for the condenser, that there is a theoretical maximum limit which cannot be exceeded by the factor G. This limit is related to the air-stream heat capacity; but is not exactly equal to it because the heat transfer, from the air, in the evaporator is not completely sensible.

Role of Expansion-Device

The type of expansion device used in almost all automobile-cooling systems is the thermostatic expansion valve TEV. The performance of this type of expansion device is essentially independent of the evaporating and condensing pressures and, hence, temperatures. The flow rate of refrigerant is governed by the amount of superheat at evaporator outlet. Accordingly, and if it is properly sized, it will respond and abide to the mass-flow requirements of the system at the balance point. But, it will not have an effective role in determining this point. Therefore, the expansion valve can be excluded from the study presented herein.

The proper selection of expansion-valve size can be easily made based on the experience and guided by the limited number of nominal capacities, specified by the manufacturer, for the different valves. The consequences of a valve malselection can be readily and qualitatively foreseen. For example, an undersized valve will result in evaporator starvation; hence, alteration of the performance expressed by Eqn. (9). This will manifest in a lower value of the factor G.

Solution of Performance Equations

The performance equations are to be simultaneously solved to yield all the operating parameters at the common balance point for the system as a whole. The results include the evaporating and condensing temperatures, the refrigeration capacity, the indicated power input to the compressor and the rate of heat rejection in the condenser.

The method of solution usually adopted, and widely acknowledged in the literature [3], is the method of successive substitution. A proposed sequence of calculations is summarized by the information-flow diagram shown in Fig. 2. The calculations start by guessing first-trial values of the evaporating and condensing temperatures. Then, new corrected values are calculated through the loop and used as input to the next iteration; till the temperatures converge to those of the common balance point. The energy exchanges of the system (i.e. the refrigeration capacity, the power input and the heat-rejection rate) are calculated in each iteration. They also eventually converge to the equilibrium or actual operating values.

With the successive-substitution method, convergence is not always guaranteed. If the sequence diverges, a different arrangement of the blocks in the information-flow diagram, other than that shown in Fig. 2, should be devised.
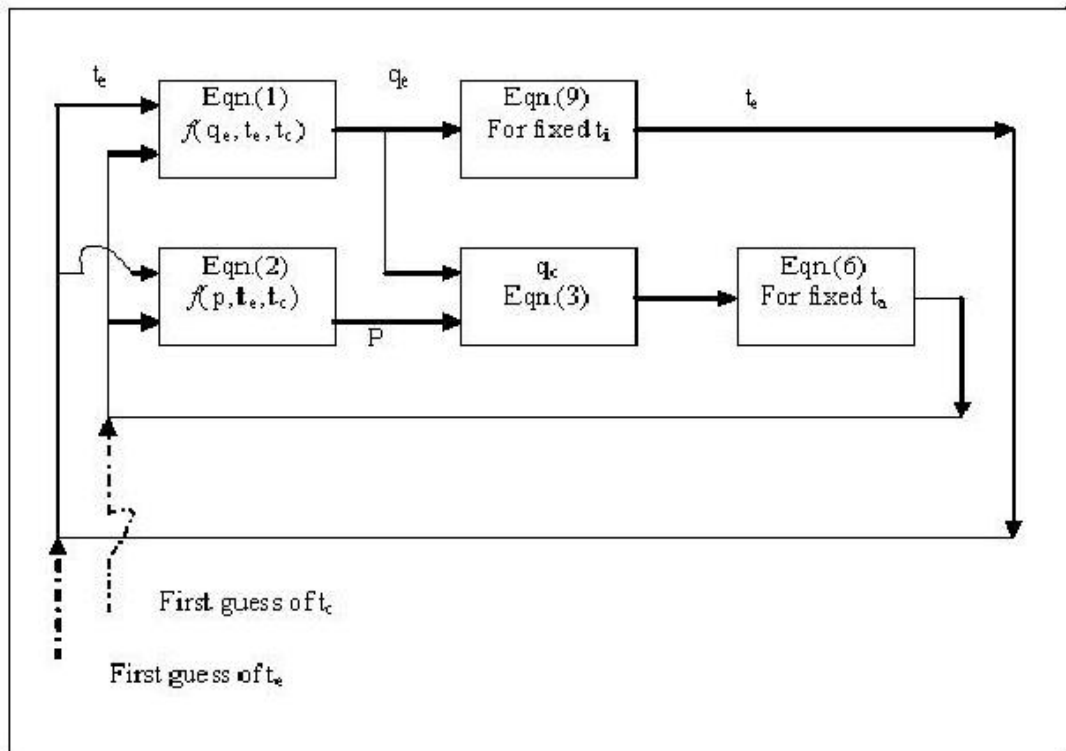
Fig. (2). Successive-substitution method (Information-flow diagram).

4. Computer Program and Computational Details

A computer program was coded to perform the computational steps of component matching; or, in other words, to solve the component-performance equations simultaneously. Another important duty of this program is to constitute or generate, as a first step, the component-performance equations in accordance with the forms explained hereinbefore. This, of course, will be based on aknowledge of the configuration, dimensions and materials of each component.

The types of heat-exchange surface used in the condenser and evaporator had to be identified before preparing the program. In automobile-cooling industry, two types of surfaces are currently in common use; these are:

1. Corrugated-plate-fin surface with louvered fins and flattened tubes with divided cross section; which is also known as "micro-channel parallel-flow exchanger" [7] and schematically displayed in Fig. 3. This type of heat-exchange surface can be used for either condenser or evaporator. When used for the evaporator, the tube internal divisions are usually removed.

2.   Circular tube bank with continuous straight plate fins ; shown in Fig. 4.

Accordingly, and in any system, we can have any one of four possible permutations of the condenser and evaporator surface types. The computer program, in turn, had to involve four different alternative routes to deal with any of the four possible combinations.

The main parts are detailed in the following overview. But, before going through the program divisions and computational details, refer to the general synoptic flow chart shown in Appendix B.

For the example shown above, number of internal tube passages is 4 and number of partitions is 3.

Fig. (3). Plate-fin surface with flattened tubes.

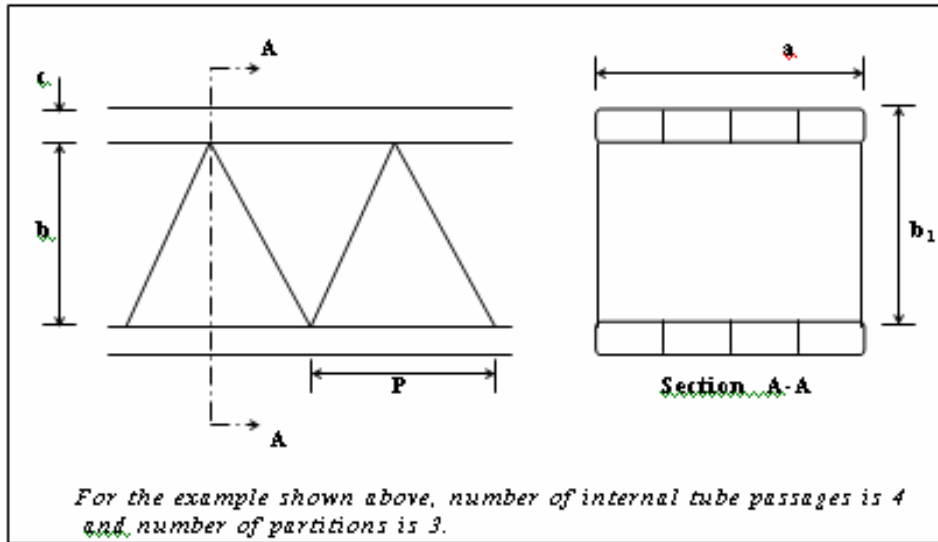**Program Input**

This section is subdivided into two subsections. The first includes the individual characteristics of the system components; and the second deals with the working conditions.
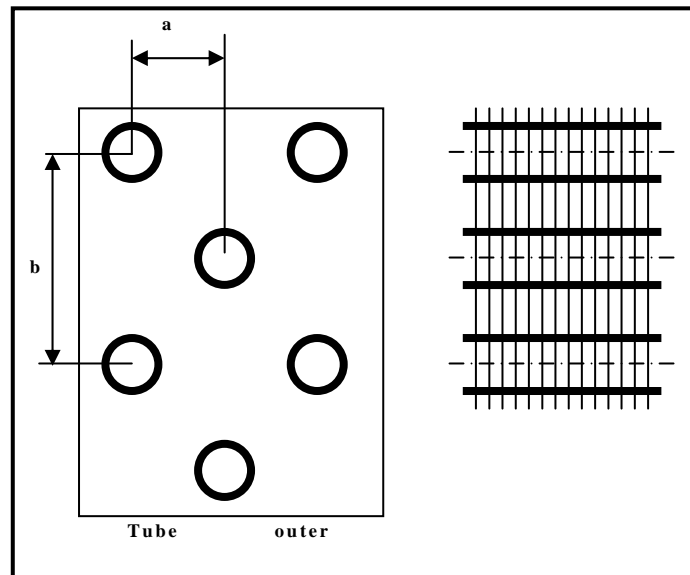

Fig. (4). Circular-tube bank with continuous straight plate fins.

Components Characteristics

Compressor: The program user is given the liberty to chose between two alternative ways of introducing the compressor characteristics. He may define the number of cylinders, the cylinder diameter and the piston stroke; or he may alternatively introduce the compressor swept volume as a lumpsum value. The choice of either way will depend on how information is obtained from the compressor catalogue.

The clearance factor should also be introduced as one of the compressor characteristics. If this factor is not known for the compressor, it may be taken from the practical ranges available in the literature. Some references specify a range of 0.04 - 0.07; while in others the range is ≤ 0.05.

Condenser and evaporator: This section includes all the geometrical dimensions and features of both the condenser and evaporator. These will define the size, flow pattern and finned-surface characteristics. In addition, the tube and fin materials are specified in terms of thermal conductivity.

The geometrical parameters, to be introduced for each heat exchanger, depend on which of the two heat-exchange surfaces is used. Lists of parameters are available [8]. Of course, these parameters should be congruous with the route followed through the program.

Working conditions
This section includes the following information:

Compressor speed
Information about Heat Source and Heat Sink: The rate of heat extraction by the evaporator depends on both the return-air temperature (cabin temperature) and the evaporator face velocity. Similarly, the rate of heat rejection from the condenser depends on the condenser face velocity in addition to the ambient-air temperature.

Accordingly, the following four parameters will be introduced to give a complete picture of the heat source and heat sink between which the cooling system operates:
1. Cabin temperature or return-air temperature t_i
2. Evaporator face velocity
3. Ambient-air temperature t_a
4. Condenser face velocity

Amount of refrigerant superheating in evaporator and sub-cooling in condenser.
Computations
Performance of individual components
The main segments constituting the computational work are those intended for working out the mathematical equations expressing the performance of the individual components. These are the steppingstones towards the simultaneous solution of the performance equations to get the collective system performance; which terminates the computational task.

Compressor performance: The ultimate objective of this section is to evaluate the coefficients c_1 to c_9 in Eqn. (1), d_1 to d_9 in Eqn. (2) and, hence, e_1 to e_9 in Eqn. (4). Along this course, a mathematical procedure is established to:
1. Construct the thermodynamic cycle (with the used refrigerant) for any pair of evaporating and condensing temperatures.
2. Calculate the relevant properties at all cycle points.
3. Calculate the refrigerant mass flow rate.
4. Calculate the three energy exchanges of the system; namely, the cooling capacity, the indicated power input and the condenser duty.

A typical theoretical cycle is shown in Fig. 5; and the required calculations are summarized in Eqns. (10-14).

$$q_e = m^{\cdot}_{ref}\left(h_3 - h_2\right) \tag{10}$$

$$P = m^{\cdot}_{ref}\left(h_4 - h_3\right) \tag{11}$$

Where;

$$m_{ref}^{.} = PD\eta_{vol}\rho_3 \tag{12}$$

$$PD = \frac{\pi D^2 LZ}{4}\left(\frac{N}{60}\right) \tag{13}$$

$$\eta_{vol} = 1 + c - c\left(\frac{P_c}{P_e}\right)^{\left(\frac{1}{n}\right)} \tag{14}$$

The constants, or coefficients, c_1 to c_9 or d_1 to d_9 are determined by equating equations (1-10) and (2-11) respectively for nine different values of condensing and evaporating temperatures; then solving the nine simultaneous equations for the required coefficients.

In this respect, the following points should be brought forth:
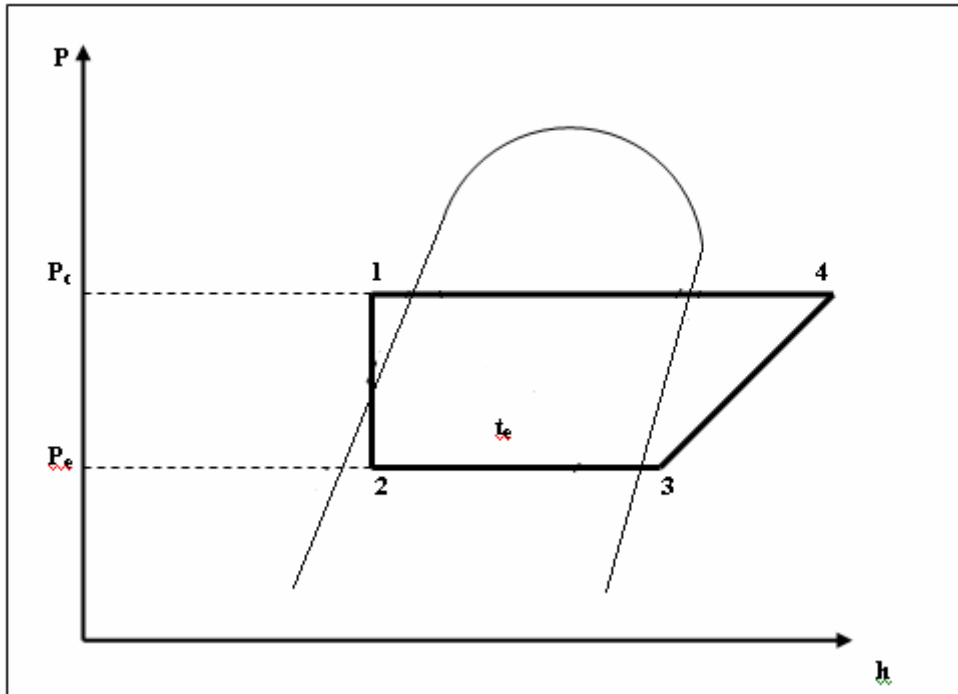
Fig. (5). Thermodynamic cycle and point designation.

1. The computer program was based on refrigerant 134a ; since it is most widely used in automobile-cooling industry. New accurate equations were derived, through curve fitting, for calculating the properties. These are given in the Appendix A.
2. The volumetric efficiency based on the clearance factor and the evaporating and condensing pressures is the apparent or clearance volumetric efficiency η_{cv}. The actual or total volumetric efficiency η_v may be considerably lower than η_{cv}. But, the actual efficiency cannot be readily calculated; the only way to determine its value is through experimentation. Therefore, the calculated apparent efficiency is multiplied by a practically-acceptable factor of 0.9 to yield the actual efficiency.
3. The calculated power input to compressor is an indicated value. The actual, or gross, power input will be higher to account for mechanical and transmission losses.

The core calculations of this section are repeated through two repetitive loops for nine pairs of evaporating and condensing temperatures t_e and t_c. Substituting in Eqn. (1) yields a system of nine simultaneous linear equations in the coefficients c_1 to c_9. Then, the principles of matrix algebra are employed to get the coefficients; the inverse of the matrix is obtained by Gauss-Jordan method.

The same technique is followed with Eqn. (2) to determine the coefficients d_1 to d_9. Then, the coefficients e_1 to e_9 are calculated using Eqn. (4).

Condenser Performance: The performance of the condenser is to be mathematically expressed in the form given by Eqn. (11). In other words, The computations in this section are dedicated to evaluating the factor F in Eqn. (6) which expresses the condenser performance. This is achieved through the following equations :

$$q_c = F (t_c - t_a)= v_f A_f \rho_a C_{pa}(t_{a,o}-t_a)= U_o A_o \frac{\left(t_{a,o} - t_a\right)}{\ln\left(\dfrac{t_c - t_{a,o}}{t_c - t_a}\right)} \tag{15}$$

where,

$$\frac{1}{U_o A_o} = \frac{1}{h_{cond} A_i} + \frac{1}{h_o\left(A_p + \eta_f A_f\right)} + \frac{\delta}{k_m A_m} \tag{16}$$

$$h_{cond} = 4050 (D_h / 0.01)^{-0.2} \tag{17}$$

The detailed geometrical characteristics of the heat-exchange surface and the heat-transfer coefficient on the air side are available [8]. The method of calculating the fin efficiency is also available in many heat-transfer textbooks [9].

The condenser capacity is evaluated at a large number of values of the ambient-air temperature and, hence, condensing temperature; through a repetitive loop. Moreover, it was concluded, through extensive computational investigations, that the factor F is highly dependent on the air flow rate represented by the face velocity of air; and had to be taken into consideration. Therefore, the repetitive calculation procedure, mentioned above, is repeated again (two nested loops) for many different values of face velocity in order to derive an expression for F in the form

$$F = A_c v_f^2 + B_c v_f + C_c \tag{18}$$

where A_c , B_c and C_c are numerical constants.

When introducing the condenser face velocity as an input item, the program user should be well versed of the practical range associated with the application in hand. For stationary, or residential, air conditioning systems, the condenser face velocity usually falls within the range 2-5 m/s. For automobile air conditioning, considerably higher values may, sometimes, be attained depending on space limitations, fan operation and velocity of air relative to the vehicle.

Evaporator performance: The evaporator performance is mathematically simulated by Eqn. (9). For any particular evaporator, the performance trends will be completely defined by evaluating the factor G. The evaporator factor, G, is calculated using the following equations:

$$q_e = G (t_i - t_e)= v_f A_f \rho_a C_{pa}(t_i-t_{a,o})= U_o A_o \frac{\left(t_i - t_{a,o}\right)}{\ln\left(\dfrac{t_i - t_e}{t_{a,o} - t_e}\right)} \tag{19}$$

$$\frac{1}{U_o A_o} = \frac{1}{h_B A_i} + \frac{1}{h_o\left(A_p + \eta_f A_f\right)} + \frac{\delta}{k_m A_m} \tag{20}$$

$$h_B = 1711 [D_h^{0.5} n_p W]^{-0.4} \tag{21}$$

Similar to the condenser and in accordance with the discussion presented before, the factor G will not be a constant. It was found to be closely related to the face velocity. Therefore, it is appropriately expressed as a function of this velocity.

The evaporator capacity is evaluated for a large number of values of the temperature difference ($t_i - t_e$) and the face velocity. The curve-fitting procedure to derive an expression for the factor G is executed in two meshed stages (two nested repetitive loops). It is based on a linear relation between the capacity and the temperature difference, for any fixed face velocity, and on a parabolic relation between the factor G and the face velocity. Thus, G will take the form

$$G = A_e \, v_f^2 + B_e \, v_f + C_e \qquad \qquad (22)$$

Due to the constraints imposed by space limitations in a car, the evaporator face velocity may be well above the practical range encountered in residential applications. This is also encouraged by the higher tolerable noise level. These considerations should be taken into account, by the program user, when introducing the evaporator face velocity among the input list.

Simultaneous solution of performance equations

This section is responsible for the simultaneous solution of the performance equations, derived in the preceding sections, to get the balance-point conditions and energy exchange rates for the whole integrated system.

The successive-substitution method was first adopted. It was successful in many cases. But, it was noticed that as the value of the factor G and/or the factor F decreases, the number of iterations required to reach the solution increased drastically ; even with trying different arrangements for the information-flow diagram. At values of F and G in the order of the first decimal place, the number of iterations was very large; as high as tens of thousands.

In fact, and with the aid of computers, the large number of iterations is not, in itself, a problem as long as a solution is finally reached. The computer-running time hardly exceeded one minute on any regular PC. The real problem was that the procedure is very sensitive to the values of F and G. At a certain sharp minimum limit, of either, the solution suddenly went into an oscillatory mode and convergence could never be reached. This limit varies from one case to another.

In automobile air conditioning applications, which are the subject in hand, both the condenser and evaporator are relatively small. Accordingly, low values of F and/or G may be frequently encountered. Therefore, and in our case, it was concluded that the traditionally-used method of successive substitution could not be always trusted. Another alternative and innovative method had to be contrived.

A new method was based on equating the cooling capacities from the compressor and evaporator sides; and equating the heat-rejection capacities from the compressor and condenser sides. This yielded two quantities R_1 and R_2 which are functions of the evaporating and condensing temperatures and should be equal to zero. The computational sequence starts from trial values of t_e and t_c. Then, the Jacobian of the transformation of R_1 and R_2 into t_e and t_c is evaluated; in a matrix form. The inverse of the Jacobian is obtained and multiplied by the vector of R_1 and R_2 to get the corrections of t_e and t_c. The new, or corrected, values of temperatures are used as input to the next iteration. This sequence continues till both t_e and t_c converge to the balance-point values; i.e. till no further significant changes are noticed in the values of t_e or t_c.

During the course of iterations, the energy exchanges of the system are repeatedly calculated; they also converge to the final operating values.

The new method of calculations represented a breakthrough in accelerating the convergence under all conditions. A large number of widely different cases were tested; the number of iterations, required to reach convergence, did not exceed a single digit. The new method of iteration is listed below

$$R1 = c_1 + c_2 t_e + c_3 t_e^2 + c_4 t_c + c_5 t_c^2 + c_6 t_e t_c + c_7 t_e^2 t_c + c_8 t_e t_c^2$$
$$+ c_9 t_e^2 t_c^2 - G \, (\, t_i - t_e \,) \qquad \qquad (23)$$
$$R2 = e_1 + e_2 t_e + e_3 t_e^2 + e_4 t_c + e_5 t_c^2 + e_6 t_e t_c + e_7 t_e^2 t_c + e_8 t_e t_c^2$$
$$+ e_9 t_e^2 t_c^2 - F \, (t_c - t_a) \qquad \qquad (24)$$

$$\begin{bmatrix} R11 & R12 \\ R21 & R22 \end{bmatrix} \begin{bmatrix} \Delta t_e \\ \Delta t_c \end{bmatrix} = \begin{bmatrix} R1 \\ R2 \end{bmatrix} \tag{25}$$

$$\text{Where } R11 = \frac{\partial R1}{\partial t_e}, \quad R12 = \frac{\partial R1}{\partial t_c}, \qquad R21 = \frac{\partial R2}{\partial t_e}, \text{ and } \quad R22 = \frac{\partial R2}{\partial t_c} \tag{26}$$

The iteration continues until the errors in the cooling and heat-rejection capacities are brought down to below arbitrarily-specified maximum limits. These limits are set, in the program, to guarantee the accuracy of calculated capacities to be of the order 0.0001 kW. This is an exaggeratively tight accuracy taking into consideration the nature of application. It would represent a percentage error well below 0.003% for all expected sizes of automobile-cooling systems. In fact, these low limits were meant to be a hard test for the solution convergence.

Whenever required, the accuracy can be easily tightened or relaxed at will. This would require just a change of the limits set in the program.

Program Output
The final results of the component-matching procedure are:
1. The equilibrium evaporating temperature at balance point.
2. The equilibrium condensing temperature at balance point.
3. The cooling capacity.
4. The indicated power input to compressor.
5. The rate of heat removal from condenser.

5. Closure

The computer program was first tested against some benchmark cases to check its integrity and accuracy. Then, it was successfully employed in a large number of design jobs; by design engineers of a specialized company. It proved to be a helpful tool for automotive air-conditioning designers.

Different alternative component combinations could be easily compared. The effects of various operating conditions could also be readily foreseen. The program could be used for any vehicle size; from small private cars up to large buses.

6. References

[1] Jolly, P. G, Tso, C. P., Wong, Y. W., Ng, S. M., "Simulation and measurement on the full-load performance of a refrigeration system in a shipping container" *International Journal of Refrigeration*, Volume 23, Issue 2, March 2000, Pages 112-126

[2] Lee, G. H. and Yoo, J. Y., "Performance analysis and simulation of automobile air conditioning" *International Journal of Refrigeration* Volume 23, Issue 3, May 2000, Pages 243-254

[3] Stoecker W. F. and Jones J. W., *Refrigeration and Air Conditioning*, TATA McGraw-Hill Publishing Company, New Delhi, 1983.

[4] Arora C. P., *Refrigeration and Air Conditioning*, TATA McGraw-Hill Publishing Company, New Delhi, 1983.

[5] Dossat R. J., *Principles of Refrigeration*, John Wiley and Sons, New York, 1961.

[6] Jabardo, J. M. S., Mamani, W. G. and Ianella, M. R., "Modeling and experimental evaluation of an automotive air conditioning system with a variable capacity compressor" *International Journal of Refrigeration*, Volume 25, Issue 8, December 2002, Pages 1157-1172

[7] Jabardo J. M. S. and Mamani W. G., "Modeling and Experimental Evaluation of Parallel Flow Micro Channel Condensers", *Journal of the Brazilian Society of Mechanical Sciences and Engineering,* Vol. 25 No. 2 Rio de Janeiro, 2003.

[8] Kays W. M. and London A. L., *Compact Heat Exchangers*, McGraw-Hill Book Company, New York, 1958.

[9] Holman J. P., Heat Transfer, McGraw-Hill Book Company, Tokyo, 1968.

7. Appendices

Appendix A : Thermodynamic properties of refrigerant 134a

1. Saturation pressure-temperature relation
    $$\ln (P) = -35.94481 + 0.265213*T - 0.6782399*10^{-3}*T^2 +$$
    $$0.6323821*10^{-6}*T^3 \qquad \text{MPa} \quad (A.1)$$

2. 2- Enthalpy of subcooled liquid
    $$h = -6.702179 + 0.1675422 *T + 0.2154294*10^{-2}*T^2 \qquad \text{kJ/kg} \quad (A.2)$$

3. 3- Enthalpy and entropy of superheated vapor
    $$h = 155.1313 + 0.8471667 * T + 0.209139 * 10^{-3} * T^2$$
    $$+P *[34.7401 - 0.3860322 * T + 0.672008*10^{-3} * T^2] \quad \text{kJ/kg} \quad (A.3)$$
    $$s = 1.100179 + 0.297224*10^{-2} * T - 0.166979* 10^{-5} * T^2$$
    $$+ P [-1.479631 + 0.67361*10^{-2} * T - 0.79838*10^{-5} * T^2] \text{kJ/kg.K} (A.4)$$

4. 4- Enthalpy and entropy of saturated vapor
    $$h = 83.23572 + 1.742258 *T - 0.2140479 *T^2 \qquad \text{kJ/kg} \quad (A.5)$$
    $$s = 1.69001 - 27.95583 / T + 10543.32 / T^2 \qquad \text{kJ/kg. K} \quad (A.6)$$

    In Eqns. (A.1) to (A.6), T is in K and P is in MPa

5. 5- Density at suction (valid for both saturated and superheated vapor)
    $$\rho = a\, t^2 + b\, t + c \qquad (A.7)$$
    where   t is the suction temperature in °C
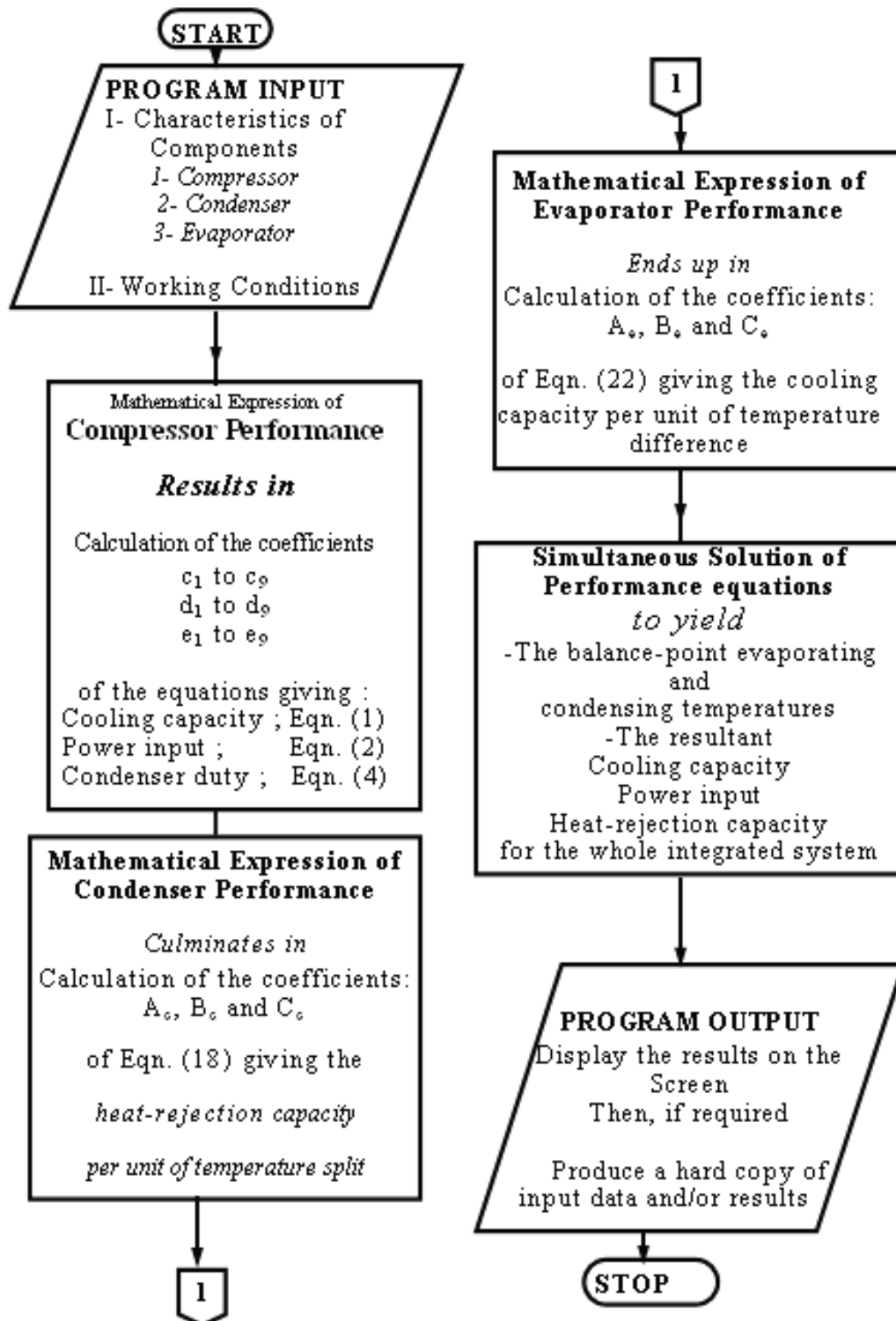 $$a = 0.00005\ P^2 + 0.0005\ P - 0.000002 \qquad (A.8)$$
    $$b = 0.0029\ P^2 - 0.2386\ P + 0.0072 \qquad (A.9)$$
    $$c = 9.63\ P^2 + 46.947\ P - 0.179 \qquad (A.10)$$
    where P is the suction pressure in MPa.

Appendix B: Program flow chart

START

PROGRAM INPUT
I- Characteristics of
Components
1- Compressor
2- Condenser
3- Evaporator

II- Working Conditions

Mathematical Expression of
Compressor Performance

Results in

Calculation of the coefficients
c_1 to c_9
d_1 to d_9
e_1 to e_9

of the equations giving :
Cooling capacity ; Eqn. (1)
Power input ;   Eqn. (2)
Condenser duty ;   Eqn. (4)

**Mathematical Expression of
Condenser Performance**

Culminates in
Calculation of the coefficients:
A_c, B_c and C_c

of Eqn. (18) giving the

heat-rejection capacity

per unit of temperature split

1

1

**Mathematical Expression of
Evaporator Performance**

Ends up in
Calculation of the coefficients:
A_e, B_e and C_e

of Eqn. (22) giving the cooling
capacity per unit of temperature
difference

**Simultaneous Solution of
Performance equations**
to yield
-The balance-point evaporating
and
condensing temperatures
-The resultant
Cooling capacity
Power input
Heat-rejection capacity
for the whole integrated system

PROGRAM OUTPUT
Display the results on the
Screen
Then, if required

Produce a hard copy of
input data and/or results

STOP

*mahmoudkassem@yahoo.com   **aymr@link.net

$\left(\text{م}٢٠٠٨/١٢/١ \qquad\qquad / / \qquad\qquad\right)$

.

.

.   .

.

A Study of Exergy Analysis for Combustion in Direct
Fired Heater (Part I)

Bahgat K. Morsy*, and Ahmed Ali Abd El-Rahman Ali**
* Mechanical Engineering Dept., Faculty of Engineering, Qassim University, bahgat@qec.edu.sa
**Mechanical Engineering, Egyptalum Company, ahmed, 3a2000@yahoo.com

Abstract. Heat transfer plants with organic media have often been able to replace or improve the classic steam–water operation. The possibility of transferring and closely controlling temperature up to $> 300\,^{\circ}C$ has provided the heat transfer media technology with many new fields of application. This growing application of heat transfer plants with liquid heat transfer media other than water has made it necessary to produce complete and accurate engineering database for combustion and its devices to continuous improvement of industrial heating. Heating is an important operation in almost all industrial fields. A large variety of heating techniques is available at the market. Some examples are fuel burning, electrical heating, and so on. The analysis of related combustion process and estimation of the effective coefficients is the first step toward a successful design. The process of combustion fuel and their combustion and combustion devices are considered in this study, direct fired heater exergy and energy analysis are performed taking into account precise calculation of chemical exergy for products of combustion.
Keywords: Exergy, Energy, Combustion, Thermal System.

Nomenclature

A	Area [m^2]	S	Distance [m]
A_{Abs}	The absolute availability of a system [-]	S_o	Entropy of a system at environmental state [J/kg]
C_p , c	Specific heat capacity [J/kgK] or heat capacity [J/kg]	S_i	Specific entropy, of substance I, [J/kgK]
E, E	Specific exergy [J/kg] or available work [J]	T	Temperature [K]
E_f	Fuel exergy [kJ/kg]	u, U	Specific internal energy [J/kg] or internal energy [J]
$e^{ch} = A_{ch}$	Chemical exergy [kJ/kg]	v, V	Specific volume [m^3/kg] or volume [m^3]
E/Q	Exergy factor [no unit, %]	σ	Stefan-Boltzmann constant [W/m^2K^4]
H, H	Specific enthalpy [J/kg] or enthalpy [J]	Є	The emissivity [-]
m_a	Mass flow rate of air [kg/s]	ώ	Exergetic efficiency [-]
m_f	Mass flow rate of fuel [kg/s]		
m_e	Mass flow rate of exhaust flue gas [kg/s]		
P	Power [kW]		
P_o	Environment pressure [bar]		
Q, Q	Specific heat [J/kg] or heat [J]		
Q, Q	Specific heat [J/kg] or heat [J]		
$\bar{R}$	Molar gas constant [J/mol K]		

1. Introduction

Traditional methods of thermal system analysis are based on the first law of thermodynamics. These methods use an energy balance on the system to determine heat transfer between the system and environment. The first law of thermodynamics introduces the concept of energy conservation, which states that energy entering a thermal system with fuel, electricity, flowing streams of matter, and so on is conserved and can not be destroyed. In general, energy balances provide no information on the quality or grades of energy crossing the thermal system boundary and no information about internal losses. By contrast, the second law of thermodynamics introduces the useful concept of exergy in the analysis of thermal systems.

Exergy is a measure of the quality or grade of energy and it can be destroyed in the thermal system. The second law states that a part of the exergy entering a thermal system with fuel, electricity, flowing streams of matter, and so on is destroyed within the system due to irreversibilities.

Energy and Exergy

In recent years, exergy analysis has played a key role in order to evaluate processes by taking into account not only the quantity of energy but also both the quantity and quality of energy. Various definitions have been used to describe the term of exergy. Exergy is defined as the maximum amount of work which can be produced by a system or a flow of matter or energy. Exergy is a measure of the potential of the system or flow to cause change, as a consequence of not being completely stable equilibrium relative to the reference environment. Unlike energy, exergy is not a subject to a conservation law (except for ideal or reversible processes). Rather exergy is consumed or destroyed due to irreversibilities in any real process. The exergy consumption during a process is proportional to the entropy created due to irreversibilities associated with the process.

Theoretical Analysis

Exergy analysis is a method using the conservation of mass and conversion of energy principles together with the second law of thermodynamic for the analysis, design and improvement of energy and other systems. An exergy balance applied to a process or a whole plant tells us how much of the usable work potential or exergy supplied as the input to the system under consideration, has been consumed by the process.

The loss of exergy or irreversibility provides a generally applicable quantitative measure of process inefficiency. In other words, an Exergy analysis is similar to an energy analysis, but it takes into account the

quality of the energy as well as the quantity. Since it includes a consideration of entropy, Exergy analysis allows a system to be analyzed more comprehensively by determining where in the system the Exergy is destroyed by internal irreversibilities, and the causes of those irreversibilities.

2. Combustion and Exergy

The purpose of combustion in industrial applications, for the most part, is to transform chemical energy available in various types of fuels to thermal energy or heat to be used in the processing of gas or liquid streams or solid objects. Typical examples involve the heating of air, water, and steam for use in heating of other processes or equipment, the heating of metals and nonmetallic minerals during production and processing, the heating of organic streams for use in refining and processing, as well as heating of air for space comfort conditioning. For all of these, it is necessary to have a workable method for evaluating the heat that is available from a combustion process. Available heat is the heat accessible for the load (useful output) and to balance all losses other than stack losses.

Exergy is a measure of the energy available for useful work in a system. This property is also referred to as Availability. Exergy is a better measure of the work that may be extracted from a system rather than properties such as the internal energy or enthalpy of the system. No device or process can extract a quantity of work greater than the availability of the system without violating the second law of thermodynamics. Thus, the availability of a system also helps to define the upper limit on the efficiency of the device/process.

The method of Exergy analysis presented in this investigation enables us to identify the location, cause and true magnitude of energy resource waste and to determine losses. Such information can be used in the design of new energy-efficient systems and for improving the performance of existing systems.

3. Exergy Balance

Exergy can be transferred by three means:
1. Exergy transfer associated with work.
2. Exergy transfer associated with heat transfer.
3. Exergy transfer associated with the matter entering and exiting a Control Volume.

Exergy is also destroyed by irreversibility within the system or control volume. Fig.1. shows exergy flow diagram. In this figure E_{tr} represent exergy transit and E_{pr} represent exergy used by process.
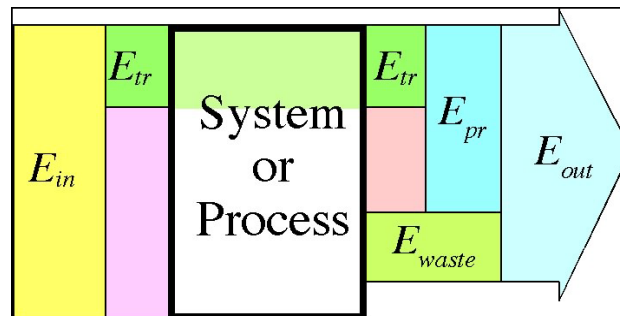

Fig. (1). Exergy flow diagram.

4. The Objective of Investigation

Direct fired heaters are the most common industrial Heating facilitates. They are readily employed for a wide range of applications and can be powered on various fuels depending on the local availability. Their many advantages and relative lack of competition has made Direct fired heaters one of the preferred devices for converting the chemical energy of fuels into thermal energy. The current work attempts to understand the destruction of exergy (availability) in combustion processes and compare it with the losses of energy, with specific application to direct fired heaters. However, the analysis is not restricted to direct fired heaters and is applicable to all combustion processes.

From the literature review, it is evident that a comprehensive second law examination of combustion processes is lacking. Such a study would provide a more fundamental understanding of combustion processes and help in identifying strategies to reduce the destruction of exergy during combustion processes. Some work has been done towards applying the second law to combustion by Dunbar and Lior [1] (constant pressure combustion) and Daw *et al*. [2] (constant pressure combustion) and Caton [3] (constant volume). These studies however, were restricted to a particular combustion process and did not strictly quantify the contribution of the various exergy terms. The current study wishes to apply the second law to the combustion process, while relaxing most of the approximations and simplifications made in the past. It is hoped that an inclusive examination of the various parameters will provide a   more fundamental and complete understanding of the combustion processes. The current work also aims to incorporate excess air ratio into the study to allow for comparison of the combustion of different equivalent ratios. For more accurate analyses chemical exergy will be calculated in this study. The combustion process analyzed will be in the (direct fired heater), used in purpose of heating of heat transfer medium (Mineral Oil MOBILTHERM 605), in plant of heating of thermal oil in EGYPTALUM company in Nag-Hammady, Egypt.

5. Thermal Oil Plant Operation

Thermal oil system is shows in Fig. (2). The figure provides an efficient means of supplying indirect heat to one or more process systems. Such systems offer both high temperature and low pressure, making them ideal for a wide variety of process heating application. The heat transfer fluid firstly heated by means of a direct fired heater then circulated through a closed loop systems to the users. Heat from the fluid is transferred to the user and then re-circulated for reheating and the cycle repeated. However, organic media has become more common and often replaces a classic steam-water operation. The heaters are made with coils made of seamless tubes. The thermal fluid is heated during the flow through the tubes. The heat is transferred to the fluid as radiant heat in the combustion chamber, where the inner cylindrical tube coil and a flat tube coil form the chamber wall and the bottom respectively. Consequently refractory concrete is avoided. The combustion gasses are hereafter cooled in the outer convection part, as the gasses pass the space between the two tube coils. The thermal design ensures a modest volume of the thermal fluid relative to the size of the heater, and allows unlimited thermal expansion due to the high fluid temperature.
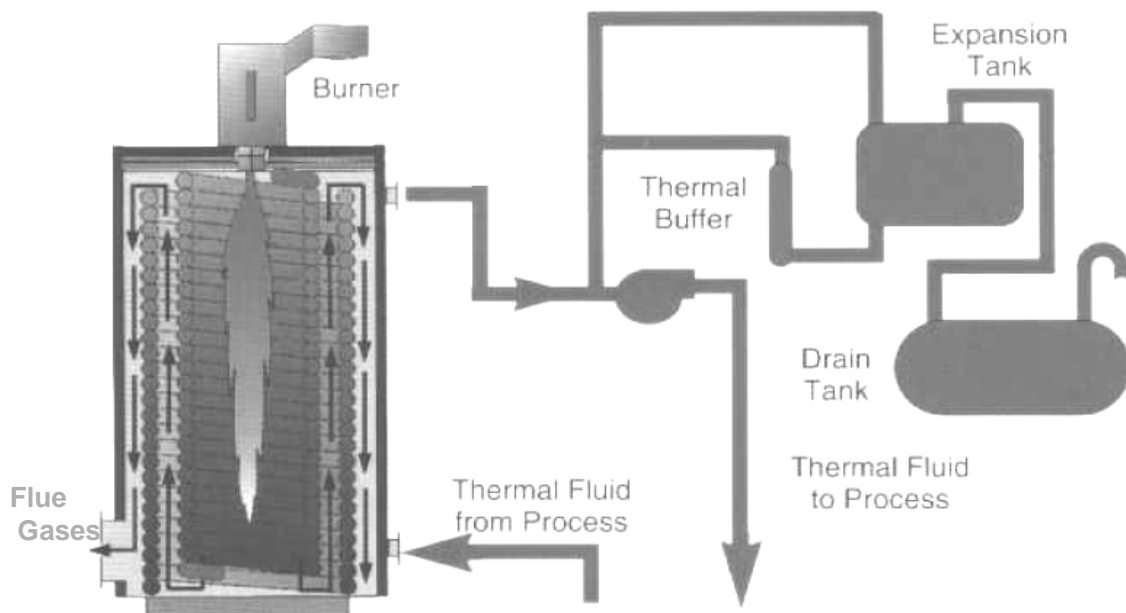

Fig. (2). Simple schematic diagram for thermal oil plant.

The fuel that will be used in this test will be fuel oil no.6 that is named in Egypt and Arab countries as (Mazout); this fuel must be heated before using because it's high viscosity at ambient temperature. Table (1) shows fuel chemical analysis for typical heavy oil No.6 by weight.

Table (1). Fuel chemical analysis for typical heavy oil no.6 by weight.

Fuel Components	C	H_2	N_2	O_2	S
% By Weight	87.87	10.33	0.14	0.50	1.16

Almost all industrial liquid fuel burners use atomization to aid vaporization by exposing the large surface area (relative to volume) of millions of droplets in the size range of 100-400 μm. Evaporation then occurs at a rapid rate even if the droplets are not exposed to furnace radiation or hot air due to enhanced mass transfer rates.

Rotary-cup atomization delivers the liquid fuel to the center of a fast-spinning cup surrounded by an air stream. Rotational speed and air pressure determine the spray angle. This is still used in some large boilers, but the moving parts near the furnace heat have proved to be too much of a maintenance problem in higher temperature process furnaces and on smaller installations where a strict preventive maintenance program could not be affected.

6. Flue Gas Analysis

The major constituents in flue gas are CO_2, O_2, N_2 and H_2O. Excess air is determined by measuring the O_2 in the flue gas. Before proceeding with measuring techniques, consider the form of the sample. A flue gas sample may be obtained on a wet or dry basis. When a sample is extracted from the gas stream, the water vapor normally condenses and the sample is considered to be on a dry basis. The sample is usually drawn through water near ambient temperature to ensure that it is dry. The major constituents of a dry sample do not include the water vapor in the flue gas.

When the gas is measured with an in situ analyzer or when precautions are taken to keep the moisture in the sample from condensing, the sample is on a wet basis. The amount of O_2 in the flue gas is significant in defining the status of the combustion process. Its presence always means that more oxygen (excess air) is being introduced than is being used. Assuming complete combustion, low values of O_2 reflect moderate excess air and normal heat losses to the stack, while higher values of O_2 mean needlessly higher stack losses. The quantity of excess O_2 is very significant since it is a nearly exact indication of excess air.

The O_2 is an equally constant indication of excess air when the gas is sampled on a wet or in situ basis because the calculated excess air result is insensitive to variations in moisture for specific types/sources of fuel. The current industry standard for heaters operation is continuous monitoring of O_2 in the flue gas with in site analyzers that measure oxygen on a wet basis. For testing, the preferred instrument is an electronic oxygen analyzer.

The flue gas analyzer unit, which measures (CO_2 SO_2) and O_2 on a dry volumetric basis, remains a trusted standard for verifying the performance of electronic equipment. The flue gas analyzer uses chemicals to absorb the (CO_2 SO_2) and O_2, and the amount of each are determined by the reduction in volume from the original flue gas sample

7. Temperature Measurements

Thermal oil inlet, thermal oil outlet, ambient temperature, fuel oil temperature, flue gas temperature and outer surface temperature, all are measured in this study for more accurate calculation. All measurements of temperature included in this investigation will be executed by PT-100 thermocouple (Type K) Fig. 3. Temperature of thermal oil inlet, thermal oil outlet, fuel oil inlet, and flue gas were measured by PT-100 thermocouple. Temperature of outer surface of heater was measured by using device which uses Infrared sensor technology to measure temperature of surfaces without contact.

8. Method of Calculation

The most commonly used indicator for the efficiency of energy conversion process is the ratio of the output of useful energy to the total energy input. This ratio is called first law efficiency. It is based on a quantitative accounting of energy, which reflects recognition of the first law of thermodynamics and the law of conservation of energy.

It is well known that the second law of thermodynamics defines the availability of energy more restrictively than the first law. Principally, first law is silent on the effectiveness with which availability is concerned. Analysis in terms of the second law of thermodynamics more closely describes the effectiveness with which systems or processes use available energy.

Each calculation of exergy and thus each exergetic analysis imply reference state called 'dead state'. If a system is in thermal and mechanical equilibrium with the reference environment that is at the environmental temperature T_O and Pressure P_O, it is said to be in a thermodynamically dead state or restricted dead state. In general it is taken as $T_O = 298$ K and $P_O = 1$ atm.

Exergy losses are calculated by making exergy balance for each component of the system. Unlike energy balance where the inflow is equal to outflow (when there is no internal energy generation or consumption), in exergy balance due to reasons of irreversibility, exergy inflow is always greater than the exergy outflow and their difference gives the exergy loss or exergy destruction. Ratio of exergy output to exergy input gives the exergetic efficiency of a system [4].

$$\omega = \text{Exergetic efficiency} = \frac{\text{Exergy output}}{\text{Exergy input}} \qquad (1)$$
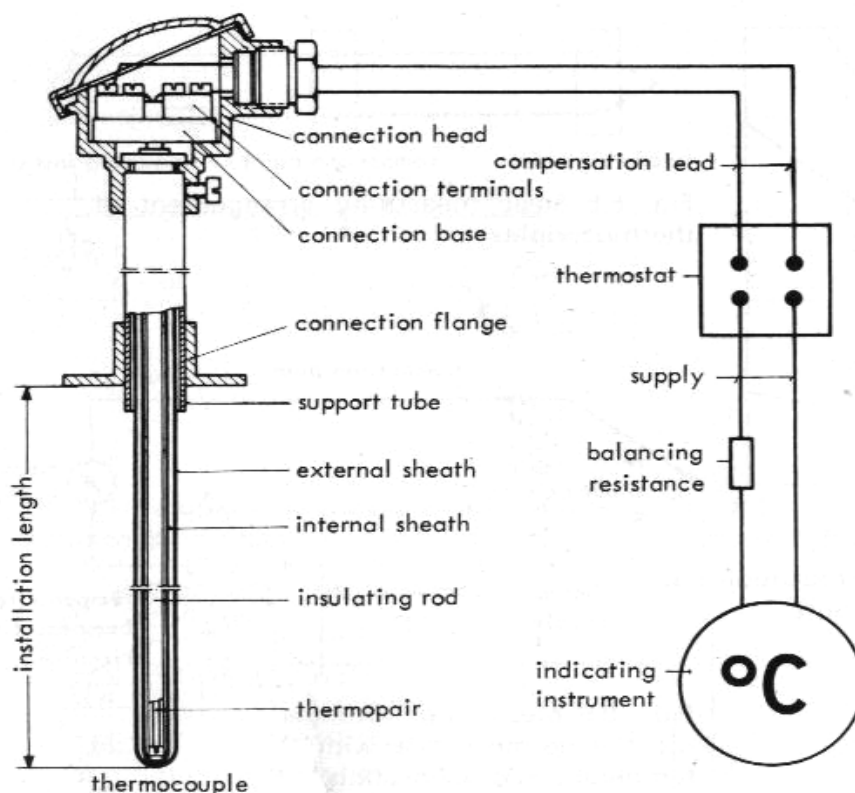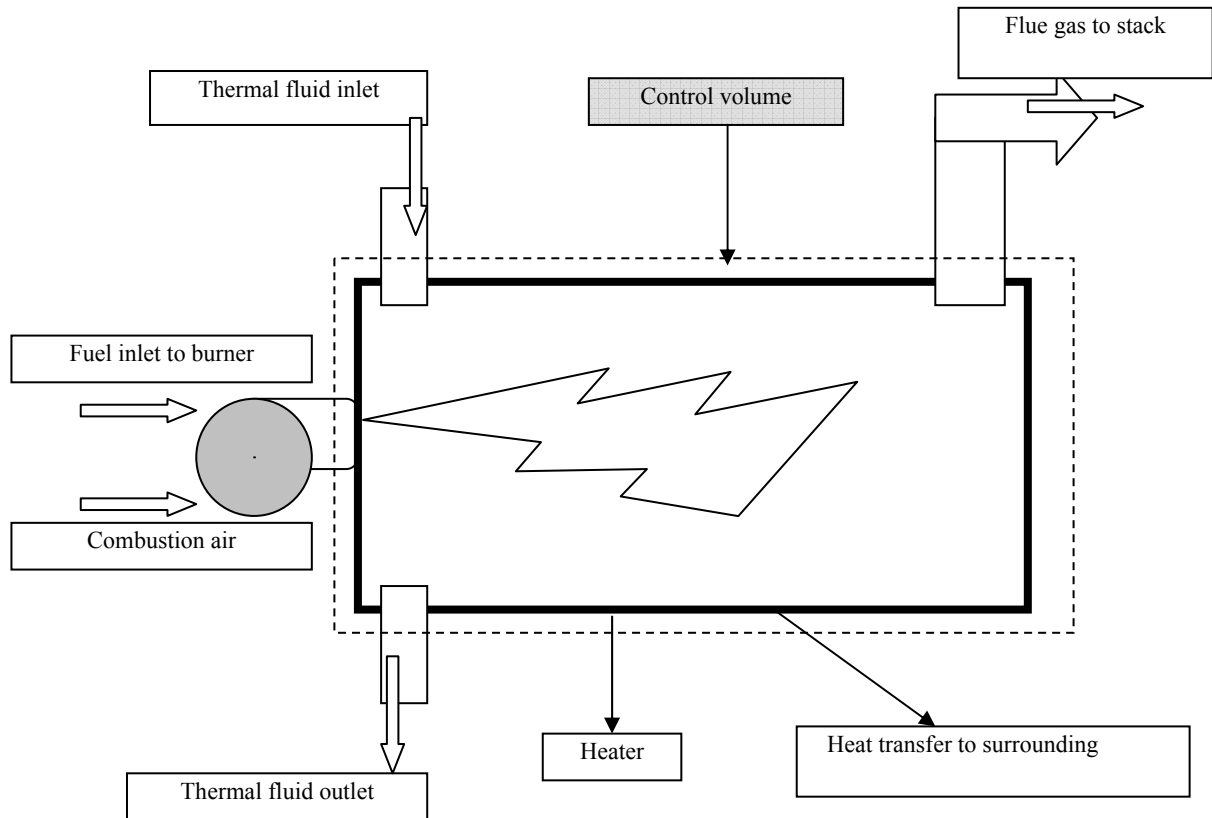

Fig. (3). PT- 100 Thermocouple (type K).

Fig. (4). Schematic diagram for the control volume of a test rig.

Exergy Calculation (Second Law of Thermodynamics)

The objective of this section is to introduce exergy analysis, a method that uses the conservation of mass and conservation of energy principles together with the second law of thermodynamics for the investigate and analysis of combustion process and thermal systems. Another term frequently used to identify exergy analysis is availability analysis.

Following usual conventions [5-7], the absolute availability, A_{Abs} of a system is defined as

$$A_{Abs} = \tilde{U}\ T_0 \tilde{S}\ P_0 V \tag{2}$$

Where U, S and V are the internal energy, entropy and volume of the system respectively, while T_0 and P_0 are the reference temperature and pressure. The work that may be extracted from a system is also limited by the reference conditions. The work that may be extracted from the system is then given by the (thermo-mechanical) availability, A_{TM}, of the system, which is defined as

$$A_{TM} = (\tilde{U}\ U^o)\ \tilde{T}_0\ (\tilde{S}\ S^o)P_0\ (\tilde{V}\ V^o) \tag{3}$$

Where U^o, S^o and V^o are the internal energy, entropy and volume of the restricted dead state respectively.

The restricted dead state is achieved by allowing the system to come to thermo-mechanical equilibrium with the environment, typically the atmosphere. The restricted dead state has the same pressure and temperature as the environment, however, the composition of the restricted dead state is the same as that of the original system and is not necessarily the same as that of the environment. The current work uses this definition of the restricted dead state, in conformance with the standard literature [5-7], with a temperature of 298.15 K and

pressure 101.325 kPa for the restricted dead state and the reference conditions. This difference in composition between the restricted dead state and the environment can be exploited to further obtain work from the system. This work, obtained by allowing the restricted dead state to come to chemical equilibrium with the environment, is referred to as the chemical exergy, A_{Ch}, of the system.

$$A_{Ch} = \sum_{k=1}^{n} N_k \left(\mu_k^0 - \mu_{k,0} \right)$$

(4)

Where N_k is the number of moles of the respective species (k) and $\mu_{k,o}$ & μ_k^o are the chemical potentials of the respective species in the restricted dead state and the environment, respectively. The chemical potentials may further be expressed as:

$$\mu_k = g_k(T_0, P_0) + \bar{R} T_0 \ln \left(\frac{p_k}{p_0} \right)$$

(5)

Where g_k is the Gibbs energy of the kth species in the mixture $\bar{R}$ is the Universal gas constant and p_k is the partial pressure of the kth species in the mixture. If the restricted dead state and the environment, both had the same constituent species, differing only in their respective compositions, the Gibbs energy term would cancel out, leaving a simpler expression for the chemical availability of the system

$$A_{Diff} = \bar{R} T_0 \sum_{k=1}^{n} N_k \ln \left(\frac{p_k^0}{p_{k,0}} \right)$$

(6)

The difference in concentrations of the various species in the system and the atmosphere may be exploited by first separating the various components in the mixture (using devices such as semi-permeable membranes) and then allowing them to expand or compress to the atmospheric partial pressures, as the case may be. Work may be gained or lost during this process and this creates an additional potential for work. Since this term may be attributed to the work obtained by allowing the species in the system to diffuse to the atmospheric concentrations, it would be appropriate to refer to this as the "diffusion availability". It may be noted that diffusion availability of a system can be positive or negative, depending on the concentrations of the various species in the system.

The diffusion availability of a system is largely ignored since its contribution is often small relative to the thermo-mechanical availability A_{TM} of the system. Also, it is not easy to extract the diffusion availability component of the availability since it would require the use of semi-permeable membranes to extract the various species in the mixture before allowing them to diffuse to atmospheric concentrations. It is also evident from the expression for the diffusion availability of a system that it depends on the composition of the environment. The assumed composition of the atmosphere therefore, makes a difference on the diffusion availability of the system. The current work uses a standard wet atmospheric unless otherwise stated.

The availability of a system, A_{Total}, incorporating the various components would then be

$$A_{Total} = (U - U_0) - T_0(S - S_0) + P_0(V - V_0) + \sum_{k=1}^{n} N_k \left(\mu_k^0 - \mu_{k,0} \right)$$

(7)

The above expression for availability is valid for closed systems. For open systems, the flow availability, $A_{Total,f}$ needs to be considered. This is defined

$$A_{Total,f} = (H - H^0) - T_0(S - S^0) + \sum_{k=1}^{n} N_k \left(\mu_k^0 - \mu_{k,0} \right) \qquad (8)$$

Where H and H^0 are enthalpies of the system and the restricted dead state respectively.

In general, then, the availability of a system, A_{Total}, may be expressed as a sum of the thermo-mechanical availability and chemical availability.

$$A_{Total} = A_{TM} A_{Ch}$$

The chemical availability term may further be split into constituents, the reactive availability and diffusive availability as:

$$A_{Total} = A_{TM} A_{Reactive} A_{Diff} \qquad (10)$$

The importance of developing thermal systems which uses fossil fuel in the process of combustion that make effective use of nonrenewable resources such as oil, natural gas, and coal is apparent. The method of Exergy analysis is particularly suited for furthering the goal of more efficient resource use, since it enables the locations, types, and true magnitudes of waste and loss to be determined. This information can be used to design thermal systems, guide efforts to reduce sources of inefficiency in existing systems, and evaluate system economics.

8.2 Exergy Analysis Formulas

The start point in the Exergy analysis is Exergy balance for a system, Exergy balance in this system can be symbolized as:

$$E_{in} = E_{oil} + E_{stack} + E_{s,loss} + E_{Destruction} \qquad (11)$$

Where, E_{in} represent chemical exergy involved in fuel oil entering to combustion chamber, also exergy of fuel oil = LHV * 1.04, [5] that means E_{in} = 41033*1.04 = 42674.32 kJ/kg fuel.

E_{oil} in above equation represent Exergy flow to thermal fluid, and is calculated here from:

$$E_{oil} = \textbf{Exergy flow to thermal fluid}$$

$$= \overset{\bullet}{m} c_p (T_{out} - T_{in} - T_o \ln \frac{T_{out}}{T_{in}}) \qquad (12)$$

Where, the value 1.04 is factor multiply in lower heating value of fuel to get exergy value contained in fuel. [5].

$\overset{\bullet}{m}$ = Thermal fluid mass flow rate kg/hr, Cp = average specific heat capacity kJ/ (kg.k)

T_{out} = Thermal fluid outlet temperature Kelvin, T_{in} = Thermal fluid inlet temperature Kelvin.

E_{stack} in above equation represents exergy flow to surrounding with flue gas and calculated here from equation:

$$E_{stack} = \underline{h - h_0 - T_0 (s-s_0)} + e^{ch} \qquad (13)$$

Where, in above eq., h and s represent the specific enthalpy and entropy, respectively, at the inlet or exit under consideration; h_0 and s_0 represent the respective values of these properties when evaluated at the dead state. Values of h, s, h_0 and s_0 are from standard tables of thermodynamics. Where the underlined term is the thermo-mechanical contribution of exergy in combustion products, e^{ch} is the chemical contribution evaluated as following:

$$\overline{e}^{ch} = \overline{R} T_0 \sum_i y_i \ln \left(\frac{y_i}{y_i^e} \right) \qquad (14)$$

Where, $\overline{R}$ = Universal Gas Constant = 8.314 kJ/kmol. K and y_i and y_i^e denote, respectively, the mole fraction of component i in the mixture of combustion products at T_0, P_0 and in the environment, with assumption that products of combustion are modeled as an ideal gas mixture at all states considered.

$E_{s.loss}$ in main equation represents exergy flow to surrounding by radiation from the surface of heater and calculated here from equation:

$$E_{s.loss} = (1 - [T_o / T_{surf}])* Q_e \tag{15}$$

Where Q_e calculate (surface losses) which is quantified macroscopically by a modified form of the Stefan–Boltzmann law equation equation:

$$Q_e = \varepsilon \sigma A (T_s^4 - T_o^4) \tag{16}$$

$E_{Destruction}$ in main equation represents Exergy Destruction inside furnace because irreversibility and are calculated by making Exergy balance for control volume in this study.

9. Results Presentation and Analysis

In this study, exergy analysis was carried out for combustion in direct fired heater. A flue gas sample for 40 runs of restricted heater was taking and input and output streams for each run were studied. Exergy and energy balance for each run was evaluated and theoretical analysis was carried out using these results. These results include a complete energy and Exergy analysis for direct fired heater, therefore energy efficiency, exergetic efficiency; exergy losses, energy losses, irreversibility and exergy destruction within the system (control volume of test rig) are calculated.

Excess air ratios at variation of fuel oil flow rate, the following operating condition are tested:
1.Fuel oil flow rate=120 kg/hr,   2.Fuel oil flow rate=144 kg/hr,   3.Fuel oil flow rate=192 kg/hr,
4.Fuel oil flow rate=240 kg/hr,   5.Fuel oil flow rate=279 kg/hr,   6.Fuel oil flow rate=298 kg/hr
7.Fuel oil flow rate=318 kg/hr,   8.Fuel oil flow rate=336 kg/hr

Fig. (5) represents the variation of energy efficiency with excess air at different levels of fuel flow rate. The figure shows that the energy efficiency, for all curves, tends to decrease with the increase of excess air level. A closer look in the figure would show that the high values of energy efficiency are achieved in the range of 8% to 20% of excess air. For all levels of fuel flow rate, the energy efficiency values are limited in the range of 60% to 82%.
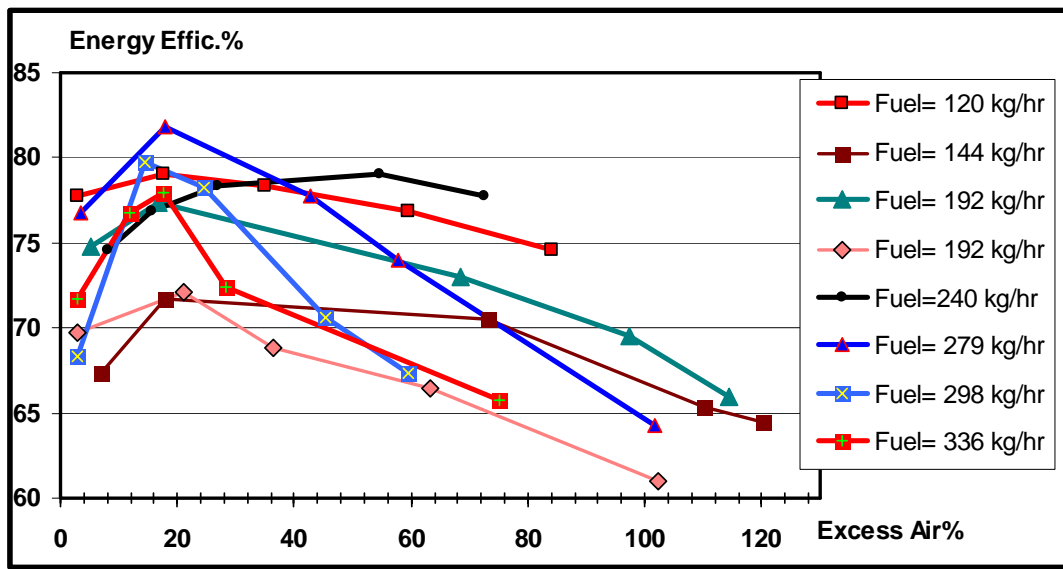

Fig. (5). Variation of the energy efficiency with excess air.

Fig. (6) shows the variation of exergy efficiency with excess air at different levels of fuel flow rate. It is clear that the trend is the same as it appears in figs. (1-5) but with change in values of exergy efficiency and energy efficiency. The figure shows that the energy efficiency reached a range of 18% to 24% instead of 60% to 82% at the same excess air of the range of 8% to 20%.
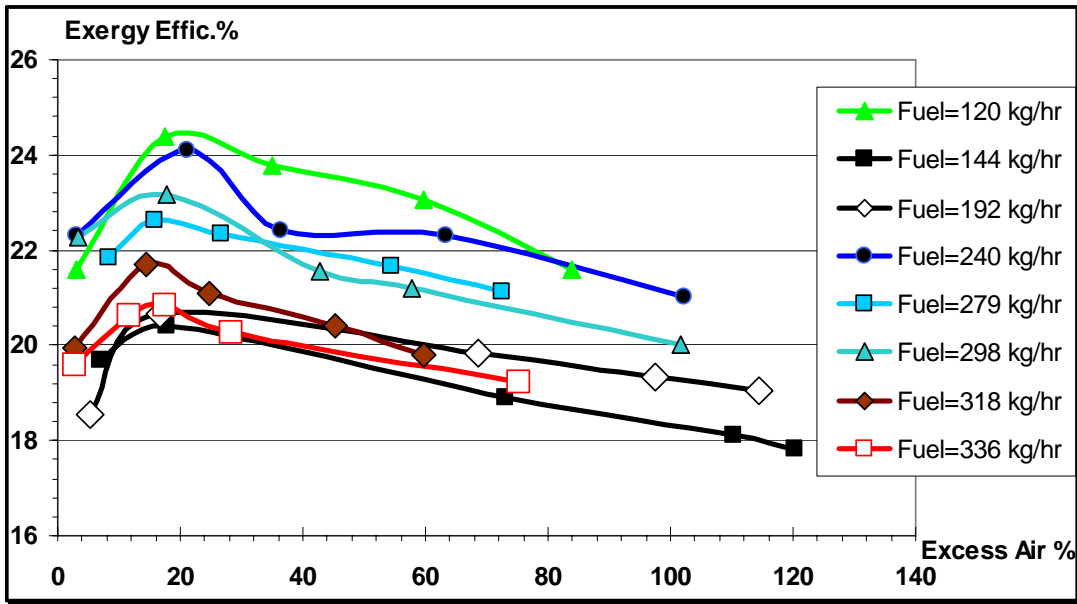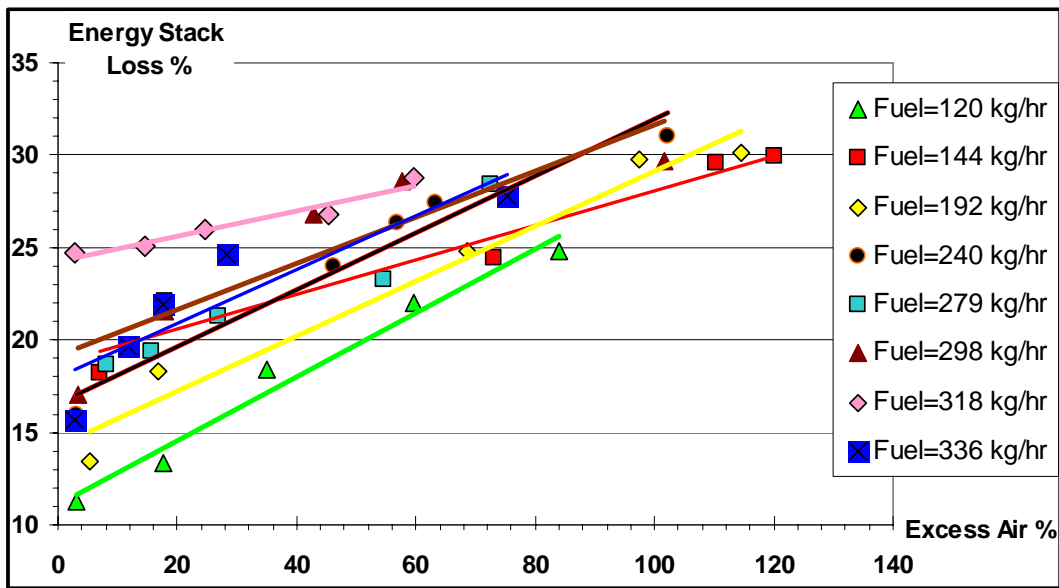
Fig. (6). Variation of the exergy efficiency with excess air.

Fig. (7) shows the variation of energy stack losses with the excess air at different level of fuel flow rate. In the figure, it is clear that general trend for the lines to go to high level of energy which goes to surrounding with flue gases with increase of excess air level, but in rang of 8% to 20% excess air stack losses decrease and return to increase again with excess air. Energy stack loss values are limited by the range 10% to 33% for all runs.

Fig. (7). Variation of the energy stacks losses with excess air.

Fig. (8) shows the variation of exergy stack losses with the excess air at different level of fuel flow rate, it is obvious that the trends of the curves are the same as they appear in Fig. 7; but with changes in value of exergy stack losses than energy stack losses, since energy stack losses vary in range of 10% to 33%, while exergy stack losses vary in range 32% to 73% for all runs.
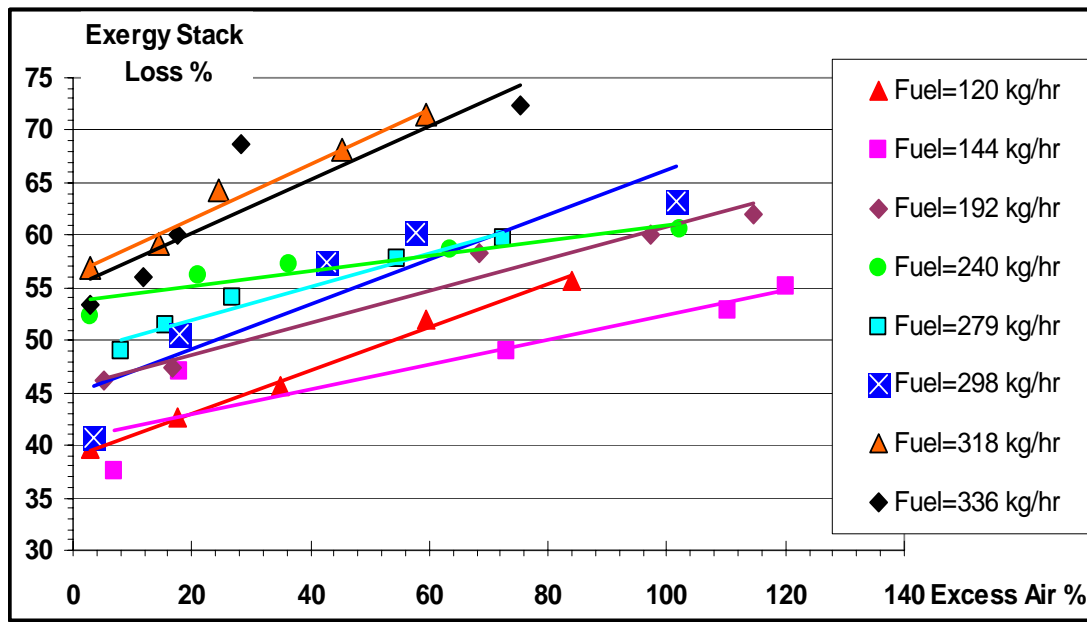
Fig. (8). The variation of exergy stack losses with variation of excess air.

Fig. (9) shows the variation of exergy destruction with the excess air at different level of fuel flow rate. In this figure, it appears that the exergy destruction within the system under investigation decreases while the excess air level increases for all runs that mean the irreversibility within the system decreases with the increase of excess air levels.
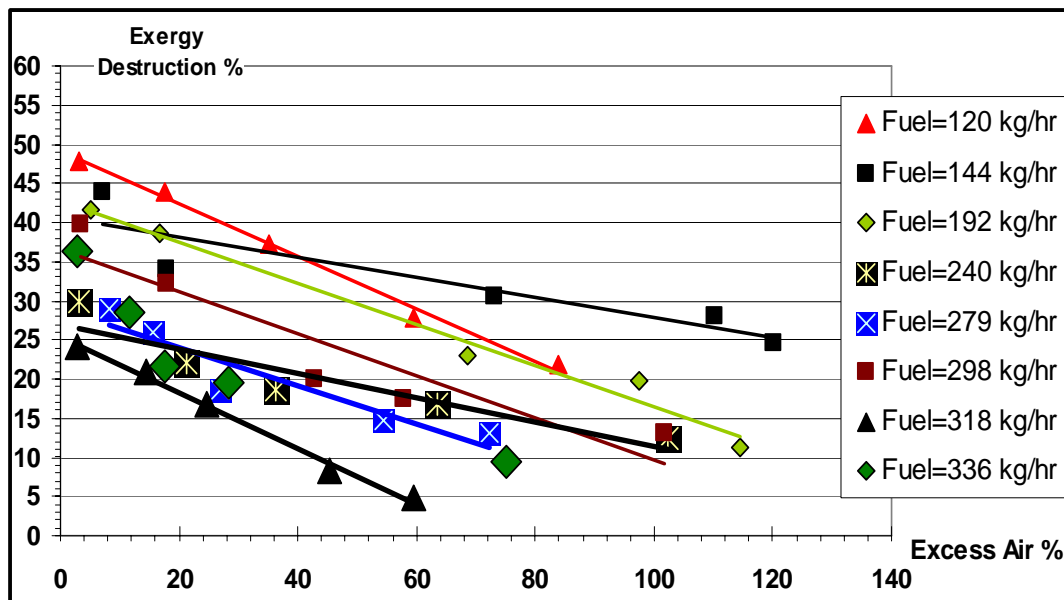

Fig. (9). The variation of exergy destruction with variation of excess air.

10. Conclusions

1. Exergy means the real work output that can be extracted from a given form of energy. According to this analysis the work output of the thermal fluid is in a very low level compared to the work input. Therefore the exergitec efficiency is very low comparing the energy efficiency in direct fired heater. The Exergy destruction is in the range of 12% to 60% in direct fired heater. The figures above show exergetic efficiency with flue gas temperature at different excess air levels.

2. The exergy loss through the flue gas is in the range of 20 % to 65 % in direct fired heater, and it is in the range of 0.004 % to 0.008 % for surface emission.

3. Depending on the previous figures the average exergetic efficiency becomes 22 % in direct fired heater. According to this analysis the minimum possible exergy losses in a direct fired heater should be within the following limits:-

Percentage exergy loss through flue gas - 20 %, percentage exergy loss through surface emission - 0.005 %. With reference to these limits the percentage exergy destruction is 60% and the exergetic efficiency is 22 %. This is the maximum possible exergetic efficiency that can be taken by maintaining the optimum running condition.

4. Reference to the previous figures, it is clear that there is a relationship between energy efficiency and exergetic efficiency. With increase of exergetic efficiency, the energy efficiency also gets increased.

5. The observable information gives a very good result:

A. Exergy destruction gets reduced with increase of flue gas temperature.

B. Exergy destruction gets increased with increase of amount of excess air at constant flue gas temperature and this effect is reduced with increase of flue gas temperature.

7. Therefore the amount of excess air is very important in exergy analysis of direct fired heater and should be maintained at the minimum possible limit. Though the exergy destruction gets reduced with increase of flue gas temperature the combined loss of exergy destruction and exergy loss through flue gas gets increased and also it increases with increase of excess air.

11. References

[1]   Dunbar, W.R., and Lior, N., "Sources of Combustion Irreversibility", Combustion Science and Technology; 103, (1994), 41-61.

[2]   Daw, S., Chakravarthy, K., Conklin, J., and Refining, G. R., "Understanding of Combustion Irreversibility", Proceedings of the Technical Meeting of the Central States, Section of the Combustion Institute, Austin, Texas, USA, March 21 – 23, (2004).

[3]   Caton, J.A., "On the Destruction of Availability (Exergy) Due to Combustion Processes – with Specific Application to Internal Combustion Engines", Energy; 25, (2002). 1097-1117.

[4]   Kotas, T.J., "The Exergy Method of Thermal Plant Analysis. Essex: Butterworth's", John Wiley and Sons Inc., New York, 1985.

[5]   Moran, M.J., and Shapiro, H.N. Fundamentals of Engineering Thermodynamics, Fourth Edition, John Wiley and Sons Inc., New York, (2004).

[6]   Moran, M.J., Availability Analysis: A Guide to Efficient Energy Use, Prentice Hall Inc., Englewood Cliffs, NJ, (1982).

[7]   Cengel, Y.A., and Boles, M.A., Thermodynamics: An Engineering Approach, Fourth Edition, McGraw Hill Publications: New York, 2002.

[8]   Kutz, M., Mechanical Engineers' Handbook: Energy and Power, Third Edition, Vol. 4, John Wiley & Sons Inc., (2006).

[9]   Caton, J.A., A Review of Investigations Using the Second Law of Thermodynamics To Study Internal Combustion Engines, SAE Technical Paper Series, Society of Automotive Engineers, (2000).

[10]   Gerpen, Van J.H., and Shapiro, H.N., "Second Law Analysis of Diesel Engine Combustion", Journal of Engineering for Gas Turbines and Power; .112, (1990), 129- 137.

[11]   Richter H.J., and Knoche, K.F., "Reversibility of Combustion Processes", Efficiency

[12]   and Costing: Second Law Analysis of Processes, ACS Symposium series, 235, and (1983), 71-85...

[13] Lutz, A.E., Larson, R.S., and Keller, J.O., "Thermodynamic Comparison of Fuel Cells to the Carnot Cycle", International Journal of Hydrogen Energy, 27, (2002), 1103- 1111.

[14] Rosen, M.A. and Dincer, I. ,"Exergy as the Confluence of Energy, Environment and

[15] Sustainable Development", Exergy, an International Journal, 1, (2001), 3-13...

[16] Cownden, R. et al., "Exergy Analysis of a Fuel Cell Power System for Transportation Applications", Exergy, an International Journal, 1, 2001), 112-121...

[17] Masanori Shukuya & Abdelaziz Hammache Introduction to the Concept of exergy - for a Better Understanding of Low-Temperature- Heating and High-Temperature-Cooling System, John Wiley and Sons Inc., New York, 2005.

(   )

**   *

                                                                    *

                                                            **

(/ /   / /   )

                                                                    .

                    .

                                                                                    .

An Optimal Algorithm for Parallel Point-wise and Block-wise Resolution
of a Triangular System on a Distributed Memory System

Mounir Marrakchi[(*)]
Management and Information System Dept. , College of Business & Economic,
Qassim University, Saudi Arabia
marrakchimounir@yahoo.fr

Abstract. We consider both point-wise and block-wise versions for solving a linear triangular system on a distributed memory machine. With p identical processors and for a problem of size N where $N/r=n=2pq+1$ ($q \geq 3$ and r being the block-size), we design an optimal parallel algorithm. We show its optimality in terms of both computing and communication costs. Finally, we determine the optimal value of the block size which minimizes the parallel execution time. A series of experimentations confirm the theoretical results.

Keywords: Communication, Optimality, Parallel Algorithms, Triangular System, Homogeneous environments

---

(*) Associate Professor and Researcher at Tunis-Elmanar University.

1. Introduction

Parallel resolution of a triangular system is an important step in resolution methods for dense systems. Many papers have been devoted to the study of this problem [1], [2], [3], [4], [5]. So far, a parallel algorithm with optimal efficiency has not been constructed yet. This is due to two reasons, i.e. processor activity has not been maximized yet, and the communication costs still predominate the computing cost due to fine granularity, especially for point-wise methods.   In this paper, our purpose is to design, using a distributed memory machine, an efficient parallel algorithm called "column oriented algorithm" (COA). Given a problem of size N that verifies N/r=n =2pq+1 where r is the block size of block, p is the number of available processors and q is an integer (q≥3), we show that in (COA) the p processors are active during the maximum possible time and communication cost is minimum. Furthermore, we determine the optimal block size minimizing the makespan. The remainder of the paper is organized as follows. In section 2, we introduce the 2-steps graph. In sections 3 and 4, we present our parallel algorithm (COA) and show its optimality by theoretically and practically analyzing its performances. Before concluding, in section 5, we determine the theoretical and practical values of the block size r_{opt} that minimizes execution time of (COA).

2. Block-wise Resolution of a Triangular System

Let us consider a triangular system (S) A x = b, where A=($a_{i,j}$), 1≤i, j≤ N, is a non singular lower triangular matrix and x, b are two vectors of size N. With reference to generality, we assume that N=nr and we split A into blocks of order rxr. We present in the following part the task decomposition {T_{ij}^r 1≤i≤n, i≤j≤n} of the lower triangular system resolution algorithm [6], [7]:

For i:=1 **To** n **Do**

Execute T_{ii}^r :<   **For** k:=(i-1)r+1 **To** ir **Do**

For   m:=(i-1)r+1 **To** k-1 **Do**

x_k:=x_k-$a_{k,m}$ x_m

EndFor

x_k := x_k/$a_{k,k}$

EndFor$^>$

For j:=i+1 **To** n **Do**

Execute T_{ij}^r :<**For** k:=(j-1)r+1 **To** jr **Do**

For   m:=(i-1)r+1 **To** ir **Do**

x_k:=x_k-$a_{k,m}$ x_m

EndFor

EndFor$^>$

EndFor

EndFor

Precedence constraints are:

(A) T_{ii}^r << T_{ij}^r 1≤i≤n, i+1≤j≤n,   (B) T_{ij}^r << $T_{i+1,j}^r$ 1≤i<n, i+1≤j≤n,

Where T<<T' means that the execution of task T precedes that of T'. In other words, data computed by T are required by T'. The task graph called 2-steps graph is depicted in figure 1 for N=6 and r=1 [6], [8]. It should be noticed, however, that T_{ii}^r corresponds to the resolution of a triangular system of size r. T_{ij}^r (i<j) corresponds to the elimination of r (already determined) unknowns in the r associated equations (Fig. 2). We note that figs (1-2) show how the task decomposition for r=2 differ from the task decomposition for r=1.

We deduce that the 2-steps graph is the precedence graph of block-wise resolution of a triangular system. In what remains, for simplicity, $T_{i,j}$ denotes T_{ij}^r. Let us precise that the 2-steps graph of size n involves n "columns", the i-th "column" C_i (1≤i≤n) being constituted by tasks $T_{1,i}$, $T_{2,i}$, ..., $T_{i,i}$ [4].

3. "Column Oriented Algorithm" (COA)

In this section, we describe a parallel algorithm for solving (S), called "Column Oriented Algorithm" (COA). As assumed in many papers [6], [9], we suppose here that we have a distributed memory machine. Each processor in this system executes just one task at a time. With reference to the generality principle, we suppose that all tasks have the same execution time equal to one unit time, i.e. r=1 and N/r=n=2pq+1 where p is the number of available processors in our system which are denoted P_1, ..., P_p and q≥3. Our objective is to keep all the processors active as long as possible. We suppose that the scheduling is performed as follows. First, at time t=0, task $T_{1,1}$ is executed by processor P_1, whereas the p-1 others are idle. The remainder of the precedence graph is then partitioned into q column-blocks of 2p "columns". Each block B_k (0≤k≤q-1) involves "columns" C_{2kp+2}, C_{2kp+3},..., $C_{(2k+2)p+1}$. The processor P_j (1≤j≤p) executes "columns" $C_{2kp+j+1}$ and $C_{2kp+2p-j+2}$ of B_k (0≤k≤q-2). For k=q-1, "columns" $C_{2kp+j+1}$ and $C_{2kp+p+j+1}$ of $B_{2(q-1)}$ are assigned to processor P_j (1≤j≤p). Suppose that C_u, C_v and C_w are three successive "columns" assigned to processor P_j, i.e., u=2kp+j+1, v=2(k+1)p-j+2 and w= 2(k+1)p+j+1 or u=2(k+1)p-j+2, v=2(k+1)p+j+1 and w=2(k+2)p-j+2 for k verified 0≤k≤q-3. Firstly, processor P_j executes alternately one task of C_u and one task of C_v until execution of task $T_{u-1,u}$. Just after that, P_j starts execution of task $T_{u,u}$. At the end of execution of C_u, it executes one task of C_v and one task of C_w. We note α_v the number of tasks belonging to C_v executed at time when execution of C_u is terminated.
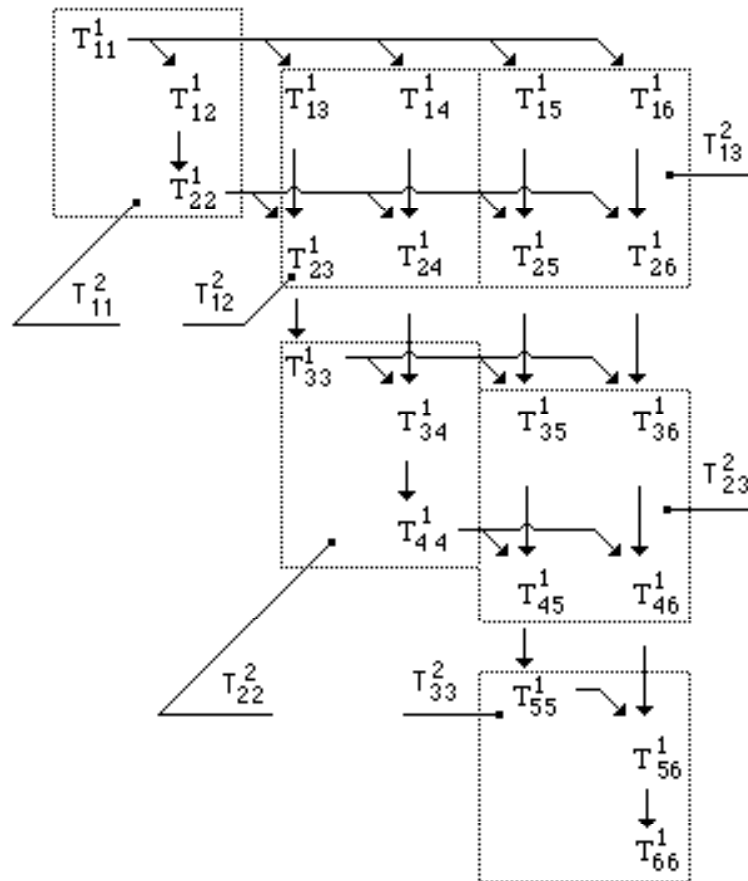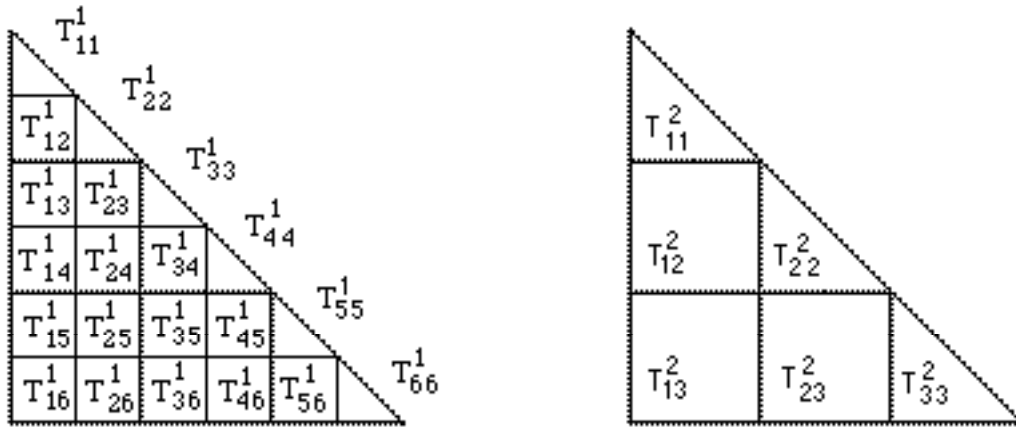

Fig. (1). 2 steps graph for n=6, r=1 and representation of tasks for n=3, r=2

Fig. (2). Correspondence between tasks and blocks (r=1 and r=2).

Lemma 1

α_v =(k+1)(2p-2j+1) (resp. (2k+1)j-(m+1)) if v=2(k+1)p+j+1 (resp. 2(k+1)p-j+2) for any j and any k verified 1≤j≤p, 0≤k≤q-2.

Proof

α_v is the number of tasks executed between end of "columns" C_t and C_u (where C_t, C_u and C_v are three successive "columns" assigned to processor P_j), i.e., the number of tasks of C_u without $T_{u-1,u}$ and $T_{u,u}$ minus α_u, and by recurrence we obtain results of lemma.

Notice that in the two above cases, we have α_v<v-1 for any v.

In the rest of this section, we will determine the date at which the execution of each task starts. We use Ex(T) to denote this date.

Lemma 2

1. $Ex((T_{11})=0$
2. $Ex(T_{uu})=2k(k-1)p+k(4p+2)+(2k+2)j$ if u=2kp+j+1 and 0≤k≤q-2
3. $Ex(T_{uu})=2(k+1)((k+2)p-j+2)$ if u=2(k+1)p-j+2 and 0≤k≤q-2

Proof

The Time at which the execution of the task T_{uu} starts is equal to the number of tasks belonging to the "columns" situated before C_u (in large sense, u≠1) and assigned to P_j plus α_v.

Notice that if the value of u increases $Ex(T_{uu})$ increases too.

In the following lemma, we determine the time at which the execution of each task not diagonally belonging to q-1 first blocks starts. Then, we will have the results in the case where j and k verified 1≤j≤p, 1≤k≤q-3:

Lemma 3

1. $Ex(T_{iv})=2i-1$ for any i and v verified 1≤i<v, v=j+1
2. $Ex(T_{iv})=2i$ for any i and v verified 1≤i<v, v=2p-j+2
3. $Ex(T_{iv})=2i+Ex(T_{uu})$ for any i, u and v verified 1≤i≤α_v, u=2(k-1)p+j+1, v=2kp+j+1
4. $Ex(T_{iv})=2i+Ex(T_{uu})$ for any i, u and v verified 1≤i≤α_v, u=2kp-j+2, v=2(k+1)p-j+2
5. $Ex(T_{iv})=2(i-\alpha_v)-1+Ex(T_{uu})$ for any i, u and v verified α_v<i<v, u=2kp-j+2, v=2kp+j+1
6. $Ex(T_{iv})=2(i-\alpha_v)-1+Ex(T_{uu})$ for any i, u and v verified α_v<i<v, u=2kp+j+1, v=2(k+1)p-j+2

The execution of the tasks belonging to the last block (k=q-1), starts with similar fashion that execution of first blocks until time t=2(k+1)((k+2)p+1)+1 where execution of task T_{uu} (u=2(k+1)p-j+2, k=q-2 and j=1) is terminated. Until this time t, each processor P_j has executed $\alpha_v+\beta_j$ tasks of its first "column" C_v (v=2(q-1)p+j+1) of the last block and it has also executed β_j tasks of the "column" of the second part of the last block C_u (u=v+p=(2q-1)p+j+1) where β_j is the number of the tasks executed by the processor P_j in each "column" of the last block just after the end of the execution of the "column" $C_{2(k+1)p-j+2}$ (k=q-2), ie., at the instant t. Hence,

$$\beta_j= [Ex(T_{2(k+1)p+1,2(k+1)p+1})-Ex(T_{2(k+1)p-j+2,2(k+1)p-j+2})]/2=(q-1)(j-1).$$

From the time where the execution of task T_{uu} (u=2(k+1)p-j+2, k=q-2 and j=1), is terminated, i.e., at the instant t = 2(k+1)((k+2)p+1)+1 where k=q-2, each processor finishes the execution of tasks of its first "column" of the last block and then it executes the other tasks not yet executed of its second "column" affected in the last block. The processor doesn't execute its tasks alternately i.e., the placement order of place of each task in its "column" gives the order of its execution by its processor affected. Lemma 4 gives the time at which the execution of each task of the last block begins. For this case, we assume v=2kp+j+1, k=q-1 and $1\leq j\leq p$ and we obtain:

Lemma 4

1. $Ex(T_{iv})=2i+ Ex(T_{2(k-1)p +j+1,2(k-1)p+j+1})$ for any i verified $1\leq i\leq\alpha_v$
2. $Ex(T_{iv})=2(i-\alpha_v)-1+Ex(T_{2kp-j+2,2kp-j+2})$ for any i verified $\alpha_v<i\leq\alpha_v +\beta_j$
3. $Ex(T_{iv})= t+\beta_j+ \alpha_v -i$ for any i verified $\beta_j+\alpha_v <i\leq v$
4. $Ex(T_{i,v+p})=2(i-\alpha_v)+Ex(T_{2kp-j+2,2kp-j+2})$ for any i verified $1\leq i\leq\beta_j$
5. $Ex(T_{i,v+p})= \beta_j -i +Ex(T_{2kp+j+1,2kp+j+1})$ for any i verified $\beta_j <i \leq v+p$

In what follows, we will show that the precedence constraints are respected. Constraint (B) is respected because the tasks of each "column" of the graph have been executed by the same processor. Constraint (A) is also respected. For this, it is sufficient to show that $Ex(T_{ii})<Ex(T_{ij})$ for all j verified $i+1\leq j\leq n$. In the first block, it is easy to show that (A) is respected (using 1 and 2 of lemma 2 and 3). In the other blocks and until the time t, the constraint (A) is also respected. As the difference $Ex(T_{i+1,i+1})-Ex(T_{ii})$ is strictly greater than 2 and as $Ex(T_{i+1,i+1})=Ex(T_{i,i+1})+1$, then $Ex(T_{ii})<Ex(T_{i,i+1})$. Moreover, using results of lemma 3 and 4 and because $\alpha_j<j-1$ for any j, we have $Ex(T_{i,i+1})=2(i-\alpha_{i+1})-1+Ex(T_{uu})\leq 2(i-\alpha_{i+1})-1+Ex(T_{ww})$ for any $w\geq u$. Using, however lemma 3, it exists $w\geq u$ where $2i+Ex(T_{ww})\leq Ex(T_{ij})$, consequently we have $Ex(T_{ii})<Ex(T_{i,i+1})\leq Ex(T_{ij})$ for any $j\geq i+1$. After time t, we show with similar fashion that the constraint (A) is also respected. Then, we have the following lemma:

Lemma 5

The (COA) parallel algorithm respects precedence constraints.

Based on generality, in the following table we will show the order of the execution of the tasks when p=2 and q=3. Hence, N=13. In this case, and after the execution of the task T_{11}, the processor P_1 (resp. P_2) executes tasks of "columns" C_2, C_5, C_6, C_9, C_{10} and C_{12} (resp. C_3, C_4, C_7, C_8, C_{11} and C_{13}). We suppose that all tasks have the same execution time equal to 1. (i,j in column P_k means processor P_k executes task T_{ij}, column $Ex(T_{ij})$ gives the date when execution of task starts):

$Ex(T_{ij})$	P_1	P_2	$Ex(T_{ij})$	P_1	P_2	$Ex(T_{ij})$	P_1	P_2
0		1,1	16	1,10	4,8	32	10,10	8,11
1	1,2	1,3	17	3,9	6,7	33	1,12	9,11
2	2,2	1,4	18	2,10	7,7	34	2,12	10,11
3	1,5	2,3	19	4,9	5,8	35	3,12	11,11
4	1,6	3,3	20	3,10	1,11	36	4,12	3,13
5	2,5	2,4	21	5,9	6,8	37	5,12	4,13
6	2,6	1,7	22	4,10	2,11	38	6,12	5,13
7	3,5	3,4	23	6,9	7,8	39	7,12	6,13
8	3,6	4,4	24	5,10	8,8	40	8,12	7,13
9	4,5	2,7	25	7,9	3,11	41	9,12	8,13
10	5,5	1,8	26	6,10	1,13	42	10,12	9,13
11	4,6	3,7	27	8,9	4,11	43	11,12	10,13
12	1,9	2,8	28	9,9	2,13	44	12,12	11,13
13	5,6	4,7	29	7,10	5,11	45	--	12,13
14	6,6	3,8	30	8,10	6,11	46	--	13,13
15	2,9	5,7	31	9,10	7,11			

4. Performance Analysis

In this section, we will present and compare both the theoretical and practical performances of the COA algorithm that was implemented on a TN310, parallel computer of T9000 Transputers. Firstly, we will determine the arithmetic cost $A_{p,r}$ of COA and secondly we will compute the communication cost of the COA algorithm. In the rest of this paper, we assume that the unit time for executing a combined multiplication-subtraction or a division is equal to t_a (4-5). The arithmetic cost of the task T_{ij} (resp. T_{kk}) is equal $r^2 t_a$ (resp. $r(r+1)t_a/2$). For the sake of simplification and as the number of tasks T_{ij} (i<j) (resp. T_{kk}) is in the order of $O(N^2/r^2)$ (resp. $O(N/r)$), we consider that execution time of any task is the same, i.e. all task are the same execution time equal to $r^2 t_a$. Then the execution times of all tasks are equal to $r^2 t_a$. Before calculating the arithmetic execution time $A_{p,r}$, we note that the number of tasks (different of T_{11}) executed by each processor P_j (1≤j≤p) is equal to q(2pq+3)+2j-p-1. $A_{p,r}$ is equal to the sum of the execution time of T_{11} ($r^2 t_a$) and the execution time of tasks affected to processor P_p (($q(2pq+3)+p-1) r^2 t_a$). In fact, the processor P_p executes the last task T_{nn} of the 2-steps graph and it is active without interruption between the end of execution of T_{11} and T_{nn}. So, the arithmetic cost of COA algorithm is $A_{p,r}= [p + q(2pq+3)] r^2 t_a$. In the paper [4], we show that the value of arithmetic cost is minimum. This is due to the fact that the number of tasks of the block B_k (0≤k≤q-2) executed by any processor is constant and independent of the number of processors.

In what follows, we determine the communication cost of (COA) algorithm. We consider a distributed memory system where we assume the following:

1. Each processor communicates with its neighbor by writing the information in its memory.

2. Communications are by message passing, and there is no overlap between time of computations and time of communications.

3. Delay of communication between one processor and its neighbor is equal to b+La where b is the start-up, a is the propagation time of an unitary number of data and L is the length of message [10].

Firstly, we remark that there are two types of communication vertical and diagonal. The cost of vertical communication is equal to 0 because each "column" of 2-steps graph has been executed by one and one processor. Then, the cost of communication is limited to the cost of diagonal communications. The diagonal communication is in fact a broadcast: when processor P_j finishes execution of affected task T_{ii}, it sends the results of all processors. For case r=1 and under the 1-port hypothesis, we choose the hypercube for linking the processors. The broadcast algorithm is: the first processor sends the data to one of its neighbors. Then the two nodes send in parallel their data to two other nodes and so on. After i steps, 2^i nodes will have received the data (10-11). The minimum time for broadcasting a message from one processor to all others under the 1-port hypothesis is equal to $\log_2(p)(b + La)$. Then, for broadcasting n values x_i, needs a time equal to $C = \log_2(p)(b + La) n$. We note that the value C is the minimum under the 1-port hypothesis [11].

For case r>1, we assume that the p processors are completely linked and it is possible to use all the links of a processor at the same time (p-ports or shouting). Then, the communication's cost is:

$$C= (b+ La) N/r =(b+ La)(2pq+1).$$

The execution time $T_{p,r}$ of (COA) is equal to $T_{p,r} =A_{p,r} + C$ where C is the communication time relatively to the topology T, i.e., the time for broadcasting n vectors of size r each. We show that the value of $T_{p,r}$ is minimum.

The (COA) algorithm has been coded in C and implemented on a TN310 parallel machine involving 10 nodes (T9000 Transputers). The size of the message is L=4 bytes (to represent a float in the TN310, it needs 4 bytes). We present in the following figures the practical results. Figure 3 presents the theoretical and the practical efficiencies for values of N=n (r=1) lower than 3000 and for p=8. It shows adequacy for the two classes of results. The differences between the theoretical and the practical values of the efficiency may be attributed to the time required to create the statements, extra synchronization variables used in the program and other program instructions which are not taken into account in our theoretical formula.

For case r>1, the p processors are completely linked. For some values of r, the efficiency of block (COA) algorithm is greater than the efficiency of the point-wise (COA) algorithm. This is due to the fact that the communication cost for the block method is less than the communication cost for point-wise method. Moreover, the practical arithmetic cost for the block algorithm is lower than for the point-wise algorithm. On the other hand, the idle time of the processors in the block resolution is greater than in the point-wise resolution. Table 1 presents two examples for showing the superiority of the block algorithm (E_B, E_P represent respectively block and point-wise practical efficiencies respectively).
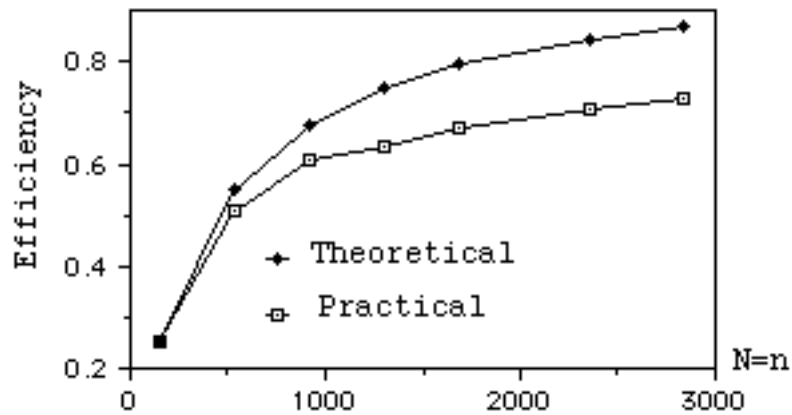
Fig. (3) Optimal theoretical and experimental efficiencies for p=8 (r=1).

5. Optimal Block Size

In this section, we will, theoretically and practically, determine the block size r_{opt} that minimizes the execution time of the (COA) algorithm. Theoretically, it is sufficient to find, for fixed values of N and p, the value of $r=r_{opt}$ that minimizes the function $T_{p,r}$. As N verifies N/r=2pq+1 where r is the block size, q is an integer verifying q≥3. Thus, we have a limited number of possible values of r. The minimum value of $T_{p,r}$, when r varies and p is fixed, is determined by comparing different values of $T_{p,r}$ for different values of r.   So, we have the following results presented in Table 2 where T. r_{opt} (resp. P. r_{opt}) means theoretical (resp. practical) value.

Hence, we note that the practical value of r_{opt} is greater than the theoretical one. This is due to the time required to create statements, DO-loop control and other program instructions which are not taken into account in $T_{p,r}$.

Table (1). Experimental efficiencies.

N	r	p	E_B	E_P
1921	20	4	0.76	0.73
2305	24	8	0.75	0.64

Table (2). Values of ropt.

N	p	T. r_{opt}	P. r_{opt}
1921	4	5	16
1921	8	12	20
2305	6	8	16
2305	8	12	24

6. Conclusion

We have presented an optimal parallel algorithm (COA) for solving a triangular system (Ax=b) of size N where N/r=n=2pq+1, where r is the block size, p is the number of processors and q≥3. It is important to notice that the arithmetic and the communication costs of (COA) are minimum. Its implementation on the parallel machine (TN310) permitted us to validate the theoretical results and showed that the weak difference between the theoretical and the practical efficiencies is satisfactory. As the algorithm executes the task graph "column-wise", thus the communication cost is reduced. In fact, only the values of x_i (1≤i≤n) are exchanged between the processors. Therefore, when the p processors are completely linked (the machine's topology is a complete graph), the number of communications is minimum, and equal to n. Note that the advantage of using block methods is the increase of task granularity, hence the reduction of overhead in synchronization and communication. We intend to implement different parallel algorithms for solving a linear system and compare different performances. Also, it is important to design scheduling for 2-steps graph in heterogeneous environments where the processors have different speeds.

7. References

[1] Heath, M. T. and Romine, C. H., "Parallel solution of triangular systems on distributed-memory multiprocessors," *SIAM J. Sci. Statist. Comput.*, Vol. 9(8) (1988), 558-588.
[2] Ibarra, O. H. and Kim, M. H., "Fast parallel algorithms for solving triangular systems of linear equations on the hypercube," *Journal of Parallel and Distributed Computing 20* (1994), 303-316.
[3] Li, G. and Coleman T. F., "A new method for solving triangular systems on distributed-memory message-passing multiprocessors," *Siam J. Sci. Stat. Comput.*, Vol. 10(2)(1989), 382-396.
[4] Marrakchi, M., "Optimal parallel scheduling algorithms for 2-steps graph with constant task cost," *Parallel Comput.*18 (1992), 169-176.
[5] Missirlis, N. M., "Scheduling parallel iterative methods on multiprocessor systems," *Parallel Comput.* 5 (1987), 295-302.
[6] Cosnard, M., Marrakchi, M., Robert, Y. and Trystram, D., "Parallel Gauss elimination on an MIMD computer," *Parallel Comput.*6 (1988), 275-296.
[7] Kwok, Y.-K. and Ahmad, I., "Static scheduling algorithms for allocating directed task graphs to multiprocessors," *ACM Computing Surveys*, Vol. 31(4)(1999), 406-471
[8] Topcuoglu, H., Hariri S. and Wu M.-Y., "Performance effective and low-complexity task scheduling for heterogeneous computing," *IEEE Tran. on para. and dis. systems*, Vol. 13(13)(2002), 260-274
[9] Honig, U., Schiffmann, W., "A meta-algorithm for scheduling multiple dags in homogeneous system environments," in: S. Q. Zheng, (PDCS'2006) Dallas 2006
[10] Saad, Y., "Data communication in parallel architectures," Rpt. DCS/461, Yale University, 1986.
[11] Rumeur, J., "*Communication dans les Réseaux de Processeurs*," France, Masson, 1994.

$$(\quad / \ / \quad\quad\quad\quad / \ / \quad\quad)$$

.

p   .

$(\quad\quad\quad r \quad\quad\quad\quad\quad\quad\quad\quad q)$ $N/r=2pq+1$

.

.

.

قواعد النشر

أهداف المجلة

تهدف المجلة إلى نشر إنتاج الباحثين من داخل الجامعة وخارجها في جميع تخصصات العلوم الهندسية وعلوم الحاسب، والمجالات الرئيسية التي تشملها المجلة هي:

● هندسة الحاسب	● الهندسة الكهربائية
● علوم الحاسب	● الهندسة المدنية
● تكنولوجيا المعلومات	● الهندسة الميكانيكية
● نظم المعلومات	● الهندسة الكيميائية
● العلوم الهندسية الأساسية	● هندسة التعدين والبترول

لغة المجلة:

تقبل المجلة البحوث باللغة الإنجليزية.

أ) المواد التي تقبلها المجلة للنشر:

١- البحث: وهو عمل أصيل للمؤلف (أو المؤلفين) يضيف جديداً للمعرفة في مجال تخصص (فرع المجلة).

٢- المقالة المرجعية: وتتناول العرض النقدي والتحليلي للبحوث والكتب ونحوها التي سبق نشرها في ميدان معين والرسائل العلمية المتميزة.

٣- المقالة القصيرة (تعليق تقني): مقالة قصيرة تحوي تطبيقاً تقنياً.

٤- الابتكارات العلمية المتميزة وبراءات الاختراع.

٥- المراسلات: وتتناول عرض فكرة أو رأي علمي أو اقتراح بحثي.

٦- انتقادات الكتب

ب) شروط النشر:

١- أن يكون البحث متسماً بالأصالة والابتكار والمنهجية العلمية وسلامة الاتجاه وصحة اللغة وجودة الأسلوب.

٢- أن لا يكون البحث قد سبق نشره أو قدم للنشر لجهة أخرى.

٣- جميع البحوث المقدمة للنشر في المجلة خاضعة للتحكيم.

ج) تعليمات النشر:

عند تقديم البحث للنشر يشترط الآتي:

١- أن يقدم الباحث طلباً بنشر بحثه، ويوضح فيه العنوان الالكتروني للمراسلات.

٢- لا يجوز إعادة نشر أبحاث المجلة في مطبوعة أخرى إلا بإذن كتابي من رئيس التحرير.

٣- يرسل الباحث بحثه باللغة الانجليزية عن طريق البريد الالكتروني على العنوان الالكتروني المذكور في فقرة المراسلات، وكذلك ملخص باللغتين العربية والإنجليزية بحيث لا تزيد كلماته عن ٢٠٠ كلمة.

٤- يكتب البحث باستخدام برنامج (Microsoft word) ويستخدم font 12 Times New Roman في كتابة المتن، مع ترك مسافة ونصف بين الأسطر.

٥- يجب ألا يزيد عدد صفحات البحث شاملا الرسومات والجداول عن ٢٠ صفحة حجم A4.

٦- أن يكتب عنوان البحث واسم الباحث وعنوانه ولقبه العلمي والجهة التي يعمل بها على الصفحة الأولى مستقلة.

٧- توضع هوامش كل صفحة أسفلها.

٨- يشار إلى المراجع داخل المتن بالأرقام حسب تسلسل ذكرها وتثبت في فهرس يلحق بآخر البحث.

أ) الدوريات: يشار إليها في المتن بأرقام داخل أقواس مربعة على مستوى السطر. أما في قائمة المراجع فيبدأ المرجع بذكر رقمه داخل قوسين مربعين فاسم عائلة المؤلف ثم الأسماء الأولى أو اختصاراتها فعنوان البحث (بين علامتي تنصيص) فاسم الدورية (تحته خط) فرقم المجلد، فرقم العدد فسنة النشر (بين قوسين) ثم أرقام الصفحات.

مثال: الحميدي، إبراهيم عبدالله. "الهجرة الداخلية في المملكة العربية السعودية حجمها واتجاهاتها." <u>مجلة كلية الآداب</u>، جامعة الملك سعود، م١٦، ع١ (٢٠٠٤م)، ١٠١-١٥١.

ب) الكتب: يشار إليها في المتن داخل قوسين مربعين مع ذكر الصفحات، مثال ذلك [٨، ص١٦]. أما في قائمة المراجع فيكتب رقم المرجع داخل قوسين مربعين متبوعاً باسم عائلة المؤلف ثم الأسماء الأولى أو اختصاراتها فعنوان الكتاب (تحته خط) فمكان النشر ثم الناشر فسنة النشر.

مثال: اليوسف، صالح سليمان. <u>المشقة تجلب التيسير: دراسة نظرية وتطبيقية</u>، الرياض: المطابع الأهلية للأوفست، ١٩٨٨م.

٩- ترفق جميع الصور والرسوم المتعلقة بالبحث في ملف مستقل.

١٠- ترقم الجداول والرسومات ترقيماً مستقلاً عن ترقيم البحث ويعنون الجدول بعنوان فوق الجدول والرسم بعنوان تحت الرسم.

١١- لا يعاد البحث إلى صاحبه سواء نشر أو لم ينشر.

١٢- يعطى الباحث نسختين من المجلة وعشرين مستلة من بحثه المنشور.

١٣- يلزم الباحث إجراء التعديلات المنصوص عليها في تقارير المحكمين، مع تعليل ما لم يعدل.

١٤- تعبر المواد المنشورة في المجلة عن آراء ونتائج مؤلفيها فقط.

هيئة التحرير

(/   )   -   ( )   ( )

المحتويات

هـ